Universität Osnabrück

Fachbereich Biologie/Chemie
Institut für Chemie

Dissertation
zur Erlangung des Grades eines Doktors der Naturwissenschaften
-Dr. rer. nat.-

Synthesis, Characterization and Host-Guest Complexation Studies of Dendritic and Linear Pyridinium Derivatives

von
Kathiresan Murugavel
aus Indien

Osnabrück 2010

This doctoral thesis was carried out at the Institut für Chemie, Fachbereich Biologie/Chemie, Universität Osnabrück, Germany, under the supervision of Prof. Dr. Lorenz Walder. The duration of the study was three years starting from June 2007 to June 2010.

Hauptberichterstatter:	Prof. Dr. Lorenz Walder, Universität Osnabrück
Zweitberichterstatter:	Prof. Dr. Heinz-Jürgen Steinhoff, Universität Osnabrück
weitere Mitglieder:	apl. Prof. Dr. Helmut Rosemeyer, Universität Osnabrück
	Dr. Karsten Kömpe, Universität Osnabrück

This thesis is dedicated to my Parents, Brother, Family members & Friends

Acknowledgements

I would like to thank Prof. Dr. L. Walder for providing me the opportunity to work in his group, for his coaching, patience and tolerance through all the haps and mishaps during the course of my work. His concerned mentorship has taught me innumerable lessons, both within and beyond the boundaries of science. Without his guidance, I wouldn't have had the ability to gain knowledge in many aspects of chemistry, from organic to analytical to supramolecular chemistry, which I believe is a great asset that will help me in whatever endeavors I pursue. For this I am grateful to him. My special thanks to GK 612 funded by DFG for the financial assistance.

I would like to thank Prof. Heinz-Jürgen Steinhoff for being my co-advisor and for his valuable suggestions during the spin-labeled dendrimers project. Also thanks to Dr. Johann P. Klare for his special guidance during this project. Thanks to Prof. Brandt, Head of the GK 612, Ms. Ludwig, for their efforts for all the official formalities related to the GK. Also I would like to thank Ms. Böhme and Ms. Krüger for all their efforts during the GK meetings.

I would like to thank apl. Prof. Helmut Rosemeyer and Prof. Uwe Beginn for their valuable suggestions and comments during our literature seminar. I would like to thank Dr. Karsten Kömpe.

I would like to thank Prof. Hans Reuter and Prof. Markus Haase for the collaborations, for allowing me to use some of the sophisticated instruments and their valuable suggestions during this time. My special thanks to Prof. Martin Steinhart.

My special thanks to Mrs. Christine Schulz-Kölbel and Mrs. Simona Webersinn for their encouragement, constant support and their help related to the administrative and laboratory work. I would like to thank Mrs. Claudia Ratermann and Mrs. Monika Dubiel for their assistance with all administrative works. I would like to thank Dr. Dirk Bongard, my

predecessor, for his valuable suggestions during the early stage of my work; most of our discussions were about the problems related to the biological applications of the dendrimers. My special thanks to Mr. Holger Oelrich and Dr. Dereje Hailu Taffa who helped me a lot from the very first day to till now regarding various things, suggestions, funny lunch sessions and for the fruitful collaborations. My special thanks Dr. Ina Rianasari. My special thanks to Ms. Veronica-Alina Constantine for her patience while teaching the basic things in the laboratory during the early days of my lab work and also for her valuable suggestions regarding viologen synthesis. I would like to thank Mr. Liang Cheng Cao who made me a senior member in the group at least in the last moment. My special thanks to Mrs. Marianne Gather who taught me the special NMR techniques.

I would like to thank Mr. Fei Ye, Mr. Ralph Beckmann, Ms. Julia Holterhaus and Mr. Christian Rickert, for the collaboration, suggestions and support.

Special thanks to Prof. Dr. R. Raghunathan, and Dr. S. Bhagavathy.

I would like to thank Dr. E. Ramesh, Dr. R. RathnaDurga and Dr. E. Elamparuthi for their constant encouragement, support and guidance during the course of my thesis.

My special thanks to Dr. T. R. Gopalakrishnan for his suggestions and discussions. Special thanks to Dr. Rajesh Komban for his suggestions and discussions.

I would like to thank International Student Office of the University of Osnabrück for their DAAD graduation aid.

I would like to thank my parents who always had faith in me and let me to go in my own way. My special thanks to my brother, my friends, all my relatives and neighbors´ for coming all along with me till this day.

I would like to thank Thiru and his family for their invitations on various occasions.

My special thanks to Mr. Sahayam (higher secondary tutor) and Mr. Daniel Arockiaraj (my UG lecturer) who oriented me and my passion towards chemistry and organic chemistry

by their excellent teaching. Also I would like to thank them for dedication and excellency in their profession.

Of course I should thank Mr. Arun Thomas, Mr. Madhusudhanan Dharmavarapu, Mr. Maniraj Bhagawati, Dr. Sunil Kumar Srivastava, Mr. Vishal Patel, Mr. Vikash Peesapati, Mr. Joy Bose, Mr. Jan Pregnitz, Miss. Eva Augenstein, Mr. Veselin Alesandrov, Mr. Alexander Knittel, Mr. Felipe, Ms. Mina Shahi and my neighbours in Jahnplatz for their friendship, for the game sessions and for their continuous support during the course of this study.

Table of Contents

List of Schemes

List of Figures

List of Tables

Thesis Abstract

Convergent and divergent strategies for the synthesis of viologen dendrimers with 1,3,5-tri-methylene branching units are presented. The synthesis of 3,5-bis(hydroxymethyl) benzyl bromide was optimized. The analysis of the crystal structure of 1-[3,5-bis(hydroxymethyl)benzyl]-4-(pyridin-4-yl) pyridinium hexafluorophosphate together with PM3 calculations opens an avenue to judge the structure and conformation of benzylic viologen dendrimers.

In order to study chemical trigger induced conformational changes, viologen dendrimers were spin-labeled via a divergent approach. 1-(2,4-dinitrophenyl)-4-(pyridin-4-yl)pyridinium hexafluorophosphate was used as the end group to yield an activated dendrimer of the respective generation. The corresponding dendrimers were spin-labeled by reacting the active functionality with 4-amino TEMPO. The products were characterized by ESR (spin-label efficiency) and conventional cyclic voltammetry. Dynamic ESR studies are planned.

New trimethylene-dipyridinium dendrimers were synthesized via a divergent approach using 4-*tert*-butylbenzyl group as the peripheral group. These dendrimers are well soluble in DMF or DMSO as PF_6 salts and they act as a host for anthraquinone-2,6-disulfonate (AQDS). They can be stoichiometrically titrated with AQDS as shown by ^{1}H-NMR, DOSY and cyclic voltammetry. Upon loading them with AQDS, the dendrimers undergo first a contraction, they reach a minimum hydrodynamic radius for complete charge compensation and they re-open when overcharging takes place. The contraction is supported by MM+ calculations. Upon stepwise loading of $\mathbf{G_2}$ (42 positive charges) with AQDS (2 negative charges), the first 3 molar equivalents (6 neg. charges) occupy the innermost dendrimer shell (consisting of 6 pos. charges), the next 6 equivalents (12 neg. charges) occupy the middle shell (12 pos. charges) and the last 12 equivalents AQDS (24 neg. charges) occupy the outermost shell of

the dendrimer (24 pos. charges), as supported by ^{1}H-NMR titrations yielding the magic equivalent numbers of 3, 9=3+6, and 21=3+6+12. Such stepwise radial complexations again in DMSO were further demonstrated using other molecular guests (mono-, di- and trianionic) as well as with on purpose synthesized viologen dendrimers.

α,ω-dibromoalkanes were bifunctionalized in two steps to yield alkyl phosphonates with pyridinium, trimethylenedipyridinium, bipyridinium or a sulfonate at their ω end. These compounds were used as surface modifiers to build biomimetic membranes on the pore walls of mesoporous TiO_2. Host-guest interaction studies with on purpose synthesized viologen compounds have been performed in collaboration.

1 Introduction

1.1 Definition

Dendrimers are nearly perfect monodisperse macromolecules with a regular and highly branched architecture. These extremely branched molecules are synthesized from identical building blocks (dendrons) that contain branching sites via an iterative reaction sequence. A

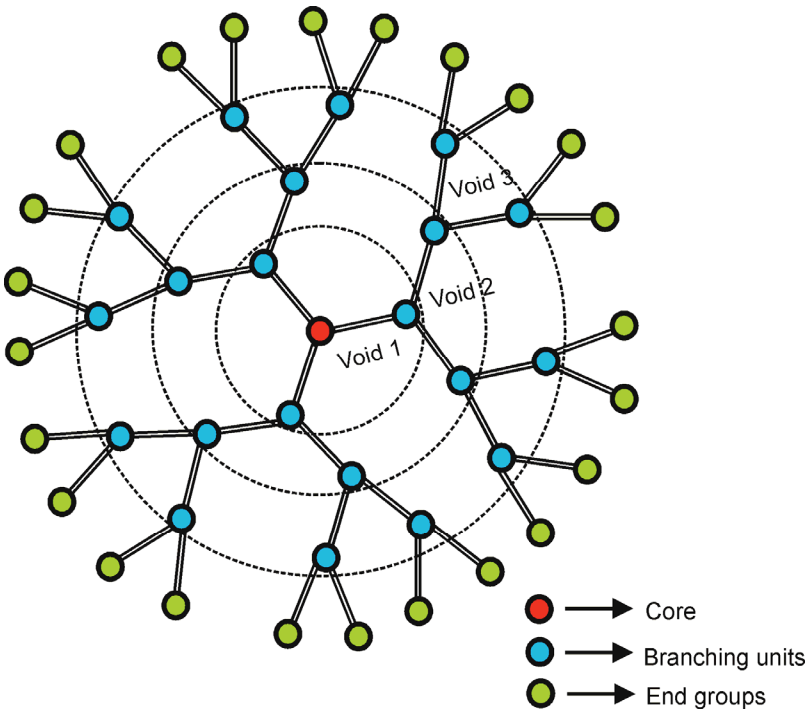

Figure 1-1: Schematic representation of a generation 2 dendrimer emanating from a trifunctional core. The microenvironments are represented as void 1, void 2 and void 3; the dotted lines indicate different layers of a typical dendrimer

dendrimer is composed of core, branching units and peripheral groups.[1] Thus, by choosing the right core, branching units and functional groups, one can precisely control the properties such as shape, dimensions, density, polarity, flexibility, and solubility of these macromolecules. The principal architecture of a dendrimer is shown in Figure 1-1.

1.2 History of Dendrimers

Dendrimer chemistry has passed three decades, in the initial years, the importance was given to their synthesis and synthetic methodologies, later emphasis was on their

functionalization and applications.[2] The first report on dendrimer synthesis was published by Voegtle in 1978.[3] A few years later, in the early 1980s, Denkewalter patented the synthesis of L-lysine-based dendrimers.[4] The first thoroughly investigated dendritic structures were Tomalia's PAMAM dendrimers[5] and Newkome's "arborol" systems[6], both of which were synthesized utilizing the divergent approach (details regarding convergent and divergent approach are discussed in the next section). In 1990, Frechet introduced the convergent approach for aromatic polyether dendrimers.[7] Moore's convergently produced phenylacetylene dendrimers[8] belong to the early reported first five classes of dendrimers. Additionally, many other types of interesting, valuable, and aesthetically pleasing dendritic systems have been developed in the past and recent years, and thus, a variety of dendritic scaffolds have become accessible with defined nanoscopic dimensions and discrete numbers of functional end groups.[9] Our own group has introduced one of the first dendrimers with electroactive branches.[10]

1.3 Classification of Dendrimers

Besides their generation, dendrimers can be classified according to the charge, symmetry, repeating units, functional groups, electro activity, etc.

Based on the charge, dendrimers can be classified as follows.

1. Cationic dendrimers – Dendrimers that carry positively charged groups in their core or periphery or branching units belong to this category. e.g., our viologen dendrimers (repeating unit is cationic), protonated PPI and PAMAM.
2. Anionic dendrimers – Dendrimers that carry negative charge in their core or periphery or branching units belong to this category. e.g., Astruc dendrimers[11] (end group is anionic).

3. Neutral dendrimers – Dendrimers that do not carry any charge are grouped in this category. e.g., polyether dendrimers, azobenzene dendrimers.[12]

Based on the electroactivity, they can be classified into

1. Electroactive dendrimers – Dendrimers that contain electroactive units in their core or branching or periphery belong to this category. Upon oxidation/reduction, they switch their state of charge. e.g., viologen dendrimers (repeating unit is electroactive), ferrocene dendrimers.[13]
2. Non-electroactive dendrimers – All the other dendrimers that do not exhibit electroactivity belong to this category.

1.4 Synthetic Approaches

Dendrimers can be synthesized using either a divergent or a convergent approach.[1]

1.4.1 Divergent approach

In the divergent approach, the synthesis starts from a central core and branches out to the periphery utilizing the branching units (dendrons), with each reaction leading to a new generation (neglecting the activation step), in contrast to a simple polymerization which result in a random distribution of molecular weights (Figure 1-2a; For an elaborated scheme and discussion using latent functionalities and activation see chapter-2). In order to have all peripheral groups transferred, every reaction has to be very selective. Often the presence of statistical defects due to incomplete reactions may hamper the product purity.

1.4.2 Convergent approach

In the convergent approach, the difficulty of divergent synthesis involving many steps on a single core unit has been overcome by starting the synthesis of these dendrimers from the

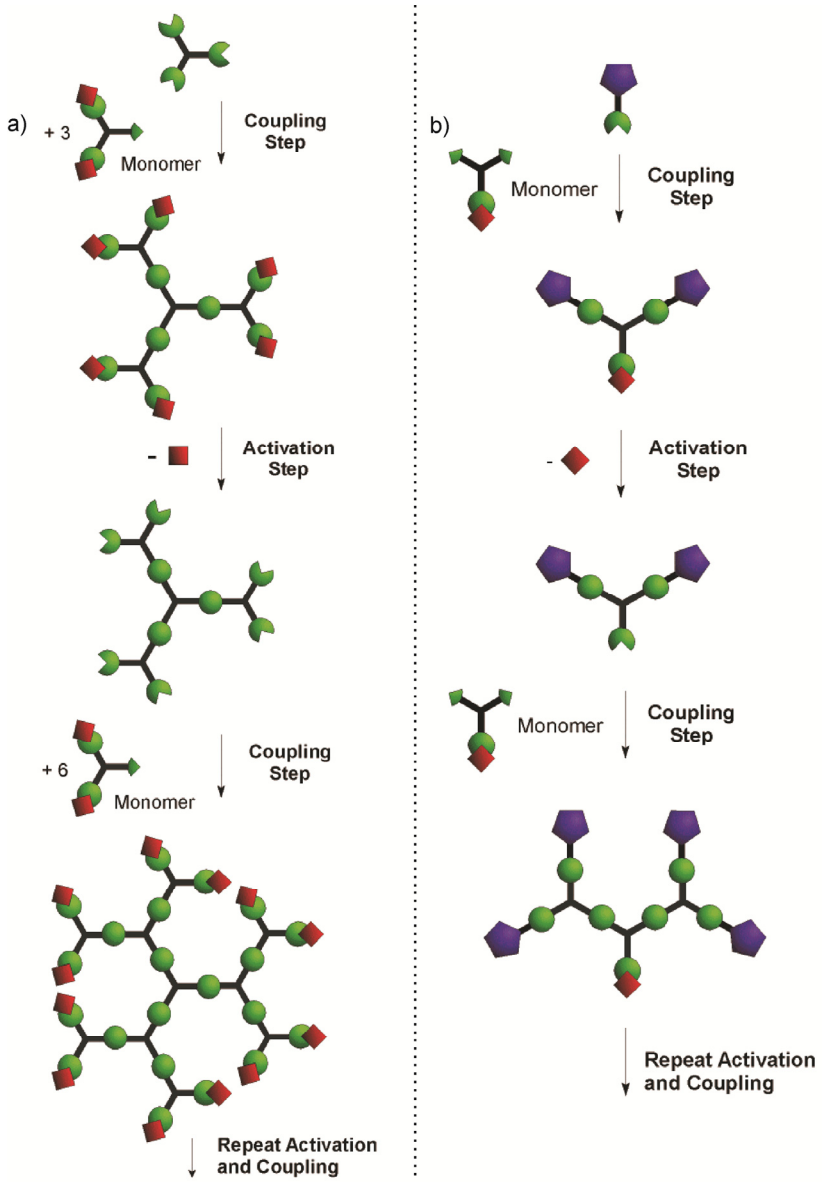

Figure 1-2: General example for a) Divergent approach; end group attachment leads to the dendrimer of defined generation; b) Convergent approach; assembly of the focal points to the core gives dendrimer of defined generation (Figures adapted as in Chemical Reviews, 2001, Vol. 101, No. 12)

periphery and ending it at the core (Figure 1-2b). In this way, a constant and low number of reaction sites are warranted throughout the synthesis. As an advantage, dendrons possessing different end groups can be anchored to the central core in a precise way. The convergent approach becomes more and more important in recent publications, because of its flexibility. The convergent approach is mainly used for the synthesis of smaller generation dendrimers, larger dendrimers are often synthesized by the divergent approach.

More recently, accelerated approaches have been developed. They combine the advantages of both divergent and convergent methods. These procedures generally maintain the versatility and product monodispersity offered by the convergent method, but reduce the number of linear synthetic steps required to access larger dendritic materials. These procedures include multigenerational coupling such as hypercore,[14] double stage convergent, hypermonomer and double exponential growth[15] utilizing orthogonal protecting group chemistry. The complicated synthetic scenario needed for their production accounts for the scarce availability of these macromolecules.

1.5 Characterization

The characterization of dendrimers is a critical and integral part of dendrimer chemistry as it provides the ability to determine accurately and confirm the structures and the purity of the compound. The dendrimers are usually characterized by standard polymer characterization techniques such as size exclusion chromatography (SEC),[16] NMR techniques such as ^{1}H NMR, ^{13}C NMR; with NMR methods, ratio of the core to the peripheral resonance reflects the quality,[17] DOSY,[11,17-18] mass spectrometry,[19] and light-scattering measurements.[17]

1.6 Properties and Applications of Dendrimers

Dendrimers are monodisperse macromolecules, because of the cascade type synthesis discussed before. They possess typical characteristics of small organic molecules like defined composition and of polymers such as high molecular weight and multitude of physical properties.[20] The volume occupied by a dendrimer increases cubically with generation whereas the molecular weight increases exponentially. With increasing generation, they undergo transition from soft polymers with flexible open structures to hard spherical particles with compact structure. Thus, higher generation dendrimers have close-packed peripheral functional groups and a hollow interior providing a unique microenvironment. Higher

generation dendrimers exhibit interesting properties due to their ability to encapsulate guest molecules. These guest molecules can be entrapped into the dendritic cavities and triggered release can be done by chemical means, eg. release of complexed eosin molecules by the addition of chloride ions to the viologen dendrimers.[21] Depending on the chemical functionality, they may be either hydrophilic or hydrophobic. Meanwhile, the surface groups of dendrimers are amenable to modification and can be tailored for specific applications (the multiple surface groups (end groups) of dendritic molecules have the potential to form multiple interactions, either with bulk solvent, or with another chemical/biological species). These surface groups are responsible for their solubility, miscibility and reactivity.

Biological properties of these macromolecules are crucial because of the growing interest in using them in biomedical applications.[22] Cationic dendrimers are generally hemolytic and cytotoxic due to their non-specific interactions with biomolecules but they cannot be excluded as there is no alternative for gene therapy applications without cationic dendrimers.[22] Their toxicity is generation-dependent, (it depends on the number of surface groups). Anionic dendrimers are biocompatible over a broad concentration range, but they do not interact with DNA.

Many potential applications for dendrimers have been proposed, studied and a lot have been reviewed in the past.[9b-d,9f,17,23] Many of these applications have focused on the dendritic interior and its use in host-guest chemistry. The applications cover a range from biological (drug delivery systems,[3] contrast reagents,[24] etc), to material sciences (polymers,[25] light harvesting devices,[9a] solid supports,[26] catalysts,[27] etc).

1.7 Electroactive Dendrimers

Electroactive dendrimers represent a class of functional materials that have potential technological applications. Different dendrimers have been prepared with an electroactive site

either at the core[28] or at the periphery. Some dendrimers with multiple electroactive sites have also been prepared. Incorporation of redox-active units in the dendritic architecture gives us information on the dendritic structure and superstructure, self-assembly processes, degree of electronic interactions, and conformational changes upon electron transfer processes.

Electroactive dendrimers are attracting increasing interest in view of their possible application as sensors,[13,29] catalysts,[13,29-30] and enzyme mimics,[31] in which a redox center is buried inside the dendritic nanoenvironment, and, last but not least, multielectron storage devices.[29] The redox properties of the electroactive dendrimers have been, in general, investigated by electrochemical techniques.

A molecular multielectron storage device should consist of multiple identical and noninteracting redox units able to reversibly exchange electrons with another molecule or an electrode. The redox-active units should exhibit chemical reversibility and fast electron transfer at easily accessible potential difference as well as chemical robustness under the working conditions. Such devices can be used as (i) redox catalysts, (ii) electrochemical sensors with signal amplification, and (iii) molecular batteries that can be foreseen to power molecular machines in the future or that can be used to construct flexible rechargeable batteries.[32]

Dendrimers are ideal scaffolds to construct these devices since: (i) a large number of redox units can be placed in the periphery and/or branching points, (ii) the dendrimer skeleton can be tuned (distance between the redox units can be tuned) to minimize electronic interaction between the redox centers and (iii) the dendrimer periphery can be optimized to get the desired solubility properties and processability to eventually deposit the dendrimers on a surface.[33] Other possible scaffolds includes polymers[34] and nanoparticles,[35] which are easier to synthesize, but they do not enable the same degree of control and tuning of the number, position, and distance of the active units.

Heinen et al have reported on the first synthesis of benzylic viologen dendrimers.[10b,10c] The study focused on generation-dependent CT complexation, generation-dependent diffusion coefficient/hydrodynamic radii and pimerization. Also in another report, they focused on the charge trapping and radial redox gradient ability of these dendrimers. Later Bongard et al[36] and Asaftei et al[37] reported the biological applications of these dendrimers. Bongard et al in their gene transfection experiments have shown that viologen dendrimers exhibit very high cytotoxicity due to their rigidity and electroactivity. The structural tuning by incorporating flexible groups has shown improved biocompatibility but the overall transfection efficiency obtained was 10-15 times lower than that obtained with PAMAM dendrimers. This is attributed to the viologen dendrimers ability to interfere in biological redox processes and their poor binding ability to the DNA molecules due to the rigidity of the biphenyl system.

The convergent synthesis and host-guest complexation studies of these dendrimers with eosin guest molecule was reported by Balzani et al.[38] Though the complexation study showed the number of eosin guest molecules complexed, a clear picture about the dendritic voids, i.e., the mechanism of filling was not clearly shown. There is one report on stepwise radial complexation of imine groups in phenylazomethine dendrimers[12,39] where the Lewis acid functionalities complexed in a step-wise manner from inside-out or outside-in. The authors stated that the incorporation of organic guest molecules quantitatively into the dendritic voids is difficult due to the random statistical distribution.[39c] Recently, Thayumanavan et al tried to explore this stepwise complexation ability by specifically installing electroactive units in every layer of dendrons. This is a tedious method as one has to specifically install the electroactive unit in every layer of dendron.[40] So, our aim is to find out if the step-wise complexation can be found in the case of electrostatic guest complexation and thus to confirm or reject the generality of this phenomenon.

1.8 Problems and Aims of the Thesis

This thesis is organized into seven chapters.

i) The first chapter is a general introduction about dendrimers, where synthetic aspects as well as their characterization, properties and applications are discussed.

ii) An efficient and selective synthesis of the viologen subunits needed for the divergent (a) and convergent (b) approach of viologen dendrimers is related to the problem of an efficient and selective synthesis of the two benzylic bromides (c) and (d).

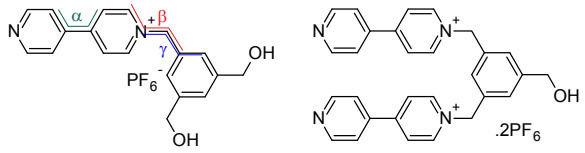

Furthermore, the conformation of the related dendrons and dendrimers is mainly governed by the dihedral angles α, β, and γ. It is therefore an important task to have access to the X-ray structure of (a) or (b) to analyze the conformation of the corresponding viologen dendrimers.

In chapter 2 of the thesis, we addressed both these problems, i.e., the synthesis of (a) and (b) as well as the X-ray structure of a compound related to (a) combined with force field calculations. The study allows for judging the conformational space of the corresponding dendrimers.

iii) The dynamics of a dendrimer, i.e., its conformational changes in time is not yet well understood. One of the most efficient methods developed for the study of intramolecular distances and dynamics of proteins is ESR which could be carried out on the appropriately spin tagged proteins. We aim at studying the conformational changes of the viologen dendrimers with respect to its chemical environment using the spin-labeled macromolecules.

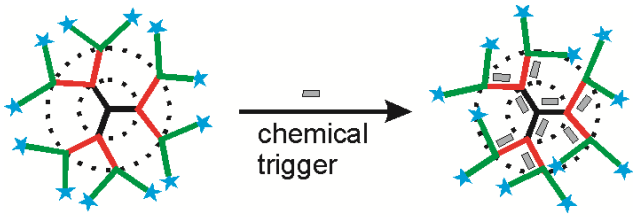

Thus a study on the synthesis of a series of viologen dendrimers (G_0*, G_1* and G_2*) equipped with peripheral N-oxide spin tags is presented in chapter 3. The ESR study was projected in collaboration with Prof. Steinhoff's group.

iv) Our group has reported earlier on a series of dendrimers and oligomers consisting of 4,4′-bipyridinium subunits. It has further been shown that the viologen dendrimers have antiviral properties and that a series of related viologen dendrimers behave as gene-transfecting agents. Typically, such applications rely on the viologen dendrimer's ability to wrap onto large biological structures. We consider their practical use in medicine as questionable because of the inherent toxicity of the viologen monomer, related to its low reduction potential. Cationic nonelectroactive dendrimers based on 4,4′-trimethylenedipyridinium subunits might show less toxicity and better conformational adaptability because of the trimethylene function disrupting the π-resonance and displaying higher flexibility.

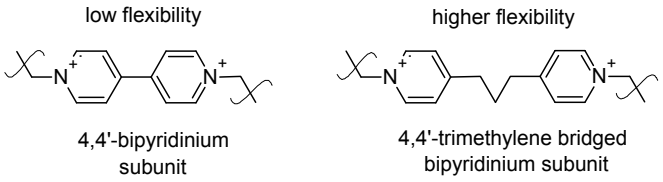

A few years ago K. Yamamoto and co-workers have reported on the sequential complexation of guest molecules (inorganic Lewis acids) by phenylazomethine dendrimers with the imine functionalities acting as Lewis base coordination sites. The authors have shown by UV/vis titration that the guest molecules fill the dendrimer radially stepwise starting with the innermost shell. There is no report on other dendrimer/guest combinations showing

the same stepwise charging mode, and the question is still not solved, if the phenomenon observed by Yamamoto is unique or of general importance.

Shell-wise occupation of dendrimer sites - a general mechanism?

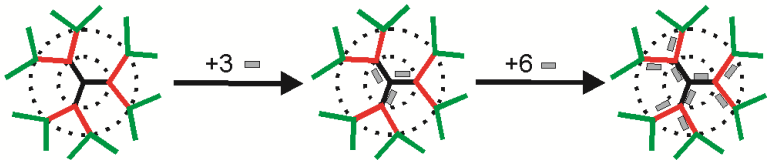

In the fourth chapter of this thesis, I have addressed on the synthesis of a new class of cationic dendrimers based on benzylic trimethylenedipyridinium subunits (flexible and non-electroactive), their characterization as well as their guest-complexing abilities towards the model anti-cancer drug anthraquinone disulfonate. We applied NMR and electrochemical techniques to solve the mechanism of complexation.

v) Is Yamamoto's theory applicable to different combinations of host dendrimers and anionic guests?

Mutual Recognition

between different guests and different host dendrimers

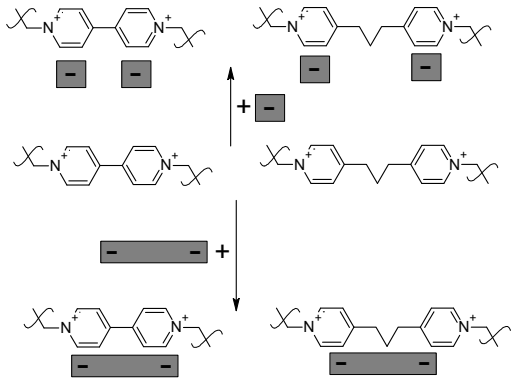

I have addressed this question in the fifth chapter. For this purpose the synthesis of viologen and trimethylenedipyridinium dendrimers carrying 4-*tert*-butylbenzyl at their periphery is discussed. Their complexing property towards mono, di and trianionic guest molecules is remarkable and contributes evidence to a general guest pick-up scenario.

vi) Organic phosphonic acids are excellent candidates for the modification of metal oxide surfaces such as TiO_2, Al_2O_3, and ZrO_2 as the phosphonic acid exhibits strong

coordination to these metal oxides. Synthesis of bifunctional linkers with one end equipped with a phosphonic acid and the other, an orthogonal functionality allows access to the fine tuning of metal oxide surfaces or the tunnels of mesoporous metal oxides. In the sixth chapter, I have presented the synthesis of linear pyridinium and sulfonic acids bearing alkyl phosphonates (bifunctional linkers) for the surface modification of metal oxides. Notably, the mono- and bipyridinium modifiers exhibit a close relationship to the dendrimers described in the other chapters and guest complexation was one of the main aspects behind this synthetic effort.

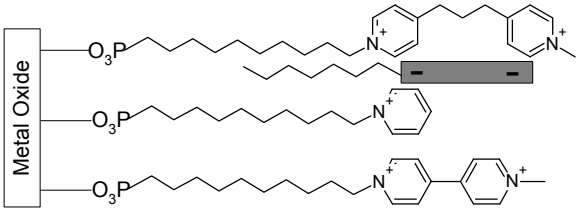

Finally a summary of the thesis is given in the last chapter.

2 Viologen based benzylic dendrimers: Selective synthesis of 3,5-bis(hydroxymethyl)benzyl bromide & conformational analysis of the corresponding viologen dendrimer sub-unit

Tetrahedron Lett. **2010**, *51*, 2188

In the last three decades, a number of methods have been reported concerning the cascade synthesis of dendrimers with trifold core using different branching units.[A] These syntheses require a trifunctional CB_2 or BC_2 type building block as the branching units with B representing a latent functionality and C representing a reactive functionality which reacts with A, where A is available by the activation of B. Depending on the synthesis (divergent or convergent), either CB_2 or BC_2 branching units are required. A representative example for the divergent approach is the synthesis of the propyl amine dendrimer from acrylonitrile (CB_2 type branching unit) with –C=C- representing C and the nitrile function representing B_2 which can be activated to A_2, A representing an amine nitrogen which can undergo double alkylation.[3] A representative example for the convergent approach is the synthesis of the poly(benzyl ether) dendrimer from 3,5-dihydroxybenzyl alcohol (C_2B type branching unit) with B representing the benzylic alcohol that can be transformed into the corresponding bromide (A) and the phenolic OH groups representing C_2.[3] A decade ago, we have introduced the synthesis of viologen dendrimers[10b] via a divergent approach using CB_2 type branching units, the corresponding convergent approach using BC_2 branching units was reported by Balzani et al[38a] (scheme 2-1). The divergent approach of the viologen dendrimers[10b] emanates from the 1,3,5-tris(bromomethyl)benzene core and the step-wise use of CB_2 branching units, where C represents the reactive pyridyl nitrogen and B_2 represents two OH groups which can

[A] This thesis follows JACS Articles style presentation

be transformed into the benzylic bromide (A). The corresponding BC_2 dicationic compound is a potential branching unit for the convergent approach.

a) Divergent approach using CB_2 branching unit

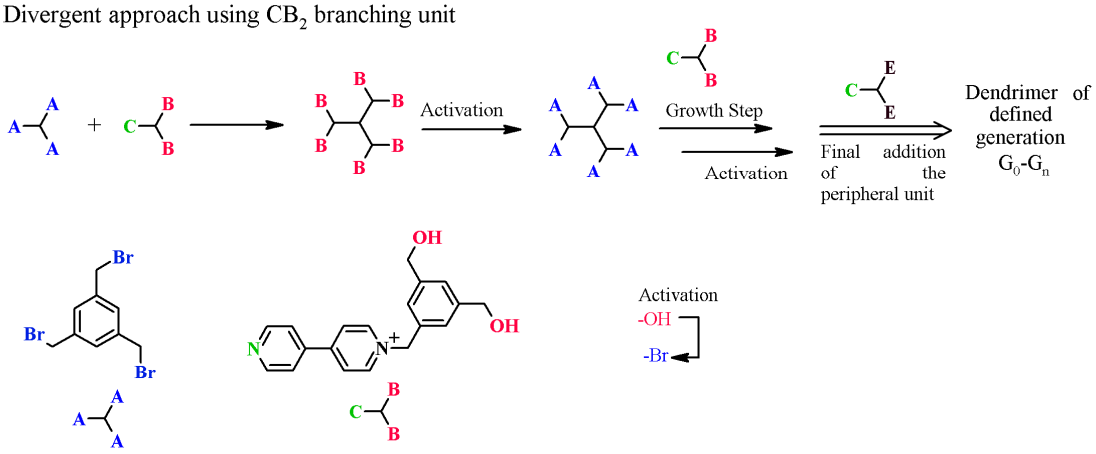

b) Convergent approach using BC_2 branching unit

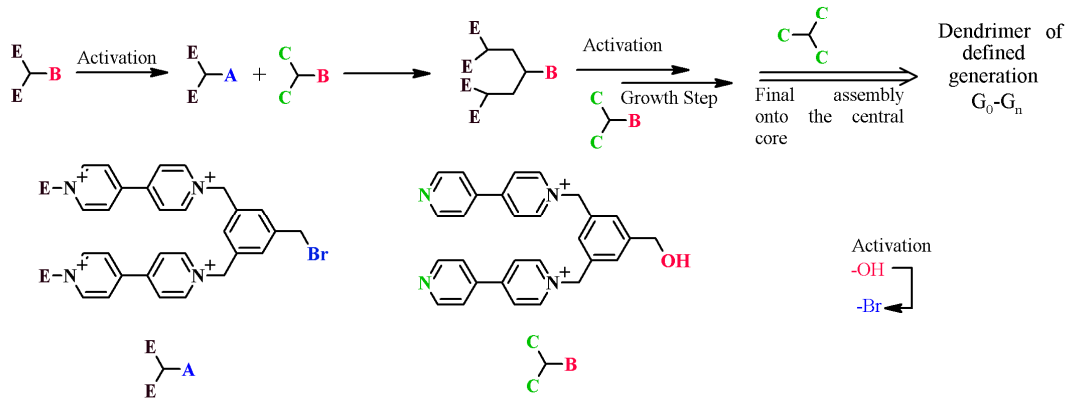

A = active functionality

B = latent functionality

C = active functionality; reaction partner of A

E = peripheral group

Scheme 2-1: Divergent and convergent strategies for benzylic viologen dendrimers

The selective monoalkylation of 4,4´-bipyridine with 1,3,5-tris(bromomethyl)benzene is possible but its further transformation to the corresponding bis(hydroxymethyl)-4-(pyridine-4yl)pyridinium salt cannot be achieved because under the typical basic condition necessary for this reaction, the bipyridinium is irreversibly attacked by OH^-. Selective double substitution of 1,3,5-tris(bromomethyl)benzene by two bipyridines is not possible as the product is prone to polymerize. Thus both "viologen" branching units CB_2 and BC_2 require

the specific synthesis of the corresponding benzylic bromides **1c** and **1d**, respectively. Procedures have been reported but the yields are not satisfactory.[41]

2.1 Results and Discussion

Possible routes for the synthesis of **1c** are presented in Scheme 2-2. These include, (I) the hydrolysis approach using 1,3,5-tris(bromomethyl)benzene **1e**, (II) the Appel method, (III) the Frechet type synthesis of **2d** followed by reduction and (IV) the bromination of diethyl-5-methylisophthalate.

(I) Hydrolysis of 1,3,5-tris(bromomethyl)benzene using different equivalents of strong or weak bases was not successful as the reaction yielded either mixture of ethers along with hydroxyl derivatives or completely hydrolyzed products, as reported for other benzylic bromide derivatives using different basic conditions.[29,42] (II) Since our first report on viologen dendrimer synthesis,[43] we use the Appel method to synthesize **1c** and **1d**. The synthesis starts with the conversion of trimesic acid to trimethyl **1a** or triethyl ester **2a** (90% in both cases), followed by the reduction of the triester **1a** with $LiAlH_4$ to yield the triol **(1b)** in 76% yield. The triol is then brominated using 1 equiv of Appel reagent to yield a mixture of the products **1c**, **1d** and **1e** which must be separated by tedious column chromatography [**1c** (36%) and **1d** (12%)]. There are two other methods tailored for higher yields of **1d**[44] (a well known linker possessing two reactive and a latent site) by Stoddart et al[41b] and by Diez-Barra et al[41a] where the former used 3 equiv of the Appel reagent in THF and the latter used 1.1 equiv of Appel reagent in CH_3CN with 43% and 52% yields, respectively, after column chromatography. No reports are available on Appel conditions favoring high yields of **1c**. The limitation of Appel method is obvious: the reaction is not specific and the necessity of separation using column chromatography which limits the work up to few hundred milligram scale. In order to overcome these problems and remembering that DIBAL-H is known to selectively reduce the

ester functionality in the presence of primary or benzylic halides,[45] we propose route **IV** involving 5-bromomethyl diethylisophthalate[46] as the key intermediate. Its reduction with 1M DIBAL-H in DCM gave **1c** in ca. 70% without the need of any column separation. We carried out the same reduction using $LiAlH_4$ at 0°C as it is reported that $LiAlH_4$ selectively reduces

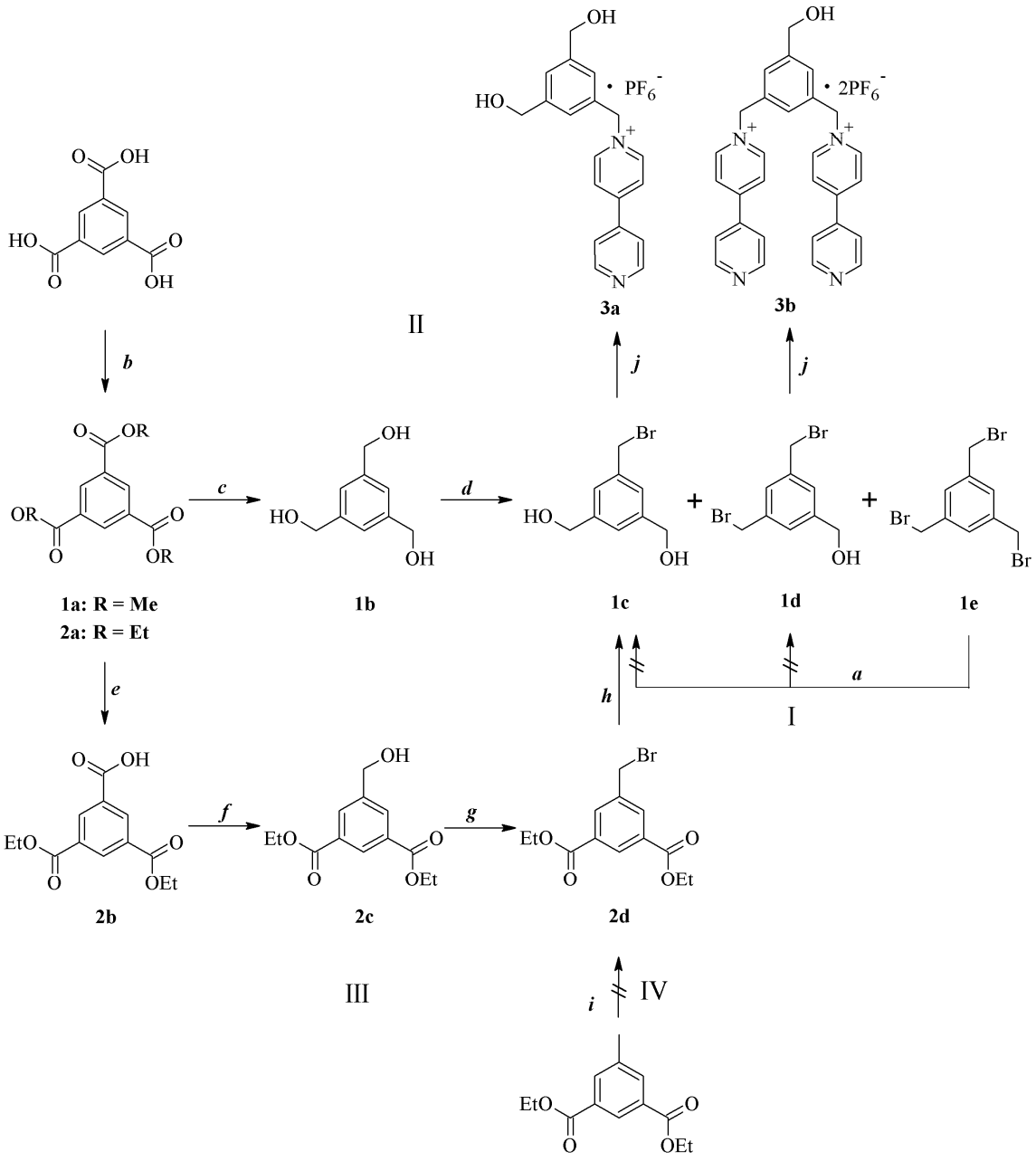

Scheme 2-2: Synthesis of hydroxymethyl- and bis(hydroxymethyl)benzylic bromides – the precursors of CB_2 and BC_2 viologen branching units; Reagents and conditions: (a) Hydrolysis under different basic conditions, (b) ROH, H_2SO_4, reflux, 24h, (c) LAH, THF, reflux, 24h, (d) CBr_4 / PPh_3, THF, 0°C-RT, 3h, (e) KOH, EtOH-THF, reflux, 24h, (f) 1M BH_3-THF, 0°C-RT, 6h, (g) 5.6M HBr-HOAc, RT, 36h, (h) 1M DIBAL-H / DCM, 0°C-RT, 6h, (i) NBS, Bz_2O_2, CCl_4, reflux, (j) (1) 4,4´-bipyridine, CH_3CN, 80°C, 24h, (2) 3M NH_4PF_6 / H_2O

ester functionality at lower temperature without reducing alkyl halides,[47] however this reaction doesn't give reproducible results. Path **III** follows a route earlier described by Frechet[46] (**2a - 2d)**, we followed the same route with some modifications. The method is based on the selective hydrolysis of 1,3,5-triethyltrimesic ester **2a** to 5-carboxy diethylisophthalate **2b** in 75% yield. The monocarboxy diester is then reduced to 5-hydroxymethyl-diethylisophthalate **2c** in 90% yield using 1M BH_3-THF complex (lit.[46] 78% using 1M BH_3-$(CH_3)_2S$). Bromination of the hydroxyl precursor using 5.6M HBr in HOAc gave 5-(bromomethyl)diethylisophthalate **2d** in 95% (lit.[46] 90%, PBr_3 as brominating agent) which is then reduced to 3,5-bis(hydroxymethyl)benzyl bromide **1c** 70% using 1M DIBAL-H in DCM following the reported procedure.[48] Notably, all these steps lead to the desired intermediates in good yield using simple recrystallization steps without column purifications. (Detailed synthetic procedure is given in the Experimental section). (IV) The intermediate **2d** can also be synthesized by brominating 5-methyldimethylisophthalate using NBS as shown in route IV but this reaction proceeds with low yield because of the electron-withdrawing effects of the two ester groups.[3]

The mono- or dialkylation of 4,4´-bipyridine is highly influenced by the solubility of the products in the solvent media. Dialkylation can be carried out only in a solvent where the monoalkylated product is partially soluble. Hence the dialkylation can be completely prevented by choosing a solvent in which the starting materials are soluble but not the monoalkylated product. In our case, we suppress the double alkylation by adding one equivalent of **1c** slowly to five equivalent excess of 4,4´-bipyridine in CH_3CN. The precipitated product is then filtered, washed with CH_3CN, dissolved in water and precipitated as hexafluorophosphate salt. The pale yellow powder thus obtained is again dissolved in water, heated to 80°C and then cooled to yield pale yellow crystals. (Note: the pale yellow crystals became light green upon exposure to air). **3b** is synthesized using the same procedure,

i.e. one equivalent of **1d** is added slowly to ten equivalents of 4,4´-bipyridine in CH_3CN and the resulting product is precipitated as hexafluorophosphate. The detailed synthetic procedures, CV and UV-vis characterizations are given in Experimental section.

2.2 X-Ray Crystallography, cyclic voltammetry and Modeling

Viologen dendrimers[10c,38a,43] and dendrons[43] have been prepared extensively from 4,4´-bipyridine and **3a** using sequential substitution and activation reactions discussed in the prior paragraph. The geometry of the resulting dendritic structure has a large impact on the pimerization of viologen subunits, i.e. their dependence on the space between viologen subunits,[43] the diffusion coefficient of the dendrimers, which in turn depends on the hydrodynamic radius,[10c,43] their internal voids and their ability to pickup large counter ions.[38a,49]

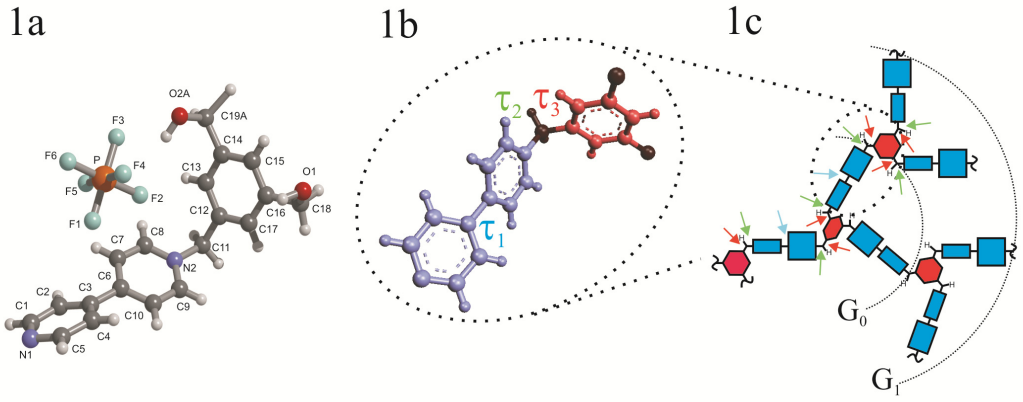

Figure 2-1: 1a) X-ray structure of 3a **with torsions τ_1 (37.8° (C_4-C_3-C_6-C_{10})), τ_2 (87.3° (C_8-N_2-C_{11}-C_{12})), and τ_3 (-80.8° (N_2-C_{11}-C_{12}-C_{13})); 1b) dendrimer subunit (based on** 3a **X-ray conformation); 1c) section of dendrimer consisting of** 3a **subunits**

A closer look at the dendrimer structure 1c in Fig. 2-1 reveals that the overall conformational space available for the branches is given by only three torsional angles, i.e. τ_1, τ_2 and τ_3, assuming that all the bending angles do not deviate much from their equilibrium value. The three torsional angles are located between the two pyridine moieties (τ_1), the methylene H and the pyridine (τ_2) and between the same methylene and the phenyl group (τ_3)

(1b in Fig. 2-1). Obviously, the salt **3a** (1a in Fig. 2-1) exhibits the same set of angles. We were able to grow crystals of **3a** and to resolve its structure by X-ray analysis[B] (Fig. 2-1 1a). The X-ray structure reveals that there are two molecules in a triclinic unit cell and the existence of an intermolecular hydrogen bond between O(1A)-H(1A) and N(1). The torsional angles found in **3a** can be used as a reasonable starting point for the discussion of the dendrimer conformation. The torsional angles τ_1 in other bipyridinium systems cover the range from 20 to 50^o in case of mono- and dialkylated viologens[40,41b,50] with no large influence of the counter ion. However, the oxidation state is of importance, thus a diphenyl viologen shows dihedral angle (τ_1) of 37^o and 1^o for the dicationic and the radical cationic state, respectively. The other two torsions τ_2 and τ_3 have been reported for dibenzyl viologen by Inoue et al[51] and by Garcia et al.[52] The former found three different τ_3 and τ_2 within a single crystallographic cell, the latter found τ_3 = -88.2° and τ_2 = 168.8°. These findings indicate no torsional angle preference, i.e. a low torsional energy profile for τ_1, τ_2 and τ_3 planes.

Semi-empirical PM3 calculations were performed using Arguslab 4.0.1[C] and Hyperchem 8.0.6.[D] When the X-ray structure is used as a starting point for geometry optimization, a local minimum is found with only minor deviation from the solid state structure (except for a lateral shift of PF_6^-), indicating that PM3 is delivering reasonable values. If the PF_6^- counter ion is omitted in the same calculation, the lowest energy torsional angles τ_{1-3} doesn't change, indicating that the counter ion is not governing the torsional angles, rather the organic structure governs the position of PF_6^-. The torsional energy barriers

[B] CCDC-756509 (for 3a) contain the supplementary crystallographic data for this paper. These data can be obtained free of charge from The Cambridge Crystallographic Data Centre via www.ccdc.cam.ac.uk/data_request/cif

[C] ArgusLab 4.0.1 Mark A. Thompson Planaria Software LLC`, Seattle`, WA http://www.arguslab.com

[D] HyperChem(TM)`, Hypercube`, Inc.`, 1115 NW 4th Street`, Gainesville`, Florida 32601`, USA

related to a 360° rotation around τ_1, τ_2, and τ_3 have been judged from single point energy calculations at 10° increments without further geometry optimization (see Experimental Section). For a 360° rotation around τ_1 (with the τ_2 and τ_3 values fixed at their X-ray values) a fourfold barrier with a height below 1 kcal/mol was found, with one of the minima identical to the X-ray value (37.9°). PM3-based Wiberg atom-atom bond order calculations[53] reveal a bond order of only 1.02 between C3 and C6 for the minimum conformation in agreement with the observed low-energy torsional profile.

Rotation along τ_2 (with the τ_1 and τ_3 values fixed at their X-ray values) shows again a low-energy barrier (2-3 kcal/mol) but two-fold, as expected for the methylene-pyridinium interaction. Finally, for the rotation around τ_3 showed a low-energy barrier but twice as that of τ_2 (5-6 kcal/mol) and two fold, as expected for the methylene-phenyl interaction.

^{1}H-NMR spectra of the viologen dendrimers with the **3a** sub-unit shows high symmetry related to faster inter-conversion conformational changes typical for flexible structures.[43] Furthermore, cyclic voltammetry studies on **3a** and **3b** do not show slow electron transfer rates, which is expected for redox couples with large activation barriers due to restricted rotation.

In summary, the conformational analysis of **3a**, based on X-ray, cyclic voltammetry and NMR data, representing a structural sub-unit of benzylic viologen dendrimers, reveals high flexibility with respect to the three torsional angles that play a role for the dendrimers shape.

2.3 Conclusions

The synthesis of viologen dendrimers with 1,3,5-tri(methyl) branching units requires facile access to the CB_2 type synthon, 1-[3,5-bis(hydroxymethyl)benzyl]-4-(pyridin-4-yl)pyridinium hexafluorophosphate (Scheme 2-1), which is in turn synthesized from **1c** and 4,4´-bipyridine (Scheme 2-2). So far the synthesis of **1c** followed route II (Scheme 2-2)

involving tedious chromatographic separation. The synthetic route III in Scheme 2-2, explored in this work, allows the production of **1c** without the need of chromatography in higher yields. The X-ray analysis of 1-[3,5-bis(hydroxymethyl)benzyl]-4-(pyridin-4-yl)pyridinium hexafluorophosphate combined with PM3 modeling studies gives a first time access to the sound estimate of the viologen dendrimer conformation.

2.4 Experimental Section

2.4.1 General Methods

All starting materials were purchased from Aldrich except $LiAlH_4$ (Merck) and 1M BH_3-THF (Alfa Aesar), and were used without further purification unless otherwise stated. All the solvents used were of analytical grade and dried if necessary according to standard procedures before use. Thin layer chromatography (TLC) was carried on aluminium sheets precoated with silica gel (0.2 mm) with fluorescent indicator (ALUGRAM SIL G/UV). Column chromatography was carried out using silica gel 63-200 μm (Baker). Melting points were measured in an Apotec melting point apparatus and the values were uncorrected. ^{1}H and ^{13}C NMR spectra were recorded on a Bruker-Avance-spectrometer at 250 and 63 MHz, respectively, using the solvent signal as an internal standard. Elemental analyses were performed on Elementar Vario microcube instrument.

2.4.2 Detailed Synthetic Procedures

The intermediates **1a, 1b, 1c, 2a, 2b, 2c, 2d, 2e, 3a** and **3b** are known compounds. **1a-c** and **3a** have been reported by Heinen, **2a-c** by different groups. In order to guarantee the quality, their spectra and elemental analysis are reported here, modified procedures are given in full detail. Compound 3b was independently prepared in our institute by Reschke.

2.4.2.1 Synthesis of bromo/hydroxyl benzylic precursors

Trimethyl-1,3,5-benzenetricarboxylate **(1a)**

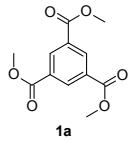

1a

Prepared according to the reported procedure.[54] m.p. 144°C (lit. 144-144.5°C), ^{1}H-NMR (250 MHz, $CDCl_3$, 25°C): δ = 8.87 (s, 3 H), 4.00 (s, 9 H); ^{13}C-NMR (63 MHz, $CDCl_3$, 25°C): δ = 165.3, 134.5, 131.1, 52.6.

1,3,5-Tris(hydroxymethyl)benzene **(1b):**

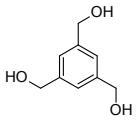

1b

Prepared according to the reported procedure.[10a] m.p. 77°C (lit.[41a] 74-76°C), ^{1}H-NMR (250 MHz, DMSO-d_6, 25°C): δ = 7.13 (s, 3 H), 5.13 (t, J(H,H) = 5.6 Hz, 3 H), 4.48 (d, J(H,H) = 5.6 Hz, 6 H); ^{13}C-NMR (63 MHz, DMSO-d_6, 25°C): δ = 142.9, 123.8, 63.9; Anal. Calc. for $C_9H_{12}O_3$: C, 64.27; H, 7.19. Found: C, 64.26; H, 7.08.

3,5-bis(hydroxymethyl)benzyl bromide **(1c)*:***

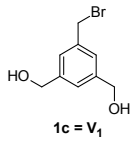

1c = V_1

Prepared according to the reported procedure.[10a] m.p. 116-117°C, ^{1}H-NMR (250 MHz, CD_3CN, 25°C): δ = 7.32 (s, 3 H), 4.70 (s, 2 H), 4.61 (d, 4 H), 3.25 (t, 2 H); ^{13}C-NMR (63 MHz, CD_3CN, 25°C): δ = 142.9, 137.9, 125.6, 124.9, 63.4, 46.3; Anal. Calc. for $C_9H_{11}BrO_2$: C, 46.78; H, 4.80. Found: C, 46.99; H, 4.72.

Triethylbenzene-1,3,5-tricarboxylate **(2a)**:

Prepared according to the reported procedure.[55] m.p. 136°C (lit.[55] 132-136°C), ^{1}H-NMR (250 MHz, DMSO-d_6, 25°C): δ = 8.66 (s, 3 H), 4.40 (q, J(H,H) = 7.2 Hz, 6 H), 1.37 (t,

J(H,H) = 7.2 Hz, 9 H). ^{13}C-NMR (63 MHz, DMSO-d_6, 25°C): δ = 165.0, 133.51, 131.56, 62.01, 14.53; Anal. Calc. for $C_{15}H_{18}O_6$: C, 61.21; H, 6.16. Found: C, 61.21; H, 6.14.

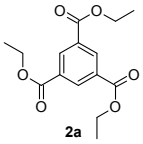

2a

***Diethyl-1,3,5-benzenetricarboxylate* (2b):**

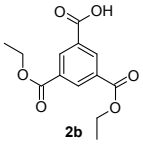

2b

A reported procedure has been followed and the ^{1}H-NMR, m.p. and the elemental analysis were found to be the same.[46]

***Diethyl-5-(hydroxymethyl)isophthalate* (2c)[46]:**

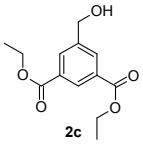

2c

Reported procedure was followed using BH_3-THF complex instead of reported BH_3-SMe_2[46] m.p. 82-83°C (lit.[46] 82-84°C); ^{1}H-NMR (250 MHz, DMSO-d_6, 25°C): δ = 8.62 (s, 1 H), 8.25 (d, 2 H), 4.84 (d, 2 H), 4.44 (q, 4 H), 1.44 (t, 6 H); ^{13}C-NMR (63 MHz, DMSO-d_6, 25°C): δ = 165.49, 144.82, 131.58, 130.79, 128.31, 62.32, 61.67, 14.61; Anal. Calc. for $C_{13}H_{16}O_5$: C, 61.89; H, 6.39. Found: C, 61.96; H, 6.27.

***Diethyl-5-(bromomethyl)isophthalate* (2d):**

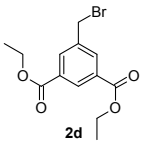

2d

Diethyl-5-(hydroxymethyl)isophthalate (3 g, 11.8 mmol) and 90 mL 5.6M HBr in HOAc were refluxed at room temperature under dark and dry condition. After 2 d, the mixture was poured into 300 mL cold water, filtered, washed with excess water until aqueous solution becomes neutral. The pale white solid was then dried, recrystallized from EtOH to give brilliant plate crystals. (3.5 g, 95%, (lit.[46] 90%)): m.p. 112-113°C (lit. 112-113°C); ^{1}H-NMR

(250 MHz, DMSO-d_6, 25°C): δ = 8.64 (s, 1 H), 8.26 (d, 2 H), 4.58 (s, 2 H), 4.44 (q, 4 H), 1.45 (t, 6 H); ^{13}C-NMR (63 MHz, DMSO-d_6, 25°C): δ = 164.84, 140.47, 134.52, 132.00, 131.47, 62.08, 32.92, 14.59; Anal. Calc. for $C_{13}H_{15}BrO_4$: C, 49.54; H, 4.80. Found: C, 49.48; H, 4.89.

3,5-bis(hydroxymethyl)benzyl bromide **(2e):**

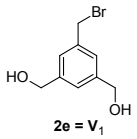

2e = V_1

Diethyl-5-(bromomethyl)isophthalate (4 g, 12.6 mmol, 1 equiv) was dissolved in 20 mL dichloromethane and the mixture was cooled to 0°C under Argon. To this solution, 82.4 mL of 1M DIBAL-H solution in dichloromethane was added dropwise over 1 h. The mixture was brought slowly to room temperature slowly and stirred for another 5 h, cooled to 0°C, 1M HCl was carefully added until the effervescence stopped. The organic layer was evaporated under reduced pressure and the white solid in aqueous layer was extracted using EtOAc. The organic layer was then washed with water, dried over anhydrous Na_2SO_4, filtered and concentrated to yield **2e** as brilliant white crystals. The NMR data and the elemental analysis results were found to be the same as **1c**.

2.4.2.2 Synthesis of viologen dendrons 3a and 3b

1-[3,5-bis(hydroxymethyl)benzyl]-4-(pyridin-4yl)pyridinium hexafluorophosphate **(3a):**

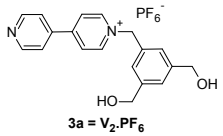

3a = V_2.PF_6

4,4′-Bipyridine (1.69 g, 10.8 mmol) was dissolved in 30 mL CH_3CN, heated to 80°C. To this stirred solution 3,5-bis(hydroxymethyl)benzyl bromide (0.5 g, 2.1 mmol) dissolved in CH_3CN (20 mL) was added slowly over 6 h. The solution was stirred for another 10 h, cooled to RT and the solvent was removed under reduced pressure. The residue was partitioned between water (100 mL) and dichloromethane (100 mL), washed with dichloromethane to

remove excess 4,4′-bipyridine. The aqueous solution was then concentrated to 50 mL, heated to 50°C, 3 mL of 3 M NH_4PF_6 solution was added. The solution turned hazy which was then immediately refrigerated for 2 h to yield **3a** as pale yellow crystals, 0.89 g (91%) of pale yellow crystals (upon aging the color changes to pale green): m.p. 190-192°C. ^{1}H-NMR (250 MHz, CD_3CN, 25°C): δ = 8.88-8.86 (m, 4 H), 8.34 (d, *J*(H,H) = 6.5 Hz, 2 H), 7.81 (d, *J*(H,H) = 6.0 Hz, 2 H), 7.44 (s, 1 H), 7.38 (s, 2 H), 5.78 (s, 2 H), 4.64 (s, 4 H); ^{13}C-NMR (63 MHz, CD_3CN, 25°C): δ = 154.5, 151.1, 144.9, 143.8, 141.1, 132.8, 126.2, 126.1, 125.8, 121.8, 64.2, 63.1; Anal. Calc. for $C_{19}H_{19}F_6N_2O_2P$: C, 50.45; H, 4.23; N, 6.19. Found: C, 50.21; H, 4.36; N, 6.22.

***5-(hydroxymethyl)-1,3-bis[4-(pyridine-4yl)pyridinium]benzene bis(hexafluorophosphate)* (3b):**

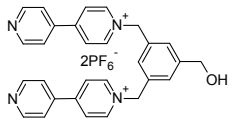

3b

4,4′-Bipyridine (2.65 g, 17 mmol, 10 equiv) was dissolved in 30 mL CH_3CN. The solution was heated to 80°C. To this solution, [3,5-bis(bromomethyl)benzene-1-yl] methanol (0.5 g, 1.7 mmol, 1 equiv) dissolved in CH_3CN (20 mL) was added over 8 h and stirred for another 14 h. The solution was cooled to RT, the solvent was removed under reduced pressure, and the residue was partitioned between water (100 mL) and dichloromethane (100 mL). The aqueous layer was washed with dichloromethane to remove excess 4,4′-bipyridine. The aqueous solution was then concentrated, precipitated by adding 4 mL of 3 M NH_4PF_6. The pale yellow precipitate was filtered, washed with water and dried to yield **3b** 0.9 g (71%); m.p. 202-204°C; ^{1}H-NMR (250 MHz, CD_3CN, 25°C): δ = 8.86 (m, 8 H), 8.36 (d, *J*(H,H) = 6.5 Hz, 4 H), 7.81 (d, *J*(H,H) = 5.5 Hz, 4 H), 7.57 (s, 2 H), 7.42 (s, 1 H), 5.79 (s, 4 H), 4.66 (s, 2 H); ^{13}C-NMR (63 MHz, CD_3CN, 25°C): δ = 154.7, 151.2, 145.1, 141.1, 134.1, 128.6, 127.5,

121.8, 63.6, 62.6; Anal. Calc. for $C_{29}H_{26}F_{12}N_4OP_2.H_2O$: C, 46.16; H, 3.74; N, 7.42. Found: C, 46.37; H, 3.78; N, 7.43. [Note: This compound was independently synthesized by Tim Reschke and reported in his Bachelor Thesis,[56], i.e., in the same year as this work was submitted to Eur.J.Org.chem (compound synthesized in March 2008)]

2.4.3 Cyclic Voltammetry and Uv-vis spectra of 3a and 3b

DMSO (puriss.) and TBA·PF_6 (puriss, electrochemical grade) were used as purchased from Fluka and used for cyclic voltammetry (CV). CVs were measured under Ar with the potentiostat PGSTAT 20 from AUTOLAB controlled by a PC running under GPES for Windows, Version 4.2 (ECO Chemie 1995); a glassy carbon electrode (GCE) from Metrohm (6.0804.010) with an active electrode surface of 0.07 cm^2 is used for CV. The electrode surface was polished with Al_2O_3 prior to each scan. The reference electrode was Ag / AgCl / KCl(sat.), separated by a salt bridge (DMSO + 0.1 M TBA.PF_6) from the cell; the counter electrode was a Pt-wire.

The cyclic voltammogram of **3a** and **3b** shows a reversible one-electron reduction wave with E_0' = -0.89V and -0.87V, respectively (Fig. 2-2), in contrast to N,N´-dialkyl bipyridinium salts which undergo two consecutive reductions in the range of -0.3V and -0.78V because of their larger π-electron conjugation. For the same concentration, compound **3b** shows a larger peak current than **3a,** i.e., 27 µA and 17 µA, respectively.

The peak current ratio can be analyzed according to[57]:

$$i_n(\theta) = n i_l(\theta)(D_p/D_m)^p = 27 = 2 * 17\,(D_p / D_m)^{1/2}$$

where

$i_n(\theta)$: current of the multi-redox center at potential θ

n : number of centers in the multi-redox system

$i_l(\theta)$: current of the one-redox system at potential θ

D_p, D_m : Diffusion coefficient of the multi-electron and the one-electron redox system, respectively

p = ½ for cyclic voltammetry

yielding: $(D_p / D_m)^{1/2} = 0.79$ and $D_p / D_m = 0.63$. This ratio is reasonable when comparing the corresponding radii ratio according to the Stokes-Einstein equation

$$D = kT / 6 \pi r \eta \text{ , yielding}$$

$$D_p / D_m = r_m / r_p$$

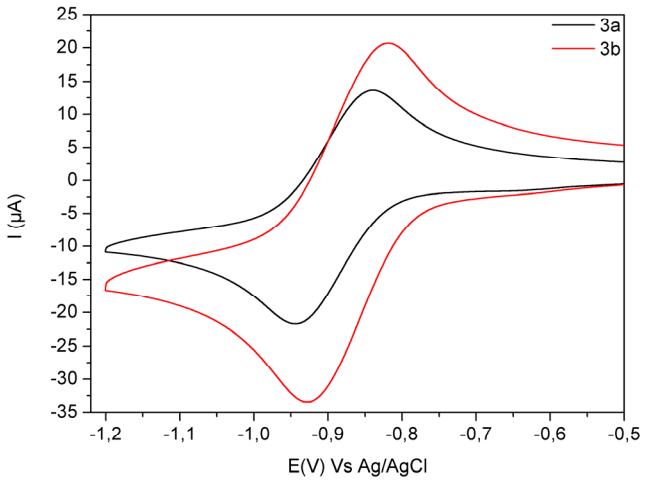

Figure 2-2: Cyclic voltammograms of 3a and 3b (c = 2 mM) in DMSO/TBA.PF_6 (0.1 M) on glassy carbon (A = 0.07cm^2) at V = 0.1 V/s, RT

The difference $E^{0\prime}$(**3b**) - $E^{0\prime}$(**3a**) = 20 mV may point to a better electrostatic stabilization of the one electron reduced species of **3b** as compared to **3a**.

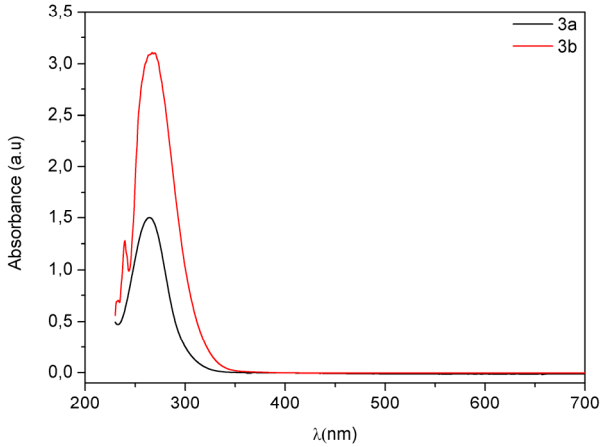

Figure 2-3: UV-Vis spectrum of 3a and 3b c = 50 µM in CH_3CN

The UV-Vis spectra of **3a** and **3b** showed absorption at (λ_{max}) 254 nm exhibiting extinction coefficients of 1.5 x 10^5 and 3.15 x 10^5, respectively (Fig. 2-3). It was not possible to get reliable spectra for the corresponding radicals as these species were not stable on the time scale of bulk electrolysis.

2.4.4 X-Ray Crystallography and Molecular Modeling

According to NMR spectroscopy which shows highly symmetric structures at RT, viologen dendrimers with trismethyl benzene branching units are quite flexible structures, with rapidly changing torsion angles. Obviously, the benzylic bending angle and the torsional angles between the benzene and the pyridinium unit as well as between the two pyridine moieties determine the structure or structural flexibility of the corresponding viologen dendrimers. Crystal data of viologens are available for their p-toluene sulfonate or tetrafluoroborate salts. In a few cases, crystallographic data of viologens with PF_6^- counter ion are reported, i.e., mono- and di-functionalized catenanes,[40,41b,50e] pyridinophane,[50c] PF_6^- .pyridine adduct of di-phenyl viologen[50b] and tris(triethylbenzyl)viologen core incorporating tetrapodal pyridinium units.[50a] Most of them are reported as adducts where the moieties can influence eachother's structure mutually. On the other hand, there are many reports on the crystal structure of the mono-alkylated bipyridine i.e., 4-(pyridin-4-yl)pyridinium salts of many metal complexes where the two pyridyl rings are found to be coplanar[50d,50f] whereas the crystal studies on some of the di-alkylated bipyridinium salts shows that the pyridyl rings lie in a different plane.[50b] Bipyridinium or 4-(pyridin-4-yl)pyridinium are extensively studied as their hexafluorophosphate salts as they are good in terms of stability, suitable for electrochemical studies in non-aqueous media, and their good solubility in wide range of organic solvents. Viologens as hexafluorophosphate salts are known to the least extent as crystals.

There are hundreds of published X-ray crystal structures containing 1,1´-dialkyl viologen dications, most commonly as methyl viologen salts or as dialkyl viologens that are part of a larger supramolecular system. Surprisingly, in the majority of the dications the two aromatic rings appear coplanar. It is possible that in many cases the apparent coplanarity of the rings is due to a dynamic solid-state structure in which the rings are twisting relative to each other, with two energy minima on either side of the coplanar structure, resulting in an averaged X-ray structure that appears to have coplanar rings.[50b] In the case of dendrimers, due to steric hindrance, these two pyridyl rings lie in different planes to avoid the steric interactions whereas in other cases it depends on the substituent effects as shown by Holger et al in the pyridine-bridged phanes[50c] where the torsion angle varies between 31° to 54° depending on the linker group. The X-ray structure of **3a** shows that the dihedral angle (Torsion angle) between the two pyridyl rings C(4) –C(3) –C(6) –C(10) is 37.9° which shows that the two pyridyl rings is torted. The torsion angles for different bipyridinium systems are shown in the Table 2-1.

Table 2-1: Representative dihedral angles for different 4,4´-bipyridinium analogues

	Atoms	angle (deg)
4-(pyridin-4-yl)pyridinium and metal complex as counter anion[50d]	C(4)-C(3)-C(6)-C(10)	50
3a	C(4)-C(3)-C(6)-C(10)	37.9
Diphenyl Viologen[50b]	C(4)-C(3)-C(6)-C(10)	37.7
Diphenyl Viologen radical cation[50b]	C(4)-C(3)-C(6)-C(10)	1.0

The angle between the pyridyl ring and the benzene ring at the benzylic position N(2) –C(11)–C(12) is 110.81 which is in close agreement with the similar bipyridinium derivatives reported[50c] and the distance between the pyridyl nitrogen N(1) and the oxygen are found to be N(1) –O(2A) = 12.08 Å and N(1) –O(1) = 11.55 Å which are in close agreement with the molecular modeling values (PM3 calculations). PM3 calculation[58] using Arguslab 4.0.1 and

Hyperchem 8.0.6 programmes at different torsion angles using single point computation showed that there is a negligible energy difference when the angle is varied between 0° - 360° in a step of 10° and we observe 4 minimas and 4 maximas from 0-360° with an interval of 45° which is an evidence for the mixed double bond and single bond characters between C(3)-C(6) i.e. between two pyridyl rings. Further Wiberg atom-atom bond order (PM3) calculations[53] using Argus lab programme showed that the bond order between C(3)-C(6) to be 1.02 suggesting mainly the single bond character between C(3)-C(6) of the two pyridyl rings but the energy profile obtained shows that there is a compensation between the single and double bond characters and the energy profile diagrams were briefly discussed in the part below the X-ray table (Table 2-2).

2.4.4.1 Crystal structure of 3a

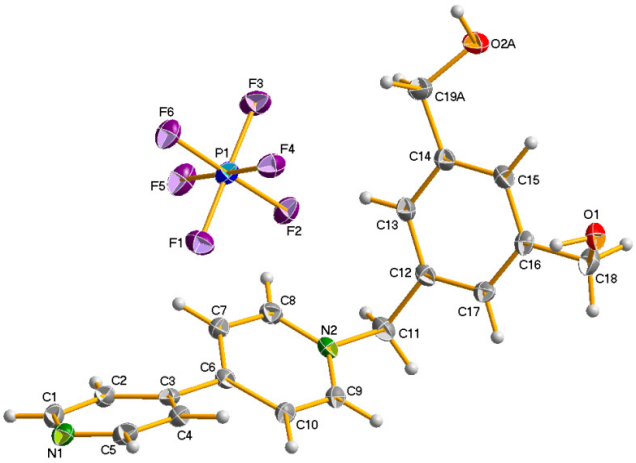

Figure 2-4: Crystal structure of 3a

Table 2-2: Crystal data of 3a

Crystal data

Empirical formula	$C_{19}H_{19}F_6N_2O_2P$
Formula weight	452.33
Temperature	100(2) K
Wavelength	0.71073 Å
Crystal system, space group	Triclinic, P-1

Unit cell dimensions	a=9.3591(3) Å α=81.646(2)°
	b=9.9891(3) Å β=83.754(2)°
	c=10.8912(4) Å γ=71.520(1)°
Volume	953.32(5) $Å^3$
Z, Calculated density	2, 1.576 Mg/m^3
Absorption coefficient	0.221 mm^{-1}
F(000)	464

2.4.4.2 Molecular Modeling

Semi-empirical PM3 calculations were performed using Arguslab 4.0.1 and Hyperchem 8.0.6.[58] When the X-ray structure is used as a starting point for geometry optimization, a local minimum is found with only minor deviation from the solid state structure (except for a lateral shift of PF_6^-), indicating that PM3 is delivering reasonable values (Fig. 2-6A). If the PF_6^- counter ion is omitted in the calculation, the lowest energy torsional angles τ_{1-3} doesn't change, indicating that the counter ion is not governing the torsional angles, but rather that the organic structure is governing the positioning of PF_6^-.

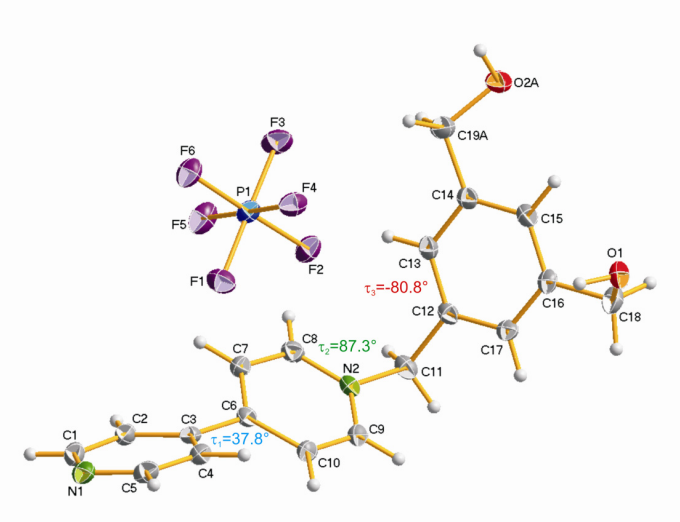

Figure 2-5: Crystal structure of 3a with τ_{1-3} indicated according to x-ray definition τ_1 C(4)-C(3)-C(6)-C(10), τ_2 C(8)-N(2)-C(11)-C(12) and τ_3 N(2)-C(11)-C(12)-C(13)

The torsional energy barriers related to a 360° rotation around τ_1, τ_2, and τ_3 can be judged from single point energy calculations at 10° increments without doing geometry

optimization. The results of such calculations (PM3 in Hyperchem) are presented in Fig. 2-7 and 2-8. For a rotation around τ_1 the values of τ_2 and τ_3 were fixed at the X-ray structure values (Fig. 2-7), and the same was the case for rotations around τ_2 or τ_3, with fixed τ_1 and τ_3, and fixed τ_1 and τ_2, respectively (Fig. 2-8).

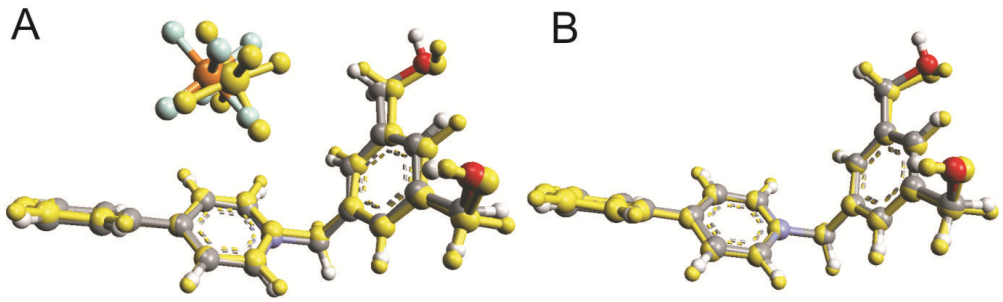

Figure 2-6: X-ray structure (grey=C, blue=N, light blue=F, orange=P, red=O, white=H) and overlaid PM3-optimized structures (yellow) A in presence and B without PF_6^- counter ion.

Rotation along τ_1:

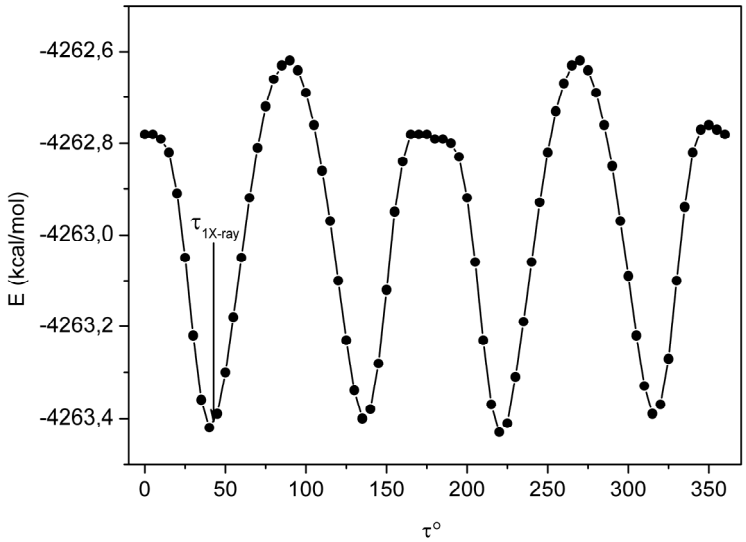

Figure 2-7: Energy changes with respect to the rotation along the C(4)-C(3)-C(6)-C(10) dihedral plane (τ_1), the black arrow indicates the observed x-ray value

The rotation along the dihedral axis C(4)-C(3)-C(6)-C(10) showed negligible energy difference i.e., the difference in energy between the maxima and minima is 0.8 kcal/mol

suggesting the free rotation along C(3)-C(6). The observed X-ray conformation (black arrow) at (τ_1) 37.8° (Fig. 2-7) corresponds to one of the minimal energy situations in the energy profile. This result is also reflected by the Wiberg-bond order calculation showing 1.02 for the C(3) - C(6) bond.

Rotation along τ_2 and τ_3:

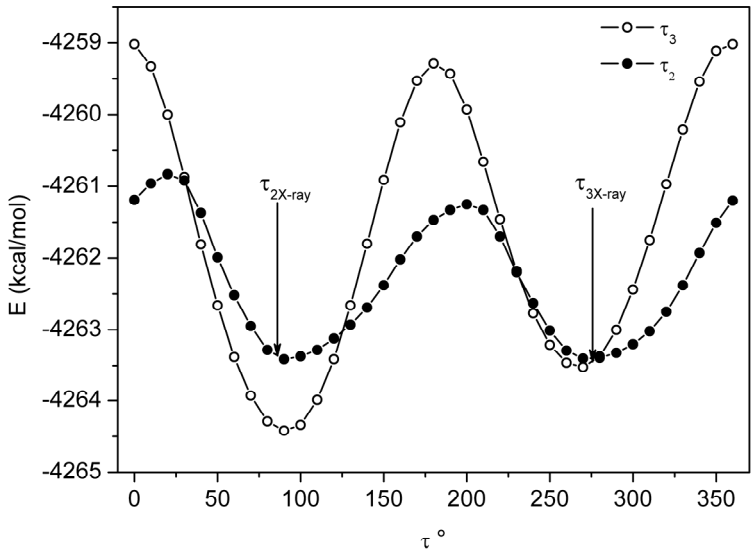

Figure 2-8: Energy changes with respect to the rotation along the C(8)-N(2)-C(11)-C(12) (τ_2) and N(2)-C(11)-C(12)-C(13) (τ_3) dihedral planes, the black arrow indicates the observed X-ray value

The rotation along the dihedral axis τ_2 as well as τ_3 showed a negligible energy difference between the maxima and minima (2 and 5 kcal/mol, respectively) suggesting the free rotation along C(11)-N(2) and C(11)-C(12) axes and the observed X-ray conformation (black arrow) at (τ_2) 87.3° and (τ_3) -80.8° (Fig. 2-8) corresponds to the minimal energy situations in the energy profile.

3 Synthesis and Characterization of Spin-labeled Viologen dendrimers

Unpublished work

Dendrimers with redox-active subunits in their core or periphery or branching units plays an important role as resulting dendritic effects concern redox protein mimics,[59] redox gradient,[60] charge-transfer complex based conductivity,[61] electron sponges[62] and redox sensors.[63] Tomalia et al. have reported several studies where PAMAM dendrimers, with low loadings of spin labels (10% of available sites). They have been used to probe interactions with other macromolecules such as DNA,[64] vesicles,[65] surfactants,[66] and polynucleotides.[67] The interpretation of the EPR data assumes a random distribution of spin-labels; however, there is no proof that this assumption is correct. Meijer et al spin-labeled all sites on five generations of DAB (polypropylene imine) dendrimers with the goal of monitoring dendrimer dynamics and hydrogen bonding between terminal groups.[68] This was done by observing the exchange interaction as evidenced in room-temperature (fluid) EPR. Moreover, Spin-labeled dendrimers have been proposed as useful relaxation agents for MRI.[69] Our aim is to introduce spin labels as the peripheral groups of the viologen dendrimer and to measure the distances between the spin labels, so that one could calculate the hydrodynamic radii of these dendrimers and their fluctuation. Apart from this, viologen dendrimers are cationic and electroactive, so upon complexation with anionic moieties, they will fold up, hence one could monitor the change in distances between the branches via ESR methods, the reduction of the viologen moieties may again stretch back as the molecule becomes neutral. We aim at studying these folding and stretching upon interactions as dendrimers mimic proteins thereby acting as a model systems by responding to the changes in their surroundings as proteins do.[22] Since the ESR experiments are under progress, the thesis will just focus on the Synthesis and

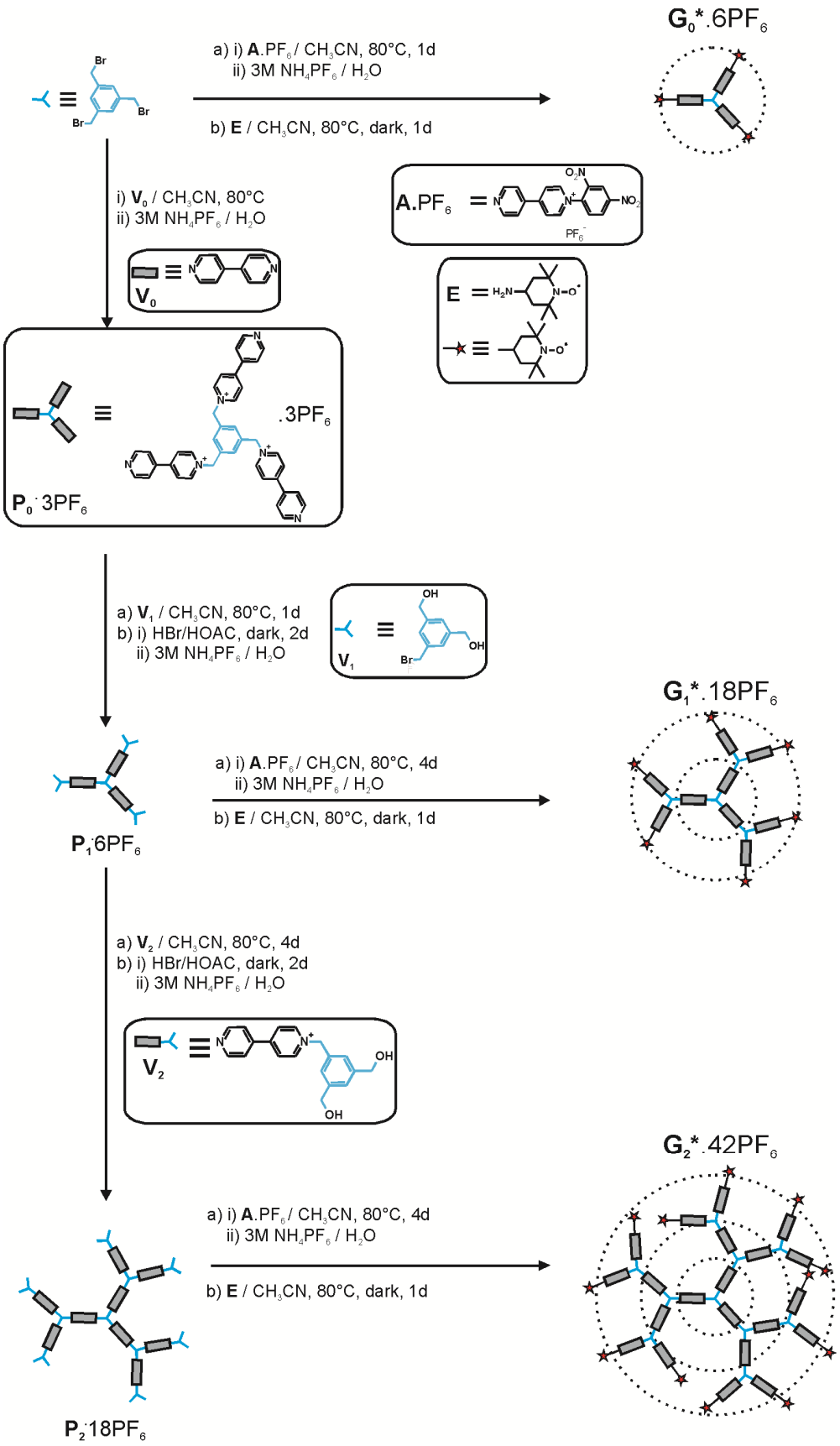

Scheme 3-1: Divergent synthesis of Spin-labeled dendrimers

Characterization of Spin-labeled Viologen dendrimers. Since final spin-labeled products are paramagnetic, NMR characterization is not possible and we characterized them by ESR and electrochemical methods.

3.1 Results and Discussion

3.1.1 Synthesis

The detailed syntheses of the starting materials V_1 and $V_2.PF_6$ were discussed in chapter 2. The synthesis follows the divergent approach (Scheme 3-1) as reported by Heinen et al.[10]

The new steps include the reaction of commercially available 1,3,5-tris(bromomethyl)benzene with 1-(2,4-dinitrophenyl)-4-(pyridin-4-yl)pyridinium hexafluoro-phosphate to yield the activated **G_0*** dendrimer (Scheme 3-1). Spin-labeling was achieved through Zincke reaction with the N-oxide **E**. Reaction of the activated **G_0*** dendrimer with 4-amino TEMPO in the dark and Argon atmosphere gives **G_0*** spin labeled dendrimer (81%). The core **P_0**.$3PF_6$ (95%) was synthesized from the reaction of **V_0** (4,4´-bipyridine) with 1,3,5-tris(bromomethyl)benzene as reported by Heinen et al. For the synthesis of higher generations we followed the same procedure. The preformed branching unit, 3,5-bis(hydroxymethyl) benzyl bromide (**V_1**) was reacted with **P_0**.$3PF_6$. The resulting hexol was activated by 5.6M HBr/HOAc to give the hexabromide **P_1**.$6PF_6$ (80%). The branching unit **V_2** with one reactive pyridine nitrogen and two latent benzylic alcohol functionalities was used for the synthesis of the precursor **P_2**.$18PF_6$. Reaction of **P_1**.$6PF_6$ with excess **V_2** yielded **P_2** alcohol which was then activated with 5.6M HBr/HOAc to give **P_2**.$18PF_6$ (60%). Reaction of **P_1.**$6PF_6$ and **P_2**.$18PF_6$ with 1-(2,4-dinitrophenyl)-4-(pyridin-4-yl)pyridinium hexafluorophosphate gave the new compounds **G_1***.$18PF_6$ and **G_2***.$42PF_6$ activated dendrimers (yields 50% & 56% respectively). The reaction of **G_1*** and **G_2*** activated dendrimers with 4-amino TEMPO gave **G_1*** and **G_2*** spin-labeled dendrimers (76% & 75%), respectively. [The intermediate product

i.e., the activated dendrimer bearing 2,4-dinitro groups at the end was purity checked by TLC. Further steps were carried out without characterizing these intermediates due to their poor solubility. The final spin-labeled dendrimers showed better solubility (soluble in CH_3CN, DMF, and DMSO) than their precursors (activated compounds)]. To standardize the ESR measurements, we additionally prepared viologen containing two spin labels on either side (Rod) as shown in Scheme 3-2 via Zincke reaction.

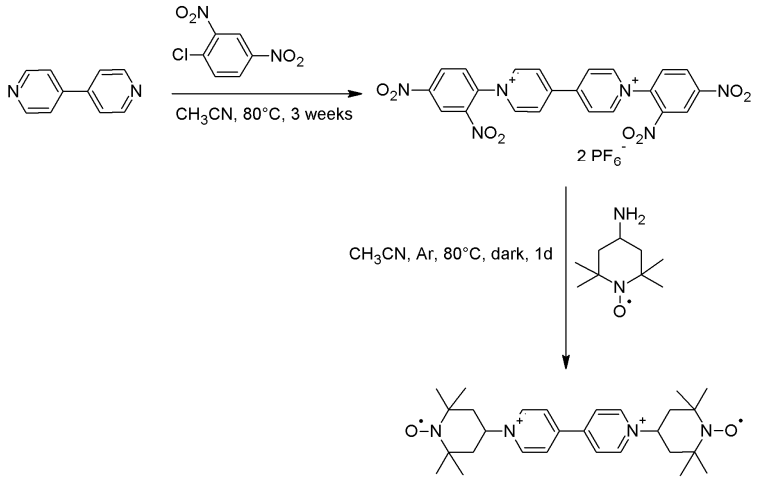

Scheme 3-2: Synthesis of the spin-labeled standard (rod-like viologen derivative)

Since the final spin-labeled dendrimers are paramagnetic, we characterized them only by TLC, elemental analysis, ESR measurement and Cyclic Voltammetry (both viologen and TEMPO moieties are electroactive). TLC showed a single spot corresponding to the dendrimer. Elemental analysis confirmed the purity of the products except for variable water content. The ESR and CV results are discussed in the following section.

Table 3-1: Physical chemical data for spin-labeled dendrimers

Generation	Mol. Wt.	No. of Spin-labels	Spin-Label Efficiency for single moiety[1] (%)	Expected distances between spin-labels[2] (nm)
G_0*	1921.21	3	84.6	2.66
G_1*	5415.09	6	72	2.82, 2.5
G_2*	12545.21	12	71	2.74, 2.66, 2.14, 1.43, 1.16, 0.83.

[1] Spin label efficiencies were calculated from the corresponding ESR spectra's of the spin-labeled dendrimers (Figure 3-1)

[2] Expected distances were calculated after geometry optimization (UFF) in Argus Lab (version 4.0)

3.1.2 ESR Characterization

In Table 3-1, the physical chemical data for the spin-labeled dendrimers are compiled. Measurement of the ESR spectrum and the corresponding correlation of the signal intensity to its concentration with that of the standard was used to calculate the spin-label efficiency (spin count) (Figure 3-1; Table 3-1)

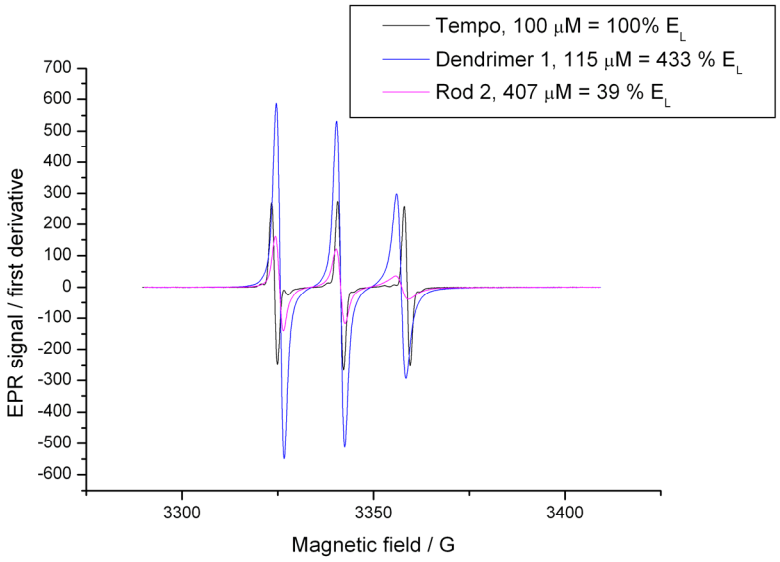

Figure 3-1: ESR spectrum of G_1* viologen dendrimer (dendrimer 1 with 6 spin-labels at its periphery); Spin-labeled standard (Rod 2) and Standard spin label (TEMPO) in (DMSO).

3.1.3 Cyclic Voltammetry

The spin labeled dendrimers were characterized by cyclic voltammetry. Figure 3-2, shows the electrochemical response of four spin-labeled dendrimers with electroactive viologen in the branching units and electroactive TEMPO at its periphery and the standard spin-labeled viologen equipped with two TEMPO units. The direct attachment of the spin-label to the standard viologen shows a potential shift of the viologen wave to more positive values as compared to viologens with alkyl substituents on N. The spin label attached to the standard spin-labeled viologen shows reversible wave at more negative potential whereas those which are attached at the dendrimer periphery (TEMPO) are shifted to positive potentials. No reduction of TEMPO in the potential < -1.0 V is observed, whereas free

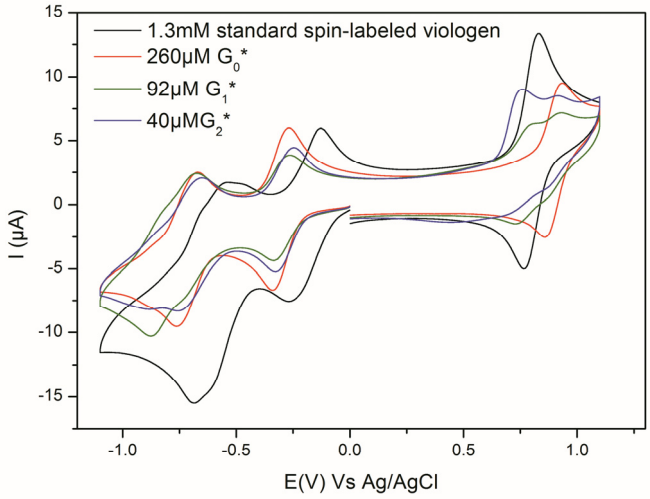

Figure 3-2: Cyclic Voltammogramms of Spin-labeled dendrimers and spin-labeled viologen standard in 0.1M TBA.PF_6 in DMF on glassy carbon (A = 0.07cm^2) at *V* = 0.1 V/s, RT

TEMPO showed reduction at -1.2 V. The missing reduction wave of TEMPO is accompanied by an increased cathodic current on the second viologen reduction wave, typical for intramolecular electrocatalysis of TEMPO reduction, according to

$$Vio^{\bullet+} + e^- \longrightarrow Vio^0$$

$$Vio^0 + TEMPO \longrightarrow TEMPO^- + Vio^{\bullet+}$$

The mutual influence of the two redox systems is also manifested by a shift or wave splitting of the TEMPO oxidation. An important quality check concerning the complete incorporation of TEMPO sites at the periphery is available from the peak current ratio of the first viologen reduction as compared to the TEMPO oxidation as shown in Table 3-2.

3.2 Conclusions

Benzylic viologen dendrimers from **G_0*** to **G_2*** bearing spin-labels (3, 6 and 12) at their periphery were synthesized via a divergent approach. The dendrimers were successfully spin-labeled by reacting the activated functionalities with 4-amino TEMPO (Zincke reaction). The final products were characterized by conventional cyclic voltammetry and ESR measurements. Cyclic voltammetry and ESR measurements showed the existence of the

additional N-O· electroactive subunit and good spin-label efficiency. The distance measurements are in progress. We intend to study chemical trigger induced conformational changes.

Table 3-2: Theoretical and Experimental ratios of viologen peak current to TEMPO peak current

Spin-labeled derivatives	Ratio of $i_{pVIOLOGEN}$ to i_{pTEMPO}	
	Theoretical	Experimental
Standard	1:2	1:1.93
G_0*	1:1	1:0.8
G_1*	1:0.66	1:0.75[a]
G_2*	1:0.57	1:0.7[a]

[a] approximated for the partly reversible double-wave of TEMPO.

3.3 Experimental Section

3.3.1 General

All starting materials and solvents were purchased from Sigma-Aldrich except 4-Amino-2,2,6,6-tetramethylpiperidine 1-Oxyl Free Radical (97%) purchased from TCI and was used without further purification. All the reactions were performed under dry conditions unless otherwise stated. HPLC grade or ACS Spectrophotometric grade solvents were used for electrochemical measurements. Elemental analyses were performed on Elementar Vario Micro cube instrument.

3.3.2 Detailed Synthetic Procedures

***1-(2,4-dinitrophenyl)-4-(pyridin-4-yl)pyridinium hexafluorophosphate (monoactivated bipyridine)* A.PF$_6$:**

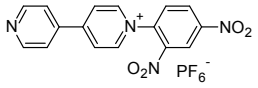

A.PF$_6$

A.PF$_6$ was prepared according to a published procedure, ^{1}H-NMR data and elemental analysis results were consistent with the reported literature.[70] The product obtained was dissolved in minimum amount of water and precipitated with 3M NH_4PF_6, the precipitate thus

obtained was washed with water and dried to yield **A**.PF_6 as a rocky brown solid, the crystals were analyzed by X-ray diffraction. The crystal structure of **A**.PF_6 is given below:

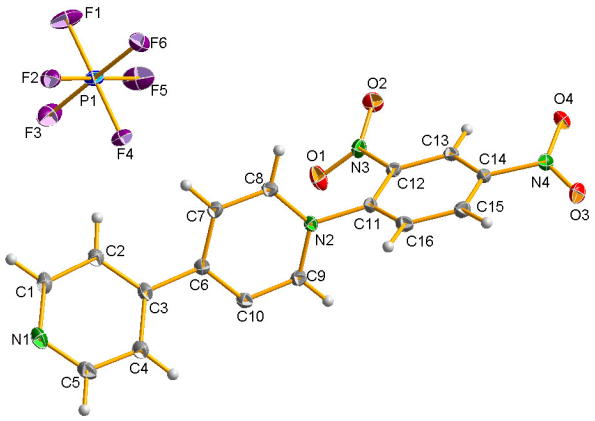

Figure 3-3: Crystal Structure of A.PF_6

Table 3-3: Crystal data for A.PF_6

Crystal data

Empirical formula	$C_{16}\ H_{11}\ F_6\ N_4\ O_4\ P$
Formula weight	468.26
Temperature	100(2) K
Wavelength	0.71073 A
Crystal system, space group	Triclinic, P-1
Unit cell dimensions	a=8.3754(7) Å α=92.533(5)°
	b=10.7018(9) Å β=106.524(5)°
	c=11.4840(9) Å γ=112.214(5)°
Volume	900.13(13) $Å^3$
Z, Calculated density	2, 1.728 Mg/m^3
Absorption coefficient	0.248 mm^{-1}
F(000)	472

G_0*.6PF_6:

1,3,5-Tris(bromomethyl)benzene (0.2g, 560 µmol) and **A**.PF_6 (1.18g, 2.5 mmol) were taken in 10 mL CH_3CN, stirred at 80°C for 1d. The solution was cooled; the precipitate was filtered and washed with CH_3CN. The residue thus obtained was dissolved in water,

precipitated with 3M NH_4PF_6, washed with water and dried to yield activated **G_0*** dendrimer (0.47g, 42%); ^{1}H-NMR (250MHz, CD_3CN) δ ppm 9.20 (d, 3H), 9.16 (d, 6H), 9.04 (d, 6H), 8.88 (dd, 3H), 8.66 (d, 6H), 8.56 (d, 6H), 8.18 (d, 3H), 7.76 (s, 3H), 5.94 (s, 6H); ^{13}C-NMR (63MHz, CD_3CN) δ ppm 152.9, 150.1, 146.8, 146.0, 143.3, 138.0, 134.9, 132.1, 131.6, 130.5, 127.9, 127.4, 122.3, 63.8. In a dry two-neck flask fitted with Ar inlet, bubbler and condenser, activated **G_0** dendrimer (0.25g, 127 μmol) and 4-amino TEMPO (0.076g, 4.4 μmol) were dissolved in 10 mL dry CH_3CN). The solution was heated to 80°C while stirring under dark condition for 1 d. The solution was cooled, precipitated with diethyl ether, filtered, washed with ether under Ar atmosphere and dried to yield **G_0*** spin-labeled dendrimer (0.2g, 81%). Anal. Calc. for $C_{66}H_{84}F_{36}N_9O_3P_6.3H_2O$: C, 40.13; H, 4.59; N, 6.38. Found: C, 40.11; H, 5.76; N, 6.59.

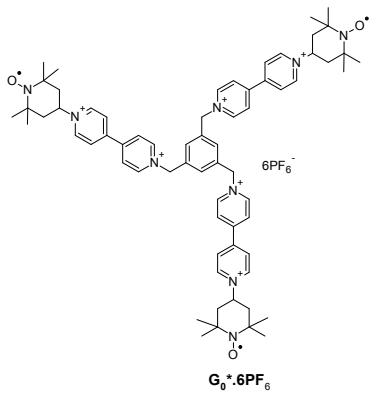

G_0*.6PF_6

P_0.3PF_6*:*

P_0.3PF_6 was prepared according to the reported procedure.[10a] The NMR data were consistent with the report.[10a] ^{1}H-NMR (250MHz, CD_3CN) δ ppm 8.88 (d, *J(H,H)* = 7.5Hz, 6H), 8.80(d, *J(H,H)* = 7.5Hz, 6H), 8.37 (d, *J(H,H)* = 7.5Hz, 6H), 7.80 (d, *J(H,H)* = 7.5Hz, 6H), 5.78 (s, 6H); ^{13}C-NMR (63MHz, CD_3CN) δ ppm 155.1, 151.2), 145.6, 141.9, 135.7, 131.5, 126.7, 122.4, 63.5.

P_1.6PF_6:

P_1.6PF_6 was prepared according to the reported procedure.[10a] The NMR data were consistent with the report.[10a] ^{1}H-NMR (250MHz, CD_3CN) δ pap 8.99 (d, *J(H,H)* = 7.5Hz,

6H), 8.94 (d, *J(H,H)* = 7.5Hz, 6H), 8.43 (d, *J(H,H)* = 7.5Hz, 12H), 7.68 (s, 3H), 7.65 (s, 3H), 7.50 (s, 6H), 5.86 (s, 6H), 5.84 (s, 6H), 4.61 (s, 12H); ^{13}C-NMR (63MHz, CD_3CN) δ pap 150.5, 145.8, 140.5, 134.8, 133.7, 131.8, 131.2, 129.7, 127.5, 64.0, 63.6, 32.0.

G_1*.18PF_6:

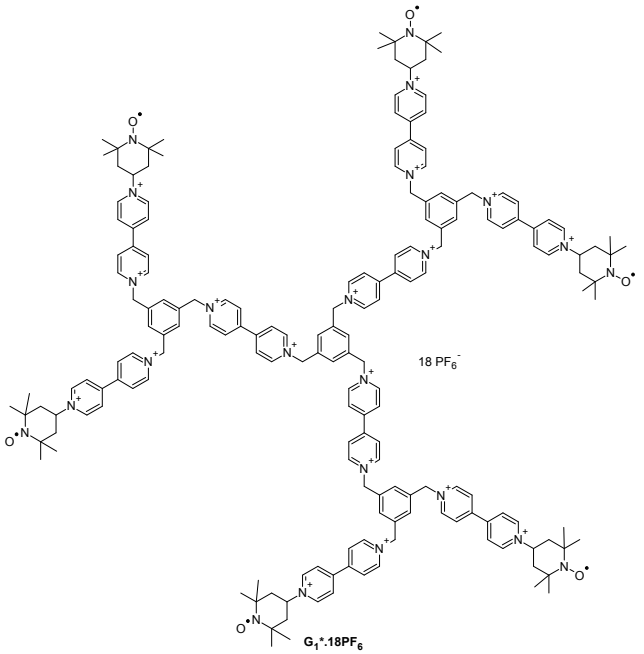

P_1.6PF_6 (0.2g, 87 μmol) and **A**.PF_6 (0.32g, 656 μmol) were dissolved in 20 mol CH_3CN, stirred at 80°C for 4d. The solution was cooled to RT, filtered, washed with CH_3CN and dried. The residue was dissolved in MeOH-H_2O (1:1) mixture, filtered to remove insoluble particles. The clear solution was then precipitated with 3M NH_4PF_6, filtered, washed and dried to yield activated **G_1*** dendrimer (0.24g, 50%); ^{1}H-NMR (250MHz, CD_3CN) δ ppm 9.18 (unresolved coupling, combined integral 18H), 8.99 (unresolved coupling, combined integral 24H), 8.65 (unresolved coupling, combined integral 36H), 8.54 (dd, 6H), 8.18 (dd, 6H), 7.74 (unresolved coupling, combined integral 12H), 5.90 (s, 24H); ^{13}C-NMR (63MHz, CD_3CN) δ ppm 152.8, 150.5, 150.1, 146.9, 146.0, 143.2, 138.0, 134.9, 132.1, 131.6, 130.5, 127.9, 127.6, 127.4, 122.3, 65.3, 63.6 [The interpretation of ^{1}H NMR and ^{13}C NMR were difficult due to the presence of unsymmetrical bipyridinium system throughout the system.

Apart from this, their poor solubility in CH_3CN lead to unresolved coupling, broad peaks, hence we looked at the total number of protons rather than individual protons].

In a dry two-neck flask fitted with Ar inlet, bubbler and condenser, activated **G_1*** dendrimer (0.2g, 36 μmol) and 4-amino TEMPO (0.047g, 273 μmol) were dissolved (10 mL dry CH_3CN). The solution was heated to 80°C under stirring in dark condition for 1d. The solution was cooled, precipitated with diethyl ether, filtered, washed with ether under Ar atmosphere and dried to yield **G_1*** spin-labeled dendrimer (0.15g, 76%). Anal. Calc. for $C_{180}H_{210}F_{108}N_{24}O_6P_{18}$: C, 39.92; H, 3.91; N, 6.20. Found: C, 39.90; H, 3.96; N, 6.18.

P_2.18PF_6:

P_2.18PF_6 was prepared according to the reported procedure.[10a] The NMR data and elemental analyses results were consistent with the report.[10a] ^{1}H-NMR (250MHz, CD_3CN) δ ppm 8.98 (s, 36H), 8.44 (s, 36H), 7.67(d, 18H), 7.55 (s, 12H), 5.85 (s, 36H), 4.61 (s, 24H); ^{13}C-NMR (63MHz, CD_3CN) δ ppm 150.51, 145.84, 140.48, 134.87, 134.30, 133.76, 131.79, 131.23, 129.72, 127.58, 63.81, 32.09, 31.62.

G_2*.42PF_6:

P_2.18PF_6 (0.2g, 32 μmol) and **A**.PF_6 (0.21g, 455 μmol) were dissolved in 40 mL CH_3CN, stirred at 80°C for 4d. The solution was cooled to RT, filtered, washed with CH_3CN and dried. The residue was dissolved in MeOH-H_2O (1:1) mixture, filtered to remove insoluble particles. The clear solution was then precipitated with 3M NH_4PF_6, filtered, washed and dried to yield activated **G_2*** dendrimer (0.23g, 56%); ^{1}H-NMR (250MHz, CD_3CN) δ ppm 9.17-9.06 (unresolved coupling, combined integral 84H), 8.90 (bs, 16H), 8.68 (bs, 18H), 8.46 (unresolved coupling, combined integral 64H), 8.19 (bs, 16 H), 7.76 (bs, 36H), 5.90 (s, 60H). ^{13}C-NMR (63MHz, CD_3CN) δ ppm 152.9, 150.5, 150.1, 146.8, 146.0, 143.3, 138.0, 134.9, 132.1, 131.6, 130.5, 127.9, 127.6, 127.4, 122.3, 65.3, 63.6 [The interpretation of ^{1}H NMR and ^{13}C NMR were difficult due to the presence of unsymmetrical bipyridinium system

throughout the system. Apart from this, their poor solubility in CH_3CN lead to unresolved coupling, broad peaks, hence we looked at the total number of protons rather than individual protons].

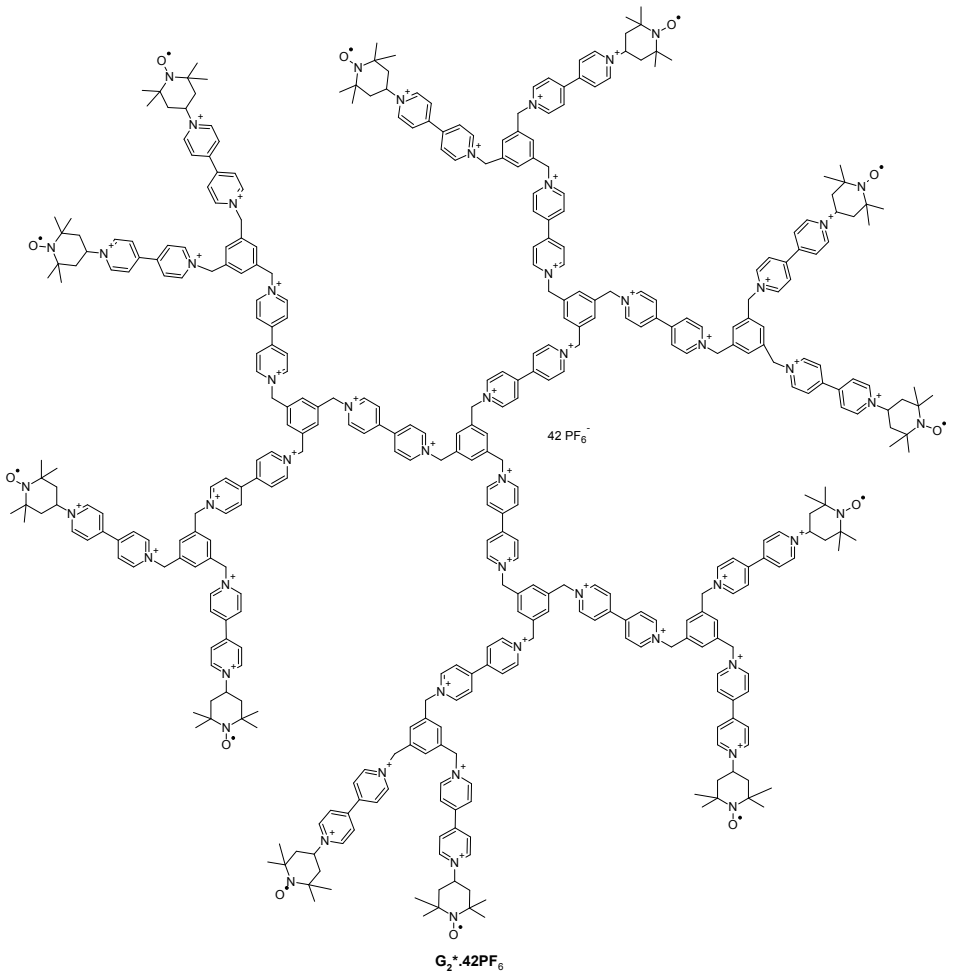

G_2*.42PF_6

In a dry two-neck flask fitted with Ar inlet, bubbler and condenser, activated **G_2** dendrimer (0.23g, 18 μmol) and 4-amino TEMPO (0.047g, 275 μmol) were dissolved in 10 mL dry CH_3CN). The solution was heated to 80°C under stirring in dark condition for 1d. The solution was cooled, precipitated with diethyl ether, filtered, washed with ether under Ar atmosphere and dried to yield **G_2** spin-labeled dendrimer (0.17g, 75%). Anal. Calc. for $C_{408}H_{462}F_{252}N_{54}O_{12}P_{42}.4H_2O$: C, 39.28; H, 3.79; N, 6.06. Found: C, 39.06; H, 3.80; N, 6.06

.

4 Trimethylenedipyridinium Dendrimers: Synthesis and Sequential Guest Complexation in Molecular Shells

Macromolecules, **2010**, *43 (22),* 9248

Dendrimers belong to a unique class of synthetic polymers with well-defined, highly branched architecture emanating from a central core through a stepwise, repetitive reaction sequence. Since the pioneering work of Vögtle,[3] Tomalia,[3] Newkome,[3]and Frechet[3] the synthesis,[3,71] special emphasis on functionalisation[72] and the tuning of their properties became a central point of research. The microenvironments in the interior and at the periphery of the dendrimers cannot be overestimated in many applications.[17,71c,73] The empty space can be occupied by molecular guests with the dendrimer playing the role of the guest.[3,74] The guest molecules can be complexed at the dendrimer periphery or in void regions within the dendrimer. Thus, the encapsulation of guest molecules into dendritic cavities[3,17,50f] is of prominent importance. Often the take-up of guest molecules is accompanied by conformational changes of the dendrimer as a consequence of the supramolecular complex formation. However, conformational changes are also known to occur upon contact with pure solvents or upon acid base reactions of dissociable groups within or at the periphery of a dendrimer.[71d,75]

Typical methods for the study of host-guest interactions involve i) ^{1}H NMR techniques (interaction accompanied by a change in chemical shift); ii) DOSY (diffusion-ordered spectroscopy) (interaction accompanied by a change of the diffusion coefficient of host or guest);[11a,17,76] iii) cyclic voltammetry – (interaction accompanied by a shift in electrochemical potential of an electroactive host or guest).[77,78] Other methods such as UV-vis, Raman

spectroscopy, Maldi-TOF, fluorescence titrations have also been used to probe the host-guest interactions.[38a,39c,79]

We have reported earlier on a similar series of dendrimers and oligomers consisting of 4,4′-bipyridinium subunits instead of 4,4′-trimethylenedipyridinium with focus on the synthesis, the generation dependent CT complexation, the molecular diode behavior, and their electrochromic properties.[10b,10c,43] Their host-guest chemistry was exploited by Balzani et al.[38] It has further been shown that the viologen dendrimers have antiviral properties and that a series of related viologen dendrimers behave as gene-transfecting agents.[36b,37] Typically, such applications rely on the viologen dendrimer's ability to wrap onto large biological structures. We consider their practical use in medicine as questionable because of the inherent toxicity of the viologen monomer, related to its low reduction potential.[80] Principally most cationic polyelectrolytes (a prerequisite for gene transfection/DNA condensation) can interact non-specifically with other cellular compounds leading ultimately to cell death, a side reaction that can be partially controlled by the dendrimers peripheral groups and its generation.[81] Di- and trimethylene bridged 4,4′-dipyridines are commercially available. Earlier work by W. Meyer in our group showed relatively low stability for the dimethylene bridged dipyridine derivatives.[82] Cationic non-electroactive dendrimers based on 4,4′-trimethylenedipyridinium subunits might show higher stability than the ethyl bridged homologues as well as less toxicity and better conformational adaptability compared to the viologen dendrimers because of the trimethylene function disrupting the π-resonance and displaying higher flexibility.

Herein we report on the synthesis of a new class of cationic dendrimers based on benzylic trimethylenedipyridinium subunits. As worked out above, this modification renders the dendrimer less electroactive (less toxic) and more flexible (more adaptive). Their medicinal value will therefore be studied in the near future. In the current article we report on

the synthesis and on fundamental complexation studies of organic anions within the voids of the cationic dendrimers.

A few years ago K. Yamamoto and coworkers have reported on the sequential complexation of guest molecules (inorganic Lewis acids) by phenylazomethine dendrimers with the imine functionalities acting as Lewis base coordination sites.[12,39c,83] The authors have shown by UV/vis titration that the guest molecules fill the dendrimer radially step-wise starting with the inner most shell. There is no report on other dendrimer/guest combinations showing the same stepwise charging mode, and the question is still not solved, if the phenomenon observed by Yamamoto is unique or of general importance. Our new dendrimers exhibit cationic complexing functionalities distributed all through the core, the branches and the periphery. Di- and trianionic guests are efficiently complexed. For the first time we describe here an evidence for an inside-out loading scenario that respects cationic dendrimer molecular shells similar to the Bohr atomic model.

Host-guest interaction studies were carried out on a model anticancer drug / DNA intercalator[84], i.e. di-anionic 2,6-anthraquinone disulfonate (AQDS). Notably, this guest is electroactive,[85] whereas the new dendrimers consisting of pyridinium sites do not show electroactivity at potentials > -1 V. The interactions between AQDS and the dendrimers were monitored using ^{1}H-NMR, DOSY and cyclic voltammetry.

4.1 Results and Discussion

4.1.1 Synthesis

The syntheses of the core, the branching and the peripheral units for a new class of polycationic dendrimers are presented in Scheme 4-1. Commercially available 4,4´-trimethylenedipyridine can be easily monoalkylated by reacting it with substoichiometric amounts of alkylating agents. The syntheses of the core $\mathbf{P_0}.3PF_6$, the branching unit for divergent ($\mathbf{V_2}.PF_6$) and for the convergent strategies ($\mathbf{W_2}.2PF_6$), as well as the corresponding

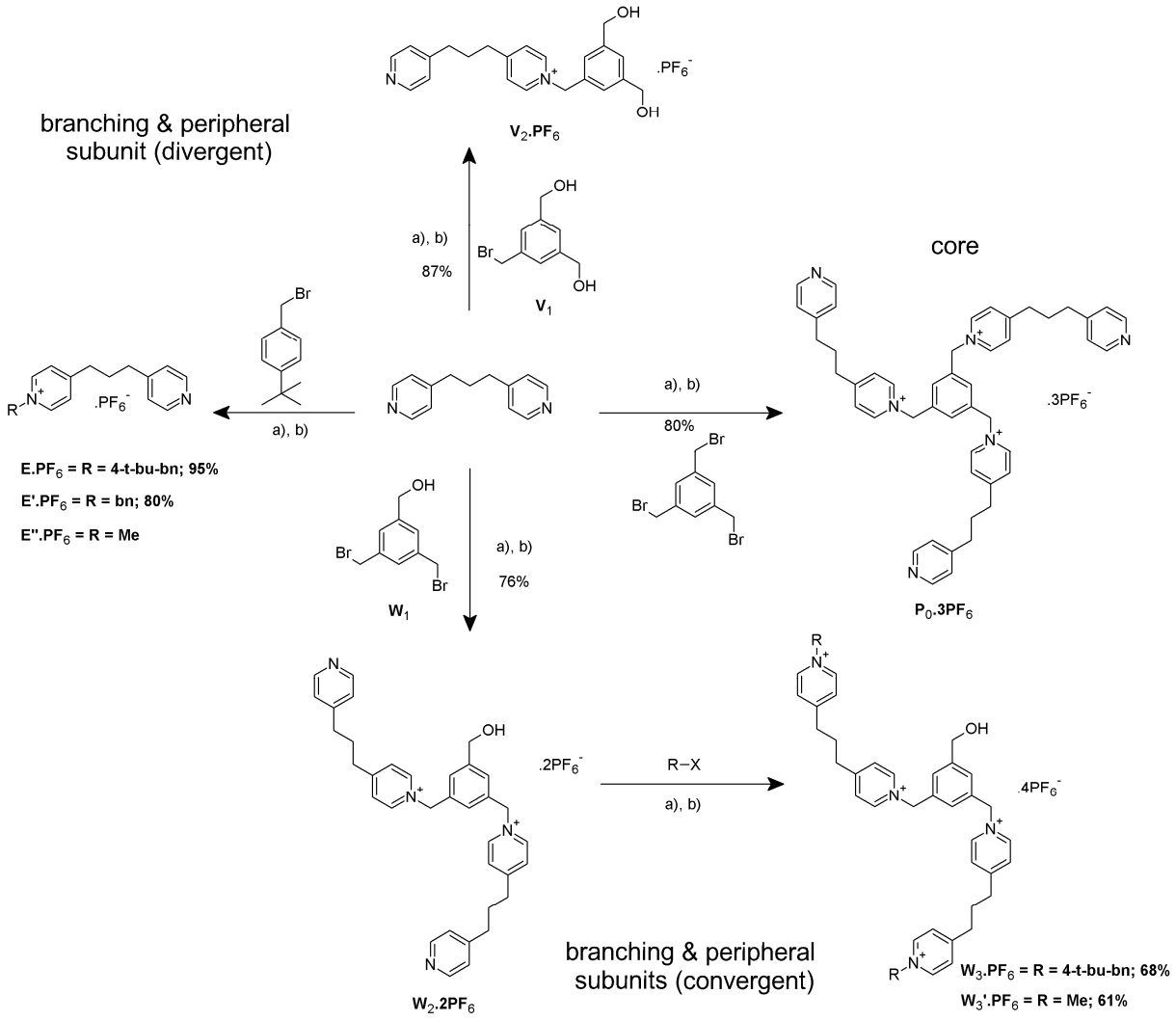

Scheme 4-1: Synthesis of core, branching and peripheral units for the divergent and convergent dendrimer synthesis; a) CH_3CN/80°C; b) 3M NH_4PF_6/H_2O

peripheral units **E**.PF_6, **E**′.PF_6 and **E**′′.PF_6, **W₃**.4PF_6 and **W₃**′.4PF_6 are shown in Scheme 4-1. In Chapter 2, we discussed on the synthesis of the benzylic bromides **V₁** and **W₁**, here they are reacted with 4,4′-trimethylenedipyridine to yield the branching units **V₂**.PF_6 and **W₂**.2PF_6. The peripheral subunits carrying the 4-*t*-Bu-Bn (**E**.PF_6), benzyl (**E**′.PF_6) and Me (**E**′′.PF_6) are easily available from the reaction of 4,4′-trimethylenedipyridine and substoichiometric amounts of 4-*t*-Bu-BnBr, BnBr or MeI, respectively. The **W₃** type peripheral groups are available from the precursor **W₂**.PF_6 using the corresponding alkylating agents. Notably, **V₂**.PF_6, **W₂**.2PF_6 and **W₃**.4PF_6 carry latent functionality (benzylic –OH) which can be

activated by bromination using HBr/HOAc. The salts obtained after each reaction are water/MeOH soluble bromides or mixed salts, for analysis and further reaction these products were converted to MeCN soluble PF_6^- salts; ion exchange was achieved by the precipitation of the bromide salts with 3M NH_4PF_6 from water/MeOH. Notably, the ion exchange step is the major purification available in these syntheses.

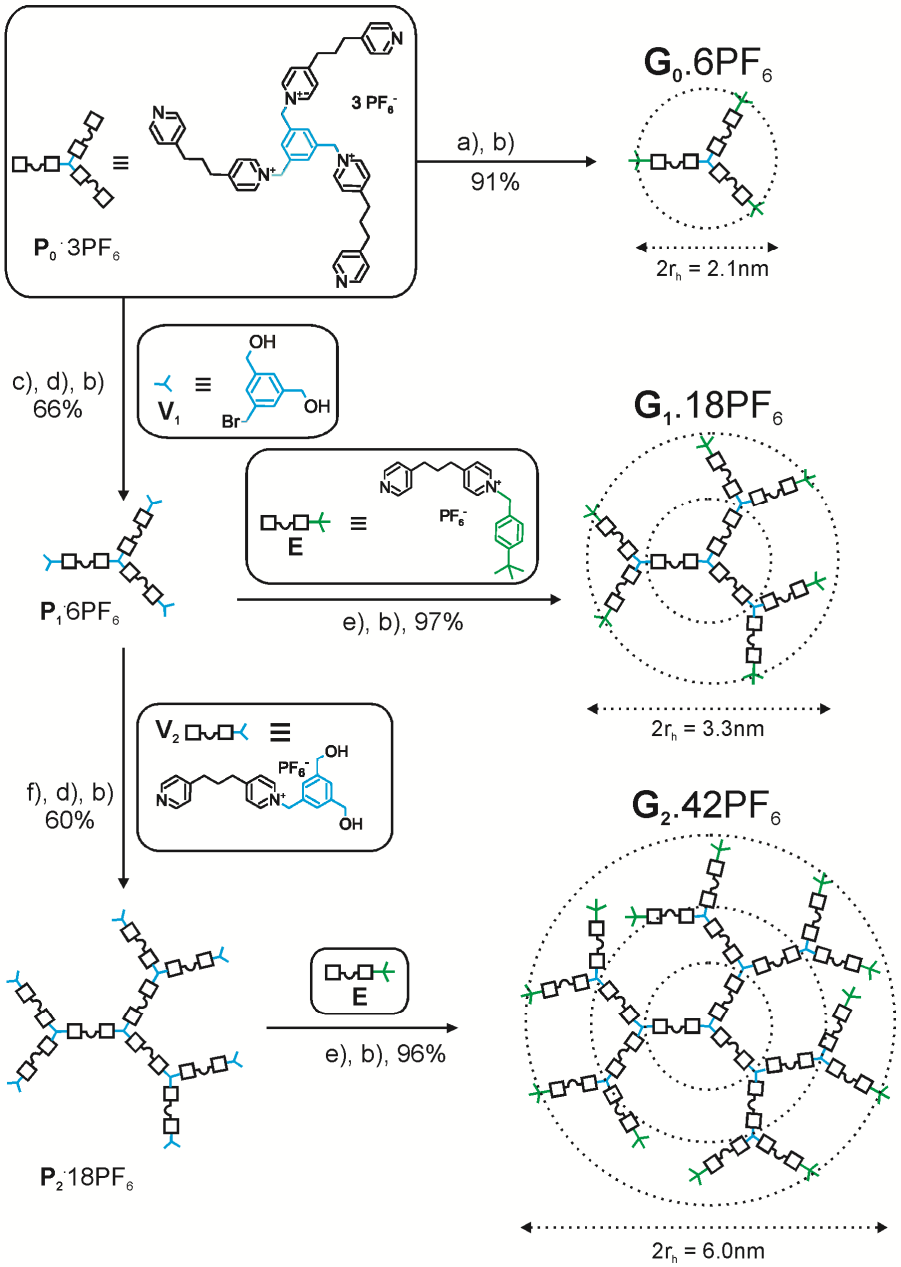

Scheme 4-2: Synthesis of polytrimethylenedipyridinium dendrimers G_0 to G_2; a) 4-*t*-Bu-BnBr/CH_3CN/80°C; b) NH_4PF_6/H_2O; c) V_1/CH_3CN/80°C; d) HBr/HOAc/RT; e) E/CH_3CN/80°C, f) V_2/CH_3CN/80°C; yields reported are the isolated yields of the title compounds; dotted circles represent generation shells, r_h is the experimental hydrodynamic radius from DOSY

The dendrimers of generations zero to two were synthesized following the "divergent method with preformed branching units" [10a,10b](Scheme 4-2). The three peripheral nitrogens in **P$_0$**.3PF$_6$ react quantitatively with excess of benzyl bromide (**G$_0$**´), methyl iodide (**G$_0$**´´) (not shown in Scheme 4-2, discussed in the Experimental Section) and 4-*t*-Bu-Bnbr. The best yield and solubility were achieved with 4-*t*-Bu-BnBr as alkylating agent. Its reaction with **P$_0$**.3PF$_6$ followed by ion exchange yielded **G$_0$**.6PF$_6$ in 91%. For the synthesis of higher generations, the preformed branching unit, 3,5-bis(hydroxymethyl)benzyl bromide (**V$_1$**) was reacted with **P$_0$**.3PF$_6$. The resulting hexol was activated by HBr/HOAc to give the hexabromide **P$_1$**.6PF$_6$. [The crude hexol was first washed with CH_3CN to remove excess **V$_1$**, and the resulting insoluble residue (mixed counter ions) was directly brominated without further characterization. After bromination, **P$_1$**.6Br is obtained as a MeOH/H_2O soluble salt]. The branching unit **V$_2$** with one reactive pyridine nitrogen and two latent benzylic alcohol functionalities was used for the synthesis of the precursor **P$_2$**.18PF$_6$. The yields of the precursors **P$_1$** and **P$_2$** were 66 and 60%, respectively, reflecting material loss in the ion exchange step. The dendrimers **G$_1$**.18PF$_6$ and **G$_2$**.42PF$_6$ were available from the reaction of the corresponding precursors **P$_1$**.6PF$_6$ and **P$_2$**.18PF$_6$ with the end group **E,** yielding 97 and 96%, respectively after ion exchange. The 4-*tert*-butyl-benzyl groups imparts better solubility, thus even dendrimers with mixed counter ions are soluble in MeOH/H_2O and subsequent ion exchange gives MeCN soluble (MeOH/H_2O insoluble) PF_6 salts (for detailed synthetic procedures see Experimental Section).

The intermediates and products were characterized by ^{1}H NMR,^{13}C NMR and DEPT measurements. The purity of the compounds was further checked by elemental analysis (samples were pure apart from variable water contents) (see Experimental Section). The completeness of N-alkylation was generally followed based on the integration of the

peripheral group as compared to the core resonances. Physical chemical data for **G_0** – **G_2** dendrimers was shown in Table 4-1.

Table 4-1: Physical Chemical data

Generation	Mol. Wt.	D x 10^{-10} (m^2/s)	r_h±0.5 (nm)
G_0	2023.45	1.12	1.07
G_1	5745.81	0.74	1.63
G_2	13190.53	0.4	3.03

4.1.2 Host-Guest complexation studies

Host-guest complexation studies were carried out with **G_0**, **G_1** and **G_2** dendrimers as host and anthraquinone-2,6-disulfonate (AQDS) as guest molecule. The molecular encapsulation of the dianion inside the dendritic voids is based on charge interactions and can be monitored using ^{1}H NMR techniques, DOSY, and cyclic voltammetry, as discussed below:

4.1.2.1 ^{1}H NMR studies

^{1}H NMR technique has been often used to evaluate the intermolecular interactions between host and guest in supramolecular chemistry. Complexation can show up (i) as cross-peaks in 2-dimensional NOESY between host and guest resonances as a function of complexation, or (ii) by a reduction of molecular symmetry and the splitting or variation in half-peak width of resonances from protons which become non-equivalent upon complexation.[40] Such host guest interaction on dendrimers monitored by NMR techniques have been reported by many research groups, e.g. by Astruc et al. (protonation of PAMAM dendrimers by different acids),[17] and Meijer et al. (hydrogen bonding interactions in adamantyl-urea functionalized PPI dendrimers).[3,74a]

Figure 4-1 shows the ^{1}H-NMR of **G_1** including the complete assignment of the proton resonances. The corresponding spectra of **G_0** and **G_2** are similar except for the ratio of internal to peripheral protons. The H_1 resonances on the pyridinium shows large splitting, whereas H_3

on the phenyl branching units show only minor splitting. This points to a preferential conformation of the methylene bearing H_5 rendering the two H_1 magnetically non-equivalent, but the three H_3 magnetically almost equivalent in the absence of the guest molecule (Experimental Section, Figure 4-10). Since the region from δ 0.9 to 4 (trimethylene and *t*-Bu end groups) is dominated by solvent peaks and tetrabutyl ammonium (counter ion of the AQDS), we focused mainly on the changes in the region δ 5.7-9.1.

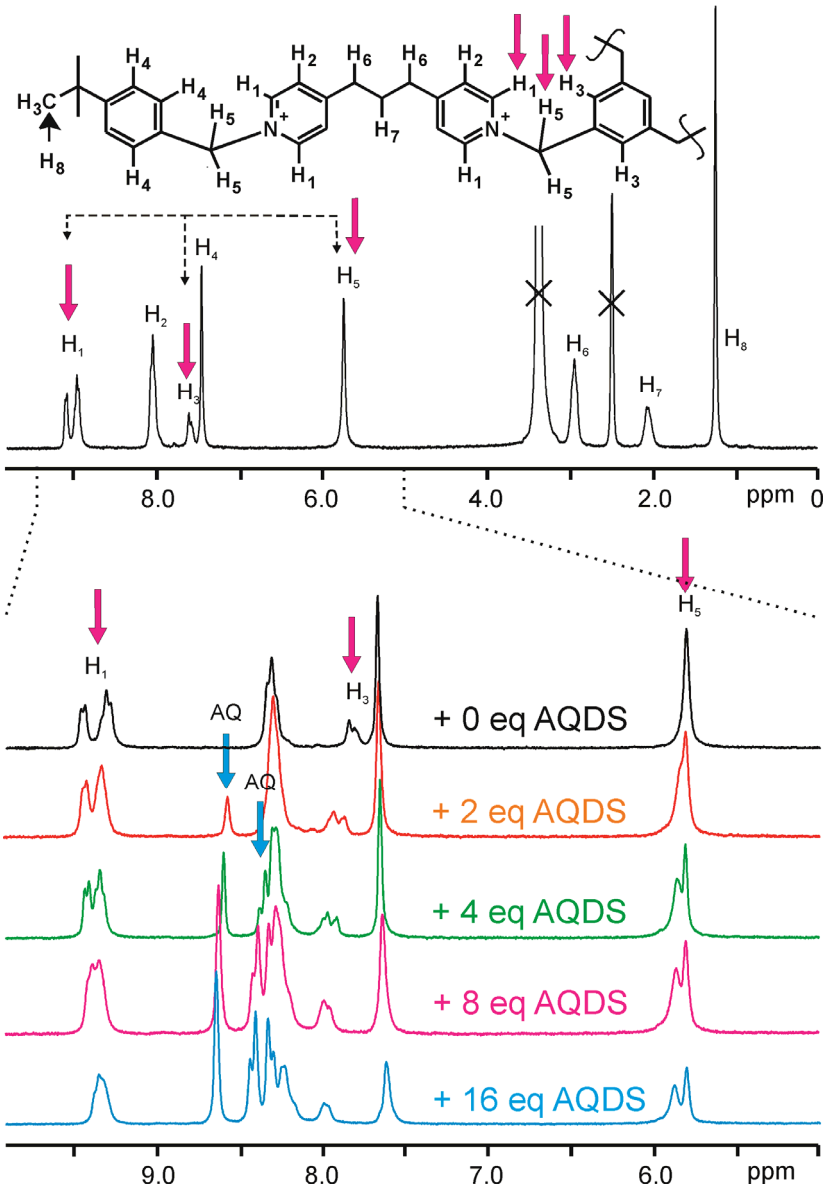

Figure 4-1: ^{1}H-NMR spectrum of G_1 (c = 2.8 mM in DMSO-d_6) with chemical shift assignment; magenta arrows: peaks monitored in guest titration (Figure 5-2); dotted-black arrows: resonances with cross peaks in NOESY (Experimental Section); AQDS equivalents present: black spectra: 0, orange: 2, green: 4, magenta: 8, blue: 16

The resonances due to meta-H_2 at pyridinium, as well as the protons at the trimethylene bridge (H_6 and H_7) show almost no splitting indicating reasonable rotational freedom of the bridge methylene groups (at least before complexation).

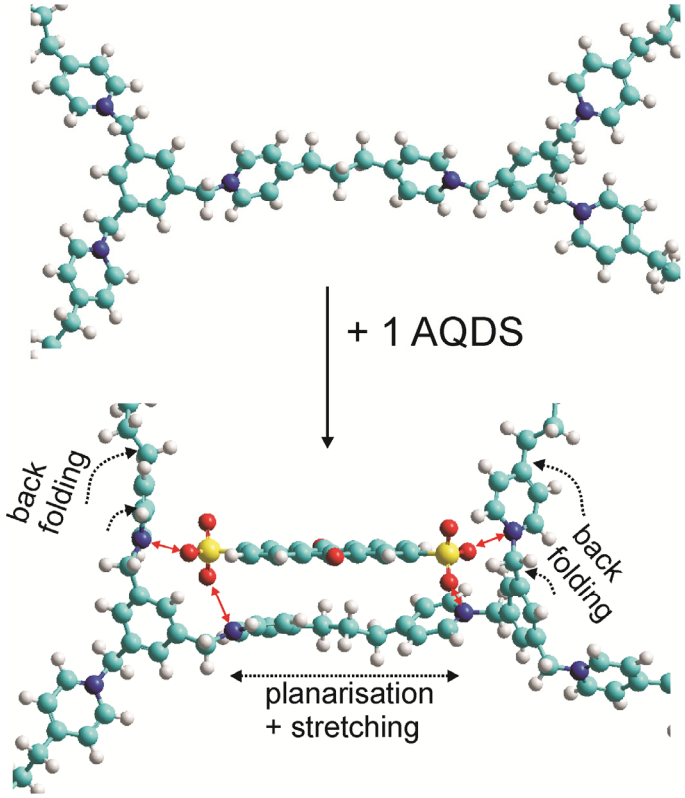

Figure 4-2: MM+ Modeling of G_1 before and after complexation of 1 AQDS; black arrows indicate major changes in G_1 conformation upon complexation; red arrows indicate electrostatic interactions

Upon addition of the dianionic guest AQDS, important shifts and changes in splitting of the host resonances H_1, H_3 and H_5 are observed as exemplified for the 18 fold positively charged **G_1** upon stepwise addition of 2,4,8,and 16 equiv AQDS (1 equiv = 2 stoichiometric negative charges). The changes in chemical shift reach a constant value after complete charge compensation, i.e. 9 equiv AQDS for **G_1**. Interestingly, only intramolecular NOESY cross peaks are observed concerning the dendrimer protons H_1, H_3 and H_5 but not between dendrimer and aromatic protons of AQDS (Experimental Section).

The main conformational changes in the dendrimer upon complexation of a single AQDS have been modeled using the MM+ force field method (Figure 4-2). A good fit

between the two sulfonates on a single AQDS and the two pyridinium nitrogens on a single propyl bispyridinium side chain is observed. Some stretching to an in-plane conformation of the propyl bridge and back-folding of the neighboring side chains is also typical.

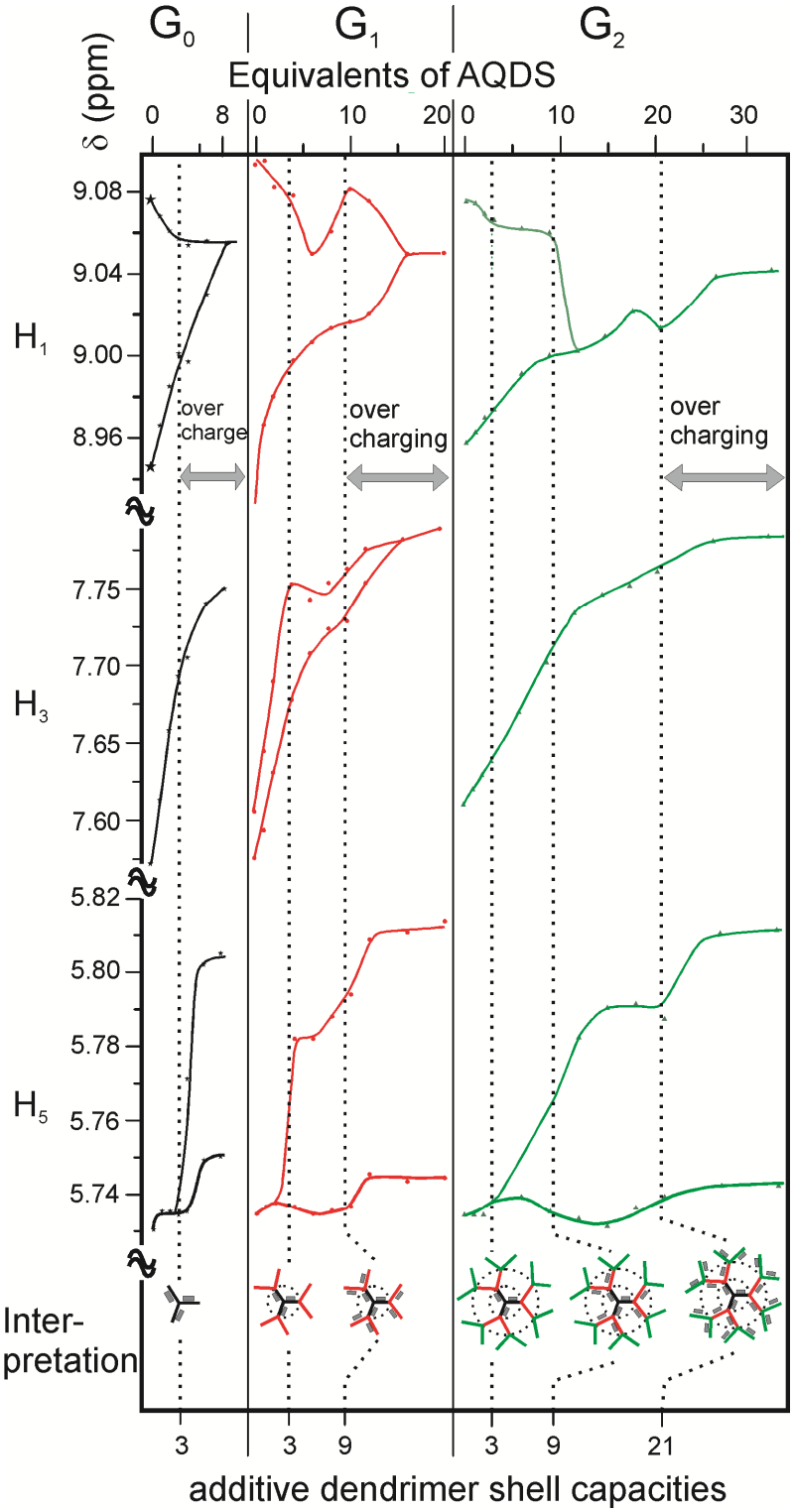

Figure 4-3: NMR titration: plots of the H_1, H_3 and H_5 dendrimer peaks of G_0, G_1 and G_2 vs. AQDS equivalent additions [G_0] = 6.9 mM; [G_1] = 2.8 mM; [G_2] = 1.1 mM; dotted lines: dendrimer shell capacity

A detailed study of the NMR shifts of the host protons H_1, H_3 and H_5 for all dendrimers **G_0-G_2** as a function of added AQDS equivalents is shown in Figure 4-3. No precipitation is observed during the titration except for **G_2**, for which the solution turned slightly hazy at the point of charge compensation. Generally changes become small above full charge compensation, but this is rather due to overcharging the dendrimer than to a low association constant (see later). Remarkably, prominent changes occur at the same number of added equivalents AQDS independent of the dendrimer generation, e.g. 3 equiv AQDS added leads to splitting of H_5 in **G_0**, **G_1** and **G_2**, or after 9 equiv added collapse of the splitting of H_1 in **G_1** and **G_2** is observed. We interpret this behavior as follows (Figure 4-3, bottom): The dendrimer **G_0** can be considered as a trimethyl benzene core with 3 doubly charged propyl bispyridinium side chains in a first shell, in **G_1** further 2*3 = 6 doubly charged propyl bispyridinium side chains are added in a second shell, and in **G_2** another set of 4*3 = 12 doubly charged side chains are added in a third shell, yielding total amounts of 3, 3+6 = 9, and 3+6+12 = 21 doubly charged side chains organized in shells for **G_0**,**G_1** and **G_2**, respectively (Figure 4-3 (bottom), Scheme 4-2). The dotted lines connecting prominent changes in the splitting at 3, 9 and 21 equiv AQDS are therefore evidence for a sequential filling of the innermost shell (3 open place), followed by the central shell (6 open places), followed by the outer most shell (12 open places).

A similar studies on the aromatic proton at δ 8.28 – 8.39 ppm of the guest molecule AQDS reveals a continuous, non-structured shift of the resonance over a range of 0.1 ppm. Notably, the shift of free AQDS is reached at 30 to 100 % excess of AQDS present in solution only. This points to overcharging the dendrimer at high AQDS concentration rather than incomplete complexation at the point of stoichiometric AQDS equivalents addition (Figure 4-4). The association constant for the first AQDS complexation by empty **G_2** (K(**G_2**)) can be

estimated K($\mathbf{G_2}$) > 1*10^5 from c($\mathbf{G_2}$)$_{initial}$ = 1.1 mM, c(AQDS) $_{initial}$ = 1.1 mM and c($\mathbf{G_2}$-AQDS)/c($\mathbf{G_2}$) $_{initial}$ > 0.9.

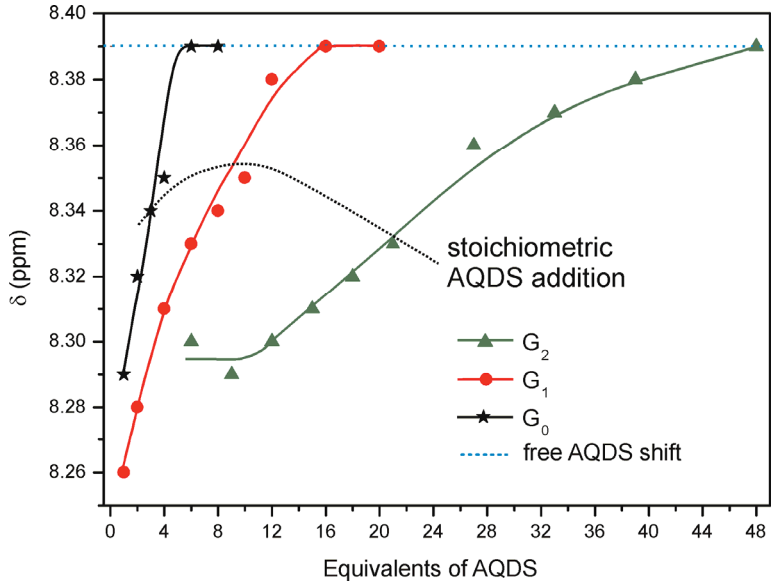

Figure 4-4: NMR titration: plots of the aromatic signal of AQDS at δ = 8.26 to 8.39, dotted blue line: shift of the proton in the absence of a dendrimer; dotted black curve: connects stoichiometric equivalent additions for the three dendrimers

4.1.2.2 Diffusion ordered spectroscopy

Diffusion ordered spectroscopy (DOSY),[86] recently emerged as an important technique in the study of host-guest complexes.[87] The prerequisite for such measurements is a sufficient difference in the diffusion coefficient of free host and free guest. Dendrimeric hosts fulfill this condition generally. DOSY has been successfully applied to probe the proton induced size variation of dendrimers terminated with –NH_2 or –COOH groups.[3] Beside from following the dendrimer diffusion coefficient, Astruc et al found diffusion breakdown of the guest molecule upon complexation eg. interaction of acetylcholine with carboxyl terminated dendrimers.[11a] Intermediate diffusion coefficient between complexed and free has been explained for small guests by a fast bound-free ligand exchange mechanism.[11a] Besides complexation studies on a single dendrimer, DOSY can be used to study the dendrimer generation dependent diffusion coefficients.[3,17] So far, very few DOSY reports are available on dendrimers size variation upon guest loading. The only report showing changes in the

dendrimer diffusion coefficient concerns a protonation induced size change,[3] other reports show no or minor size changes upon guest complexation.[11a,50f]

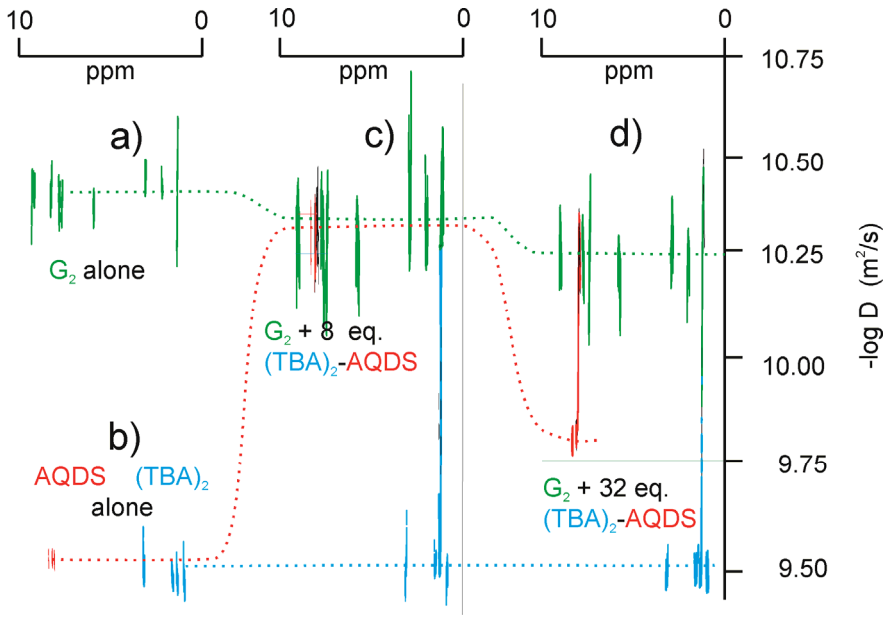

Figure 4-5: DOSY spectra a) G_2 dendrimer b) AQDS.$(TBA)_2$ c) G_2 dendrimer + 8equiv AQDS and d) G_2 dendrimer + 32equiv AQDS

The diffusion coefficients of the dendrimers **G_0**, **G_1** and **G_2** were measured in DMSO-d_6. In the non-complexed state each dendrimer displays relatively a narrow band of signals centered on its average diffusion coefficient (ca +/- 20 % in *D* maxima and minima with respect to the average). The trimethylene signals appear consistently at somewhat smaller *D* possibly due to overlapping with the solvent signals (Figure 4-5).[76] The diffusion coefficients of **G_0**, **G_1** and **G_2** in the absence of AQDS are given in Table 1 (first line, n=0). They cover a range of ca. 1.2 to 0.4×10^{-10} m^2/s corresponding to the hydrodynamic radii of 1.1 to 3.0 nm, respectively. In accordance, AQDS alone with its counter ion tetrabutylammonium (TBA) displays D_{AQDS} = 3.2 x 10^{-10} m^2/s and D_{TBA} = 3.5 x 10^{-10} m^2/s (Figure 4-5b). (The hydrodynamic radii (r_h) were calculated using a hard sphere model with the Stokes-Einstein equation.

$$r_h = kT/6\pi\nu D$$

where k is the Boltzmann constant, T= is the temperature in Kelvin, v is the kinematic viscosity, $v = \mu/\rho$, μ is the viscosity[88] and ρ, the density of the solvent, D is the diffusion coefficient).

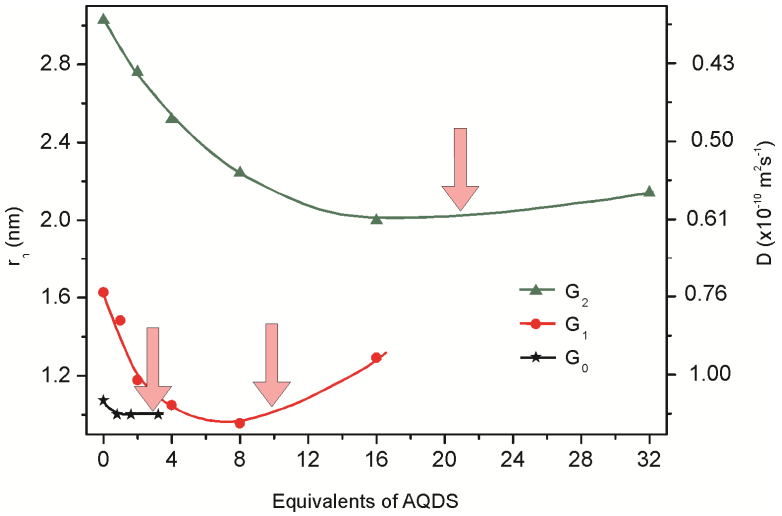

Figure 4-6: Diffusion coefficient (*D*) and hydrodynamic radii r_h as a function of the equivalents of AQDS, DOSY titrations; pink arrows indicate formal charge compensation; [G_0] = 6.7 mM; [G_1] = 2 mM; [G_2] = 0.97 mM

Dendrimer generation dependent size studies have previously been reported.[3,17] The more interesting results in the current stem from a study of the dendrimer DOSY spectra as a function of added guest molecules, i.e. equivalents of AQDS.$(TBA)_2$ (Figure 4-5 and 4-6). In Figure 4-5 c) we present **G_2** in the presence of 8 equiv AQDS.$(TBA)_2$. The dendrimer shows a slightly faster diffusion coefficient than non-complexed (dotted green line in Figure 4-5); the AQDS appears at the dendrimer diffusion coefficient (dotted red line, and its counter ion remains at its original value clearly indicating complex formation). Upon further addition of AQDS.$(TBA)_2$ equivalents – with equiv = 32 notably into the excess (overcharge) region a further increase of the dendrimer diffusion coefficient is observed with the AQDS appearing in the dendrimer as well as at a diffusion coefficient intermediate between free AQDS.$(TBA)_2$ and complexed, indicating fast exchange between the free and complexed state (Figure 4-5d).[11a,50f]

In Figure 4-6 and in Table 4-2, we resume the complete set of results on the diffusion coefficients of **G_0**, **G_1** and **G_2** as a function of AQDS added (in equivalents). Obviously all the polycationic host dendrimers shrink upon addition of the dianionic guest and reach the minimum size in the range of complete charge compensation. The shrinking concerns ca. 30 % for **G_1** and **G_2**, but it is only very small for **G_0**. Upon further addition of AQDS (overcharging), the dendrimers **G_1** and **G_2** grow again in size. This is the first DOSY study

Table 4-2: Diffusion coefficients (*D*) and hydrodynamic radii (r_h) of dendrimers in the presence of different AQDS equivalent additions (n)

G_0			G_1			G_2		
n	*D* x 10^{-10} (m^2/s) [a]	r_h±0.05 (nm)	*n*	*D* x 10^{-10} (m^2/s) [a]	r_h±0.05 (nm)	*n*	*D* x 10^{-10} (m^2/s) [a]	r_h±0.05 (nm)
0	1.12	1.07	0	0.74	1.63	0	0.40	3.03
0.8	1.20	1.00	1	0.81	1.48	2	0.44	2.76
1.6	1.20	1.00	2	1.02	1.18	4	0.48	2.52
3.2	1.20	1.00	4	1.15	1.05	8	0.54	2.24
			8	1.26	0.96	16	0.60	2.00
			16	0.93	1.29	32	0.56	2.14

[a] Reproducibility and analysis error is ± 5% [E]
[b] r_h is the hydrodynamic radius calculated for a hard sphere model;
$\boldsymbol{D}_{AQDS}$ = 3.23 x 10^{-10} m^2/s (r_h = 0.37nm); $\boldsymbol{D}_{TBA}$ = 3.46 x 10^{-10} m^2/s (r_h = 0.35nm); [G_0] = 6.7 mM; [G_1] = 2 mM; [G_2] = 0.97 mM

shows the mutual influence of complexation on host and guest diffusion coefficients in such an impressive manner. Probably it is related (i) to the fact that periphery and branches are carrier of fixed and persistent positive charge (endosystem in contrast to exosystem),[3,38a] and (ii) to the fact that there exists a good fit of the two cationic sites on the propyl bispyridinium chain (preformed acceptor site) and the two sulfonate groups on the AQDS.

A lower limit for the association constant for the first AQDS complexation by empty **G_2** (K(**G_2**)) can be estimated assuming more than 90% complexation (this is very

[E] The diffusion coefficients reported are median values of the distribution. The error estimations reported in this work were the difference between maximum and minimum diffusion values.

conservative, as there is no indication of free AQDS even at 8 equiv addition!), thus yielding $K(\mathbf{G_2}) > 1*10^5$ (see Experimental Section).

4.1.2.3 Cyclic voltammetry

Cyclic voltammetry (CV) has been used in several cases to elucidate the interaction of redox-active guests with different supramolecular hosts. The CV-curves deliver mechanistic, kinetic, and thermodynamic information about supramolecular host-guest interaction.[78a]

The dianionic AQDS alone shows two reversible reduction/oxidation waves on glassy carbon in DMF / 0.1 M TBA.PF_6 with $E^{0'}{}_{1\_AQDS}$ = -0.826 and $E^{0''}{}_{2\_AQDS}$ = -1.526 (vs. Ag/AgCl) according to

$$AQDS^{2-} + e^- \rightleftharpoons AQDS^{3-}$$

$$AQDS^{3-} + e^- \rightleftharpoons AQDS^{4-}$$

The dendrimers in the same solvent electrolyte system show two irreversible reductions with cathodic peak potentials in the range of -1.136 to -1.379 V depending on the generation and related to the reduction of the pyridinium moieties (Figure 4-7). A related modified electrode consisting of polypyrrole with pyridinium side chains and AQDS as a guest has earlier been reported.[85] However, this electrode was used in aqueous solution and AQDS under these conditions exhibits a two-electron-two-proton wave.

In Figure 4-7, the cyclic voltammograms of $\mathbf{G_0}$, $\mathbf{G_1}$ and $\mathbf{G_2}$ in the presence of different equivalents of AQDS are presented (number of equivalents added are given in proximity of the corresponding CV). The scan was limited to the first reduction of AQDS, i.e. 0 to -1.0 V *vs.* Ag/AgCl. The peak potentials of free AQDS (in the absence of dendrimers) are indicated by two vertical black lines. In the presence of dendrimers, the AQDS redox couple appears at more positive potentials. This is related to the preferential stabilization of the tri-anionic $AQDS^{3-}$ over the di-anionic $AQDS^{2-}$ oxidation state by cationic dendrimer sites (Experimental

Section-scheme of squares). For relative small equiv additions, a small broad cathodic peak (I_c, II_c) and a larger symmetric anodic peak (I) is observed (as exemplified for **G_1** in Fig. 4-7). The larger anodic and highly symmetric peak (I) is mainly due to adsorption of the complex

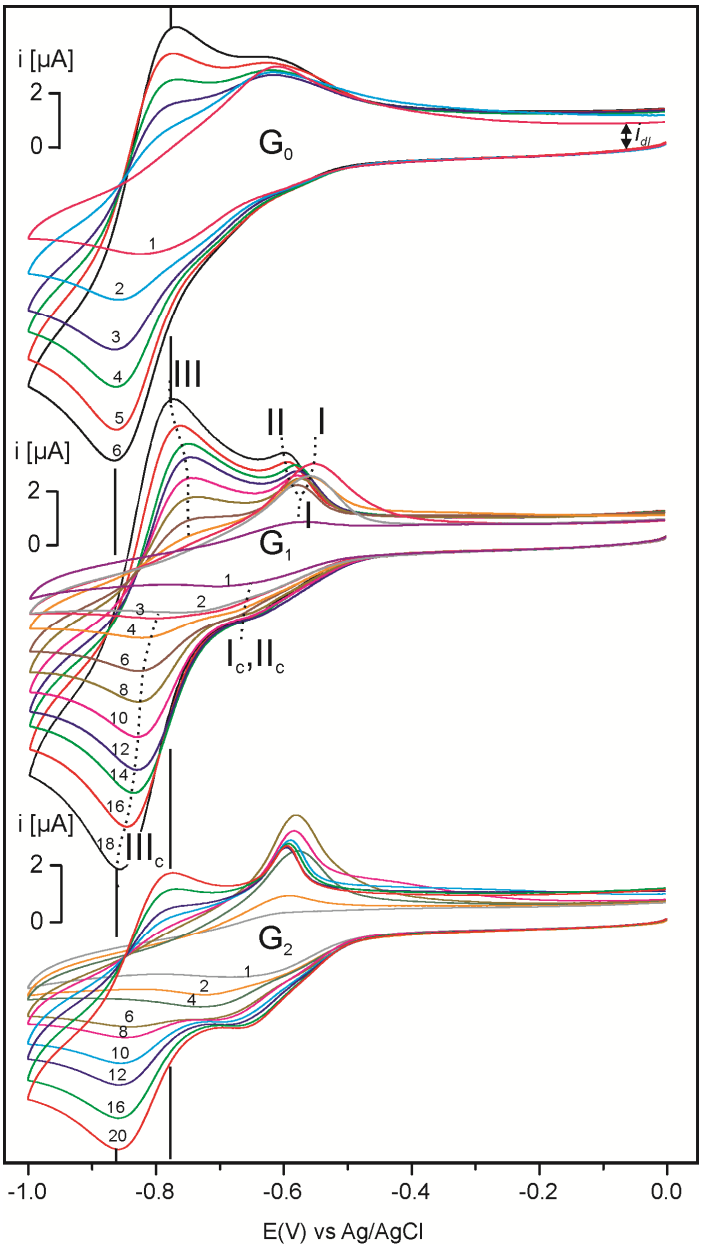

Figure 4-7: CV titration of G_0, G_1 and G_2 dendrimer *vs.* AQDS in DMF / 0.1M TBA.PF_6; [G_0] = 165 µM; [G_1] = 58 µM and [G_2] = 35 µM; numbers on each voltammogram indicate the number of added equivalents of AQDS

upon reduction as confirmed by the electrode capacitance measurement (Figure 4-8). Upon further AQDS additions anodic peak II (diffusion controlled) develops, whereas the corresponding cathodic peak (I_c, II_c) becomes plateau shaped, accompanied by an increase in

the electrode capacitance in the concentration range of total charge compensation. A new wave close to the potential of free AQDS develops for 4 and more equiv as a reversible wave with E_{pc} III_c and E_{pa} III. A closer look reveals that in spite of its proximity to the free AQDS couple (black vertical lines) –AQDS is complexed by the dendrimer (see curved black dotted lines moving into the peak potentials of free AQDS for large guest concentration).

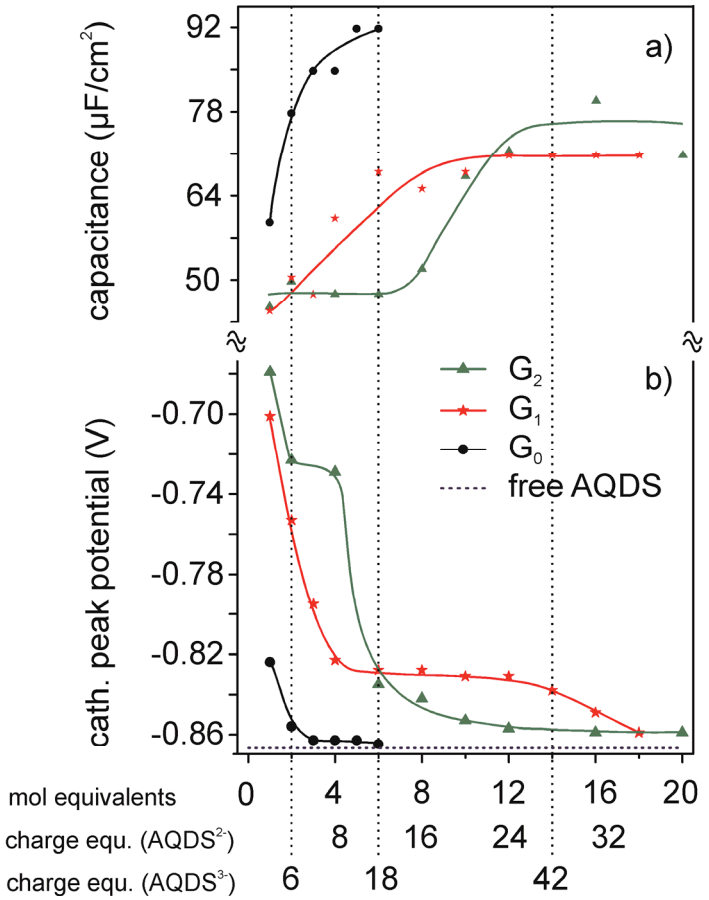

Figure 4-8: Plot of (a) the specific capacitance of the glassy carbon electrode at 0 V and (b) the cath. peak potential vs. equivalents of AQDS as dianion or triple anion; [G_0] = 165 µM; [G_1] = 58 µM; [G_2] = 35 µM; specific capacitance of AQDS = 257 µF/cm²; G_0 = 207 µF/cm²; G_1 = 163 µF/cm²; G_2 = 157 µF/cm²

In Figure 4-8a and b, the electrode capacitance and the reduction peak potential are plotted against AQDS equivalents. The capacitance curve shows prominent points at 6 equiv for **G_1** (corresponding to 9 equiv charge-corrected), 14 equiv for **G_2** (corresponding to 21 equiv if charge corrected). These points reflect a decrease of thickness of the adsorbate at the point of complete charge compensation influencing the pseudo-capacitance, C_p with

$$C_p = (I_{dl}/\nu)$$

where I_{dl} is the double-layer capacitance (Figure 4-7), ν is the scan rate.[89]

From this equation, surface specific capacitance will be given by C_p/A, where A is the surface area of the working electrode.

A persistent adsorbat layer could explain the plateau character of peak I_c, II_c by the catalytic current related to the delivery of electrons through the adsorbate onto complexed dendrimers in solution. More important in the context of the description of the AQDS-dendrimer complex is the appearance of the shell capacity numbers (corrected for an additional charge because of the reduction), whatsoever, the correlation is less pronounced than in the NMR study.

4.1.2.4 Modeling

Force field modeling MM+ implemented on Hyperchem 8.08[F] was used to judge the structure and size of the dendrimers as a function of the generation and upon guest complexation (Figure 4-9). Notably, these are gas phase calculation and therefore the charge interaction (each pyridinium carries +1 and each sulfonate oxygen -0.33) is severely over-estimated. However, the general trends are in agreement with our experimental observations. $\mathbf{G_0}$ is almost flat except for the *tert*-butylbenzyl end groups, whereas $\mathbf{G_1}$ and especially $\mathbf{G_2}$ show a dumbbell type ellipsoidal structure. Crude estimates of the large radii of the ellipsoids are given in Figure 4-9 a). The ellipsoidal radii are 50 to 100 % larger as compared to the hydrodynamic radii calculated from the diffusion coefficients (DOSY, Table 2) and a hard sphere model. However, all calculated structures are very "open" and allow much conformational freedom; definitely they are not hard spheres. Because of the unfavorable charge interaction the simulation drives the branches at maximum distance from each other. A limiting generation seems to be far away. Upon reaction with 5 equiv AQDS, as exemplified

[F] HyperChem(TM) Professional 8.0.8, Hypercube, Inc., 1115 NW 4th Street, Gainesville, Florida 32601, USA

for the case of **G_1** in Figure 4-9 b), the arms fold back, the ellipsoidal radius decreases by ca 20 % ($r_{calc(free)}$ = 3.45, $r_{calc(5AQDS)}$ = 2.75) to be compared with the experiment showing a ca. 35 % decrease ($r_{h(free)}$ = 1.63, $r_{h(5AQDS)}$ = ca. 1.02, Table 1). Other calculations also indicate severe contraction of the radii, if the dendrimer charge is counter balanced by anions carrying a single negative charge such as I^- or PF_6^- (Experimental Section).

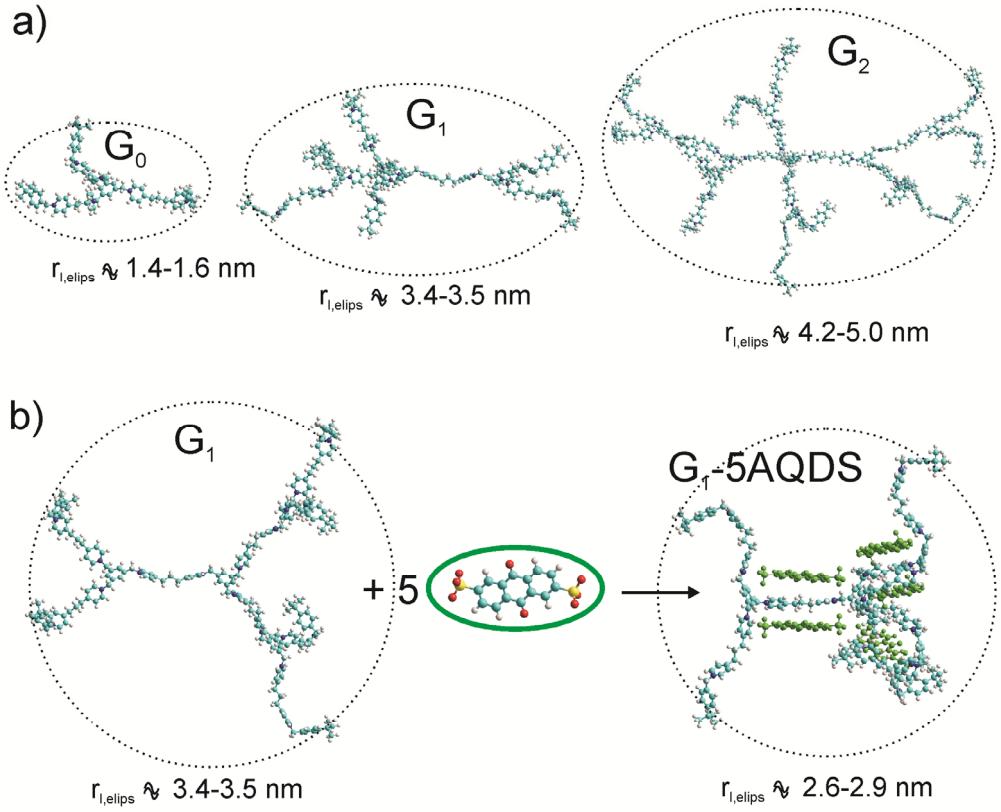

Figure 4-9: MM+ Modeling of the dendrimers: a) G_0, G_1 and G_2 MM+ geometry optimized without counter ions; unfavorable electrostatic interactions push the side chains at maximum distance from each other yielding dumbbell-type ellipsoidal structures for higher generations; presented ca. 70° out of the main ellipsoidal plane. b) G_1 relaxed as in a) but at 20° out of the main plane alone and after complexation of 5 molecules AQDS bearing one negative charge on each sulfonate
$R_{l,ellips}$ = large radius of the ellipsoidal structures

4.2 Conclusions

In this work we have introduced a new class of highly charged cationic dendrimers based on 1,3,5-tris-methylbenzene branching units interconnected by trimethylene dipyridinium. The synthetic strategy follows here a divergent approach but the intermediates necessary for a convergent route are also reported. The syntheses described are conceptually

similar to the synthesis of the corresponding viologen dendrimers.[10a,43] In contrast to the viologen (4,4′-bipyridinium) dendrimers, the new trimethylendipyridinium dendrimers show no reversible electrochemistry (disruption of conjugation), they show higher flexibility (additional trimethylene), and they are expected to have a higher limiting generation (0.3 nm larger distance between the trimethylbenzene branching units). According to MM+ calculations (neglecting counter ions and solvent) generation 0 has a disk conformation whereas generation 1 and 2 adopt open dumbbell type ellipsoidal conformations in order to minimize unfavorable charge interactions between the pyridinium moieties (Figure 9). The flexibility and the neglect of counter ions account for a considerable overestimation of the corresponding theoretical hydrodynamic radii. In contrast, the use of a hard sphere model to calculate the hydrodynamic radius from the diffusion coefficient (from DOSY experiments) underestimates this parameter.

The model anti-cancer drug anthraquinone-2,6-disulfonic acid (AQDS)[84b] is a tailored guest for the new dendrimers. The two sets of negatively charged sulfonate oxygens (distance 1.1 nm) correspond well to the distance between the pyridinium nitrogens (distance 1.1 nm) in the trimethylenedipyridinium unit (Figure 2) Upon addition of substoichiometric amounts of the AQDS guest, the dendrimers contract and reach their smallest diameter (ca 2/3 of their original hydrodynamic radius) in the range of total charge compensation (Figure 6). Overcharging with the AQDS guest is possible as evidenced by NMR (NMR titration, Figure 3) and cyclic voltammetry and leads to re-opening of the dendrimer structure (increase of the hydrodynamic radius).

The dendrimers $\mathbf{G_0}$, $\mathbf{G_1}$ and $\mathbf{G_2}$ consist of 1, 2 and 3 concentric shells. The first shell can accommodate 6 counter ions (3 equiv AQDS), the second can accommodate 12 counter ions (6 equiv AQDS) and the third can host 24 counter ions (12 equiv AQDS). If charging occurs shell by shell we expect - in analogy to the Bohr atomic model - prominent changes in

experimental observables for **G_2** at 3, 9 and 21 equiv AQDS added, if – and only if – the dendrimer is loaded "shell-wise" starting with the innermost shell. The appearance of such "magic numbers" was first and so far exclusively reported by Yamamoto et al for dendrimer-guest complexation based on Lewis base-Lewis acid interactions.[12,39c,83] We found – to the best of our knowledge for the first time for cationic dendrimers– clear evidence for a stepwise shell charging of the dendrimer from inside towards the periphery (Figure 3).

Preliminary experiments with other molecular guests and other cationic dendrimers point to the generality of the principle of stepwise guest filling in molecular shells. These further results are the subject of a forthcoming paper. We finally conclude from our results and from structural analogy that the trimethylene pyridinium dendrimers are appropriate transport vehicles for many negatively charged drugs (dianionic guests). Their expected low toxicity and their high flexibility make them also suitable candidates for gene transfection.

4.3 Experimental Section

4.3.1 General

The synthetic procedure of the benzylic bromide precursors **V_1**, **W_1** were discussed in chapter 2. All starting materials and solvents were purchased from Sigma-Aldrich and used without further purification. All reactions were performed under dry conditions. HPLC grade or ACS Spectrophotometric grade solvents were used for electrochemical measurements. Elemental analyses were performed on Elementar Vario Micro cube instrument. For the host-guest interaction studies, commercially available anthraquinone-2,6-disulfonic acid disodium salt was ion-exchanged using TBA.Br in DCM/H_2O and the obtained tetrabutylammonium salts were NMR pure [slight excess of TBA.Br was noticed].

NMR spectra were recorded on Bruker 250 Avance spectrometer at 25°C, ^{1}H NMR spectra were measured at 250 MHz; ^{13}C NMR spectra were measured at 63 MHz using

CD_3CN or DMSO-d_6 as a solvent and internal reference. All chemical shifts are reported in parts per million (δ, ppm) with respect to internal standard. ^1H NMR titrations were recorded on Bruker Avance 250 spectrometer. DOSY and NOESY spectra were recorded on a Bruker Avance III 500 MHz spectrometer. Diffusion measurements were performed at different guest concentrations using a ^1H NMR pulsed-gradient experiment: the simulated spin-echo sequence which leads to the measurement of the diffusion coefficient D, where D is the slope of the straight line obtained when ln(I) is displayed against the gradient-pulse power's square according to the following equation: $\ln(I) = -\gamma^2G^2D\delta^2(\Delta-\delta/3)$, where I is the relative intensity of a chosen resonance, γ is the proton gyromagnetic ratio, Δ is the intergradient delay (60 ms), δ is the gradient pulse duration (varied between 1.5 ms to 5 ms), and G is the gradient intensity.

Electrochemistry: Cyclic voltammograms were measured under Ar with a PGSTAT 20 potentiostat from AUTOLAB controlled by a PC running under GPES for Windows, Version 4.2 (ECO Chemie 1995); a glassy carbon electrode (GCE) from Metrohm (6.0804.010) with an active electrode surface of 0.07 cm^2 at v = 0.1 V/s was used at RT. The electrode surface was polished with Al_2O_3 prior to each scan. The reference electrode was Ag / AgCl / KCl(sat.), separated by a salt bridge (DMF + 0.1 M TBA.PF_6) from the cell; the counter electrode was a Pt-wire.

4.3.2 Detailed Synthetic Procedures

4.3.2.1 Synthesis of benzylic TMDPy dendrimers using divergent strategy

1-(3,5-bis(hydroxymethyl)benzyl)-4-(3-(pyridin-4-yl)propyl)pyridinium hexafluorophosphate (V) **$V_2.PF_6$**

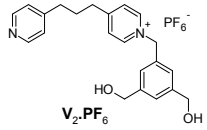

4,4´-Trimethylenedipyridine (2.14 g, 10.8 mmol) was dissolved in 30 mL CH_3CN and heated to 80°C under stirring. To this solution 3,5-bis(hydroxymethyl)benzyl bromide **V_1** (0.5

g, 2.16 mmol) dissolved in CH_3CN (20 mL) was added slowly over 6 h. The solution was stirred for another 10 h, cooled to RT and the solvent was removed under reduced pressure. The residue was partitioned between water (100 mL) and CH_2Cl_2 (100 mL), washed with CH_2Cl_2 to remove excess 4,4′-trimethylenedipyridine. The aqueous solution was then concentrated to 50 mL, 3 mL of 3M NH_4PF_6 solution was added and a viscous liquid settled down, the aqueous layer was decanted, washed with water and dried to yield $\mathbf{V_2}.PF_6$ as brown viscous liquid, 0.96 g (89%); ^{1}H-NMR (250 MHz, (*$CD_3)_2CO$*) δ ppm 8.98 (d, 2H), 8.34 (dd, 2H), 8.05 (d, 2H), 7.36 (s, 3H), 7.20 (dd, 2H), 5.85 (s, 2H), 4.56 (s, 4H), 3.02 (t, 2H), 2.73 (t, 2H), 2.16-2.04 (m, 2H). ^{13}C NMR (63 MHz, (*$CD_3)_2CO$*) δ ppm 163.4, 151.4, 148.7, 143.9, 133.3, 128.3, 125.7, 125.3, 124.1, 63.9, 63.1, 34.7, 34.1, 29.6.

1-(2-ammonioethyl)-4-[3-(pyridin-4-yl)propyl]pyridinium hexafluorophosphate(V): (not discussed in the main text)

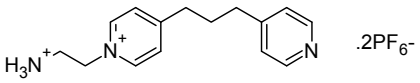

4,4′-Trimethylenedipyridine (2.5 g, 12.6 mmol) was dissolved in 30 mL CH_3CN, heated to 80°C under stirring. To this solution 2-bromoethylammonium bromide (0.516 g, 2.52 mmol) dissolved in MeOH (10 mL) was added slowly over 6 h. The solution was stirred for another 10 h, cooled to RT and the solvent was removed under reduced pressure. The residue was partitioned between water (100 mL) and CH_2Cl_2 (100 mL), washed with CH_2Cl_2 to remove excess 4,4′-trimethylenedipyridine. The aqueous solution was then concentrated to 50 mL, 3 mL of 3M NH_4PF_6 solution was added. The clear aqueous solution was kept in the refrigerator for 2 days to obtain a white powder which was then washed with water and dried to yield 1-(2-ammonioethyl)-4-[3-(pyridin-4-yl)propyl]pyridinium hexafluorophosphate(V), 0.96 g (94%); ^{1}H-NMR (250 MHz, (*CD_3CN*) δ ppm 8.56 (d, 4H), 7.92 (d, 2H), 7.51 (d, 2H), 4.63 (t, 2H), 4.28 (bs, 3H), 3.44 (t, 2H), 3.01 (t, 2H), 2.86 (t, 2H), 2.1 (m, 2H); ^{13}C NMR (63

MHz, ($CD_3)_2CO$) δ ppm 163.8, 155.8, 146.3, 144.2, 128.2, 125.3, 59.1, 40.5, 34.5, 34.2, 29.4; Anal. Calcd for $C_{15}H_{21}N_3P_2F_{12}$: C, 33.78; H, 3.97; N, 7.88. Found C, 33.59; H, 4.06; N, 7.93.

1-benzyl-4-(3-(pyridin-4-yl)propyl)pyridinium hexafluorophosphate(V) **E′.PF$_6$**

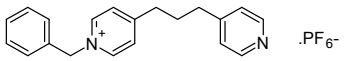

The above mentioned procedure is followed. Brown viscous liquid, 1.02 g (80%); ^{1}H-NMR (250 MHz, CD_3CN) δ ppm 8.64 (d, 2H), 8.49 (d, 2H), 7.88 (d, 2H), 7.49 (s, 5H), 7.26 (d, 2H), 5.68 (s, 2H), 2.96 (t, 2H), 2.74 (t, 2H), 1.97 (s, 2H). ^{13}C-NMR (63 MHz, CD_3CN) δ ppm 163.6, 151.2, 149.1, 143.7, 133.2, 129.8, 129.5, 129.0, 128.3, 124.1, 63.7, 34.6, 33.9, 29.7.

1-(4-tert-butylbenzyl)-4-(3-(pyridin-4-yl)propyl)pyridinium hexafluorophosphate(V) **E.PF$_6$**

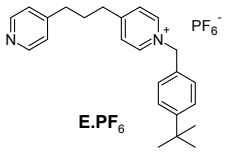

1-(4-*tert*-butylbenzyl)-4-(3-(pyridin-4-yl)propyl)pyridinium hexafluorophosphate(V) was synthesized by reacting 4,4′-trimethylenedipyridine (1.74 g, 8.8 mmol) and 4-*tert*-butylbenzyl bromide (4-*t*-BuBnBr) (1 g, 4.4 mmol) in 50 mL EtOAc under refluxing conditions. The solution was stirred for 6 h, cooled to RT and the precipitate was filtered, washed with excess EtOAc. The residue was dissolved in water, 3 mL of 3M NH_4PF_6 solution was added, the product settled down as a viscous liquid, the aqueous layer was decanted, washed with water and dried to yield **E**.PF_6 as white solid, 2.05 g (95%); ^{1}H-NMR (250 MHz, CD_3CN) δ ppm 8.61 (d, 2H), 8.49 (s, 2H), 7.86 (d, 2H), 7.54 (d, 2H), 7.38 (d, 2H), 7.24 (d, 2H), 5.63 (s, 2H), 2.95 (t, 2H), 2.73 (t, 2H), 2.12-2.01 (m, 2H), 1.33 (s, 9H); ^{13}C-NMR (63 MHz, CD_3CN) δ ppm 163.6, 153.1, 150.9, 149.3, 143.5, 130.3, 128.7, 128.3, 126.4, 124.1, 63.4, 34.6, 34.4, 30.4, 29.7; Anal. Calcd for $C_{24}H_{29}N_2PF_6.H_2O$: C, 56.69; H, 6.14; N, 5.51. Found C, 56.56; H, 6.04; N, 5.53.

1,1′,1′′-(benzene-1,3,5-triyltris(methylene))tris(4-(3-(pyridin-4-yl)propyl)pyridinium) hexafluorophosphate(V) **$P_0.3PF_6$**

4,4′-Trimethylenedipyridine (6.25 g, 31.5 mmol) was dissolved in 50 mL CH_3CN and heated to 80°C under stirring. To this solution 1,3,5-tris(bromomethyl)benzene (0.75 g, 2.1 mmol) dissolved in CH_3CN (20 mL) was added slowly over 8 h. The solution was stirred overnight, cooled to RT and the solvent was removed under reduced pressure. The residue was partitioned between water (100 mL) and CH_2Cl_2 (100 mL), washed with DCM to remove

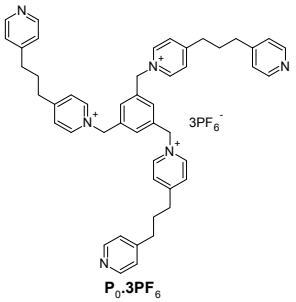

$P_0.3PF_6$

excess 4,4′-trimethylenedipyridine. The aqueous layer was then concentrated to 50 mL, 3 mL of 3M NH_4PF_6 solution was added, viscous liquid settled down, the aqueous layer was decanted, washed with water and the sample was dried to yield **P_0**.$3PF_6$ as a brown solid, 1.92 g (80%); ^{1}H-NMR (250 MHz, *CD_3CN*) δ ppm 8.51 (dd, 12H), 7.85 (d, 6H), 7.49 (s, 3H), 7.29 (d, 6H), 5.65 (d, 6H), 2.96 (t, 6H), 2.76 (t, 6H), 2.07 (m, 6H); ^{13}C-NMR (63 MHz, *CD_3CN*) δ ppm 163.9, 152.2, 148.5, 143.8, 135.4, 130.9, 128.3, 124.4, 62.6, 34.6, 34.0, 29.6; Anal. Calcd for $C_{48}H_{51}N_6P_3F_{18}.4H_2O$: C, 47.30; H, 4.88; N, 6.89. Found C, 47.12; H, 4.23; N, 7.02.

$G_0.6PF_6$:

P_0.$3PF_6$ (0.2 g, 0.17 mmol) and 4-*t*-BuBnBr (0.19 mL, 1.04 mmol) were dissolved in 20mL CH_3CN, refluxed for 1 d. The solution was cooled, solvent was removed under reduced pressure and the residue was washed with EtOAc to remove excess 4-*t*-BuBnBr. The residue was then dissolved in MeOH/H_2O, precipitated with 3M NH_4PF_6, filtered, washed with H_2O and dried to yield **G_0**.$6PF_6$ as a brown solid, 0.32 g (91%); ^{1}H-NMR (250 MHz, *CD_3CN*) δ ppm 8.61 (dd, 12H), 7.89 (s, 12H), 7.54 (d, 9H), 7.38 (s, 6H), 5.64 (s, 12H), 2.98 (t, 12H),

2.09 (m, 6H), 1.33 (s, 27H); ^{13}C-NMR (63 MHz, *CD_3CN*) δ ppm 163.2, 162.8, 153.1, 143.9, 143.7, 135.3, 131.0, 128.8, 128.3, 126.4, 63.5, 62.6, 34.3, 30.4, 28.8; Anal. Calcd for $C_{81}H_{96}N_6P_6F_{36}.3H_2O$: C, 46.83; H, 4.95; N, 4.05. Found C, 46.87; H, 5.27; N, 4.15.

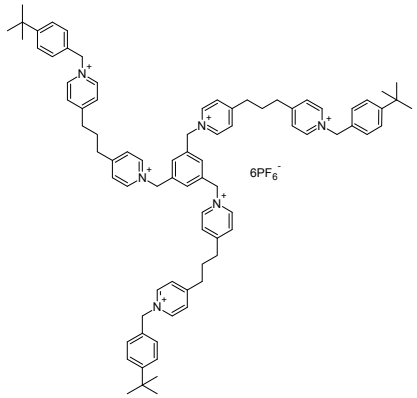

$G_0.6PF_6$

$G_0'.6PF_6$:

Brown solid; Yield: 75%; ^{1}H-NMR (250 MHz, *CD_3CN*) δ ppm 8.61 (dd, 12H), 7.89 (d, 12H), 7.40 (m, 18H), 5.69 (d, 12H), 3.00 (s, 12H), 2.12 (m, 6H); ^{13}C-NMR (63 MHz, *CD_3CN*) δ ppm 163.3, 162.9, 143.9, 143.8, 135.3, 133.1, 131.0, 129.8, 129.5, 129.0, 128.8, 128.4, 128.3, 63.8, 62.7, 34.3, 28.7; Anal. Calcd for $C_{69}H_{72}N_6P_6F_{36}.H_2O$: C, 44.24; H, 3.98; N, 4.48. Found C, 44.36; H, 4.02; N, 4.45.

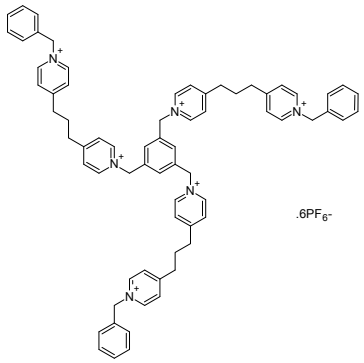

$G_0''.6PF_6$:

Pale brown solid, Yield: 73%; ^{1}H-NMR (250 MHz, *CD_3CN*) δ ppm 8.55 (dd, 12H), 7.49 (s, 3H), 5.66 (s, 6H), 4.28 (s, 9H), 3.00 (s, 12H), 2.15-2.03 (m, 6H); ^{13}C-NMR (63 MHz, *CD_3CN*) δ ppm 163.3, 161.9, 144.7, 143.9, 135.3, 131.0, 128.4, 127.8, 62.7, 47.6, 34.3, 34.3,

28.8; Anal. Calcd for $C_{51}H_{60}N_6P_6F_{36}$: C, 37.65; H, 3.72; N, 5.16. Found C, 37.71; H, 4.18; N, 5.15.

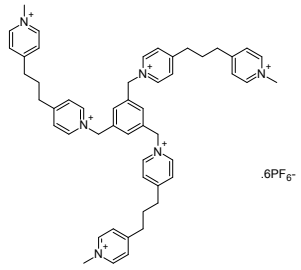

P_1.6PF_6:

P_0.3PF_6 (0.75 g, 0.65 mmol) and 3,5-bis(hydroxymethyl)benzyl bromide **V_1** (0.56 g, 2.42 mmol) were dissolved in 20mL CH_3CN, refluxed for 1 d. (Note: After alkylation, the product is insoluble, hence bromination was carried out with the insoluble residue which became soluble in 5.6M HBr/HOAc upon refluxing at RT. The resulting brominated product was soluble in either H_2O or MeOH/H_2O with a little residue left behind; hence the solution was filtered before converting it into the PF_6 salt. As prolonged exposure to air causes

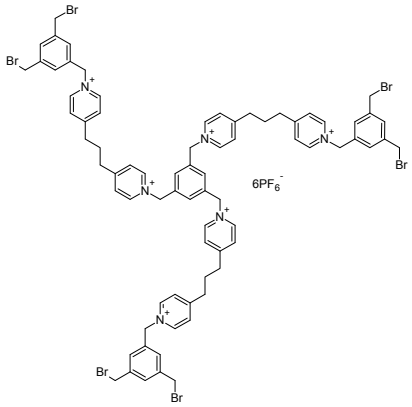

P_1.6PF_6

decomposition of the hexabromide and insolubility, the product is stored at 4°C under argon). The aqueous solution was cooled; the solvent was removed under reduced pressure, brominated using 200 mL 5.6M HBr/HOAc for 2 d. The acid was removed under reduced pressure, the residue was dissolved in H_2O or MeOH/H_2O, precipitated with 3M NH_4PF_6,

filtered, washed with excess water and dried to yield **P$_1$**.6PF$_6$ as a pale brown powder, 1.05 g (66%); ^{1}H-NMR (250 MHz, *CD$_3$CN*) δ ppm 8.66-8.57 (m, 12H), 7.91 (d, 12H), 7.6-7.45 (m, 12H), 5.66 (d, 12H), 4.59 (s, 12H), 2.99 (t, 12H), 2.10 (m, 6H); ^{13}C-NMR (63 MHz, *CD$_3$CN*) δ ppm 163.2, 144.0, 140.4, 135.3, 134.4, 131.0, 129.4, 128.4, 63.0, 62.6, 34.4, 32.1, 28.8; Anal. Calcd for $C_{75}H_{78}N_6Br_6P_6F_{36}.2H_2O$: C, 36.79; H, 3.37; N, 3.43. Found C, 37.06; H, 3.38; N, 3.43.

G$_1$.18PF$_6$:

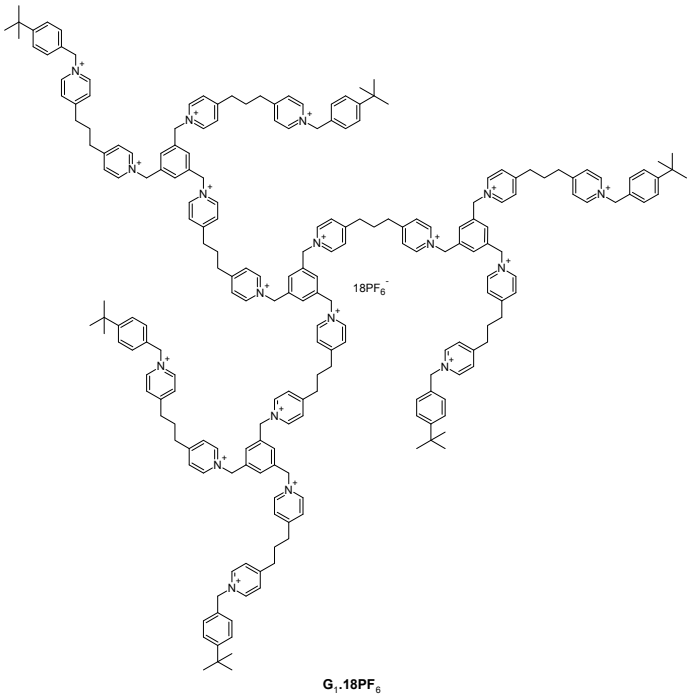

P$_1$.6PF$_6$ (0.15 g, 62 μmol) and **E**.PF$_6$ (0.228 g, 466 μmol) were dissolved in 30 mL CH_3CN, refluxed for 4 d. The solvent was removed under reduced pressure, the residue was dissolved in MeOH/H_2O, precipitated with 3M NH_4PF_6, filtered, washed with H_2O and dried to yield **G$_1$**.18PF$_6$ as a dark brown solid, 0.348 g (97%); ^{1}H-NMR (250 MHz, *DMSO-d$_6$*) δ ppm 8.98 (dd, 36H), 8.04 (bs, 36H), 7.60-7.57 (m, 12H), 7.45 (s, 24H), 5.74 (s, 36H), 2.95 (bs, 36H), 2.08 (m, 18H), 1.25 (s, 54H); ^{13}C-NMR (63 MHz, *DMSO-d$_6$*) δ ppm 162.8, 162.2, 152.4, 144.6, 136.3, 131.9, 128.9, 128.4, 126.5, 62.9, 62.3, 34.9, 34.5, 31.4, 31.1, 28.6; Anal.

Calcd for $C_{219}H_{252}N_{18}P_{18}F_{108}.18H_2O$: C, 43.33; H, 4.78; N, 4.15. Found C, 43.04; H, 4.96; N, 3.70.

$P_2.18PF_6$:

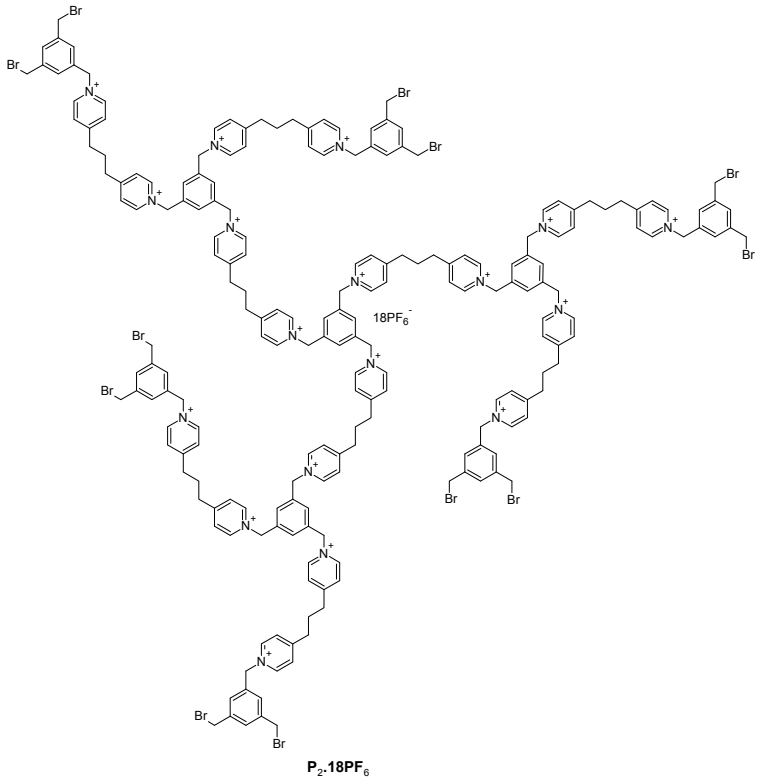

P_1.$6PF_6$ (0.4 g, 0.174 mmol) and **V_2**.PF_6 (0.576 g, 1.27 mmol) were dissolved in 40mL CH_3CN, refluxed for 4 d. The solution was cooled; the solvent was removed under reduced pressure, brominated using 200 mL 5.6M HBr/HOAc for 2 d. The acid was removed under reduced pressure, the residue was dissolved in $MeOH/H_2O$, precipitated with 3M NH_4PF_6, filtered, washed with excess water and dried to yield **P_2**.$18PF_6$ as a pale brown powder, 0.65 g (60%); ^{1}H-NMR (250 MHz, *CD_3CN*) δ ppm 8.61 (m, 36H), 7.91 (m, 36H), 7.52 (m, 30H), 5.65 (s, 36H), 4.59 (s, 24H), 3.01 (t, 36H), 2.06 (m, 18H); ^{13}C-NMR (63 MHz, *CD_3CN*) δ ppm 163.2, 144.0, 140.4, 135.3, 134.4, 131.0, 129.4, 128.3, 63.0, 62.7, 34.4, 32.2, 28.8; Anal. Calcd for $C_{207}H_{216}N_{18}Br_{12}P_{18}F_{108}$: C, 38.11; H, 3.34; N, 3.86. Found C, 38.07; H, 3.31; N, 3.84.

G_2.42PF_6:

P_2.18PF_6 (0.15 g, 23 μmol) and **E**.PF_6 (0.158 g, 322 μmol) were dissolved in 50 mL CH_3CN, refluxed for 7 d. The solvent was removed under reduced pressure, the residue was dissolved in MeOH/H_2O, precipitated with 3M NH_4PF_6, filtered, washed with H_2O and dried to yield **G_2**.42PF_6^- as a dark brown solid, 0.292 g (96%); ^{1}H-NMR (250 MHz, *DMSO-d_6*) δ ppm 8.97 (m, 84H), 8.04 (m, 84H), 7.61 (m, 30H), 7.45 (s, 48H), 5.74 (s, 84H), 2.95 (m, 84H), 2.08 (m, 42H), 1.24 (s, 108H); ^{13}C-NMR (63 MHz, *DMSO-d_6*) δ ppm 162.8, 162.2, 152.4, 144.7, 144.5, 136.4, 131.9, 128.9, 128.5, 126.5, 62.8, 62.3, 34.9, 34.6, 31.4, 28.6; Anal. Calcd for $C_{495}H_{564}N_{42}P_{42}F_{252}$.42$H_2O$: C, 42.63; H, 4.68; N, 4.22. Found C, 41.87; H, 4.76; N, 3.83.

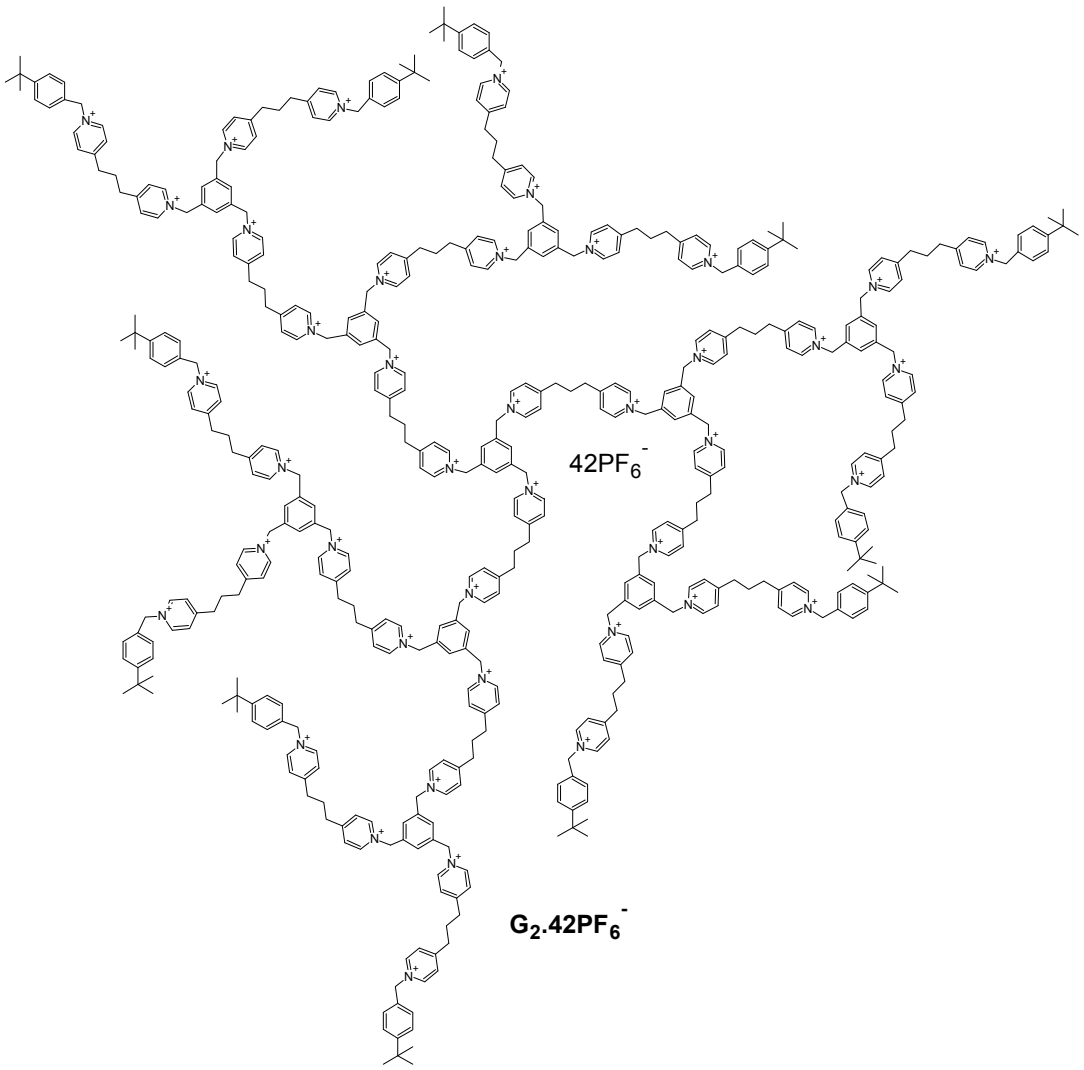

4.3.2.2 Synthesis of the convergent dendrons

1,1′-(5-(hydroxymethyl)-1,3-phenylene)bis(methylene)bis(4-(3-(pyridin-4-yl)propyl)pyridinium) hexafluorophosphate(V) **$W_2.2PF_6$**

4,4′-Trimethylenedipyridine (5.06 g, 25 mmol) was dissolved in 30 mL CH_3CN, heated to 80°C under stirring. To this solution 5-hydroxymethyl-1,3-bis(bromomethyl)benzene, **W_1** (0.75 g, 2.5 mmol) dissolved in CH_3CN (20 mL) was added slowly over 8 h. The solution was stirred for another 12 h, cooled to RT and the solvent was removed under reduced pressure. The residue was partitioned between water (100 mL) and

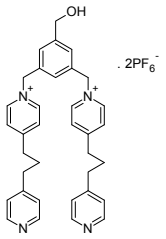

CH_2Cl_2 (100 mL), washed with CH_2Cl_2 to remove excess 4,4′-trimethylenedipyridine. The aqueous solution was then concentrated to 50 mL, 3 mL of 3M NH_4PF_6 solution was added, viscous liquid settled down, the aqueous layer was decanted, washed with water and dried to yield **$W_2.2PF_6$** as a brown solid, 1.6 g (76%); ^{1}H-NMR (250 MHz, *CD_3CN*) δ ppm 8.6-8.4 (unresolved coupling, 8H), 7.83 (s, 4H), 7.34 (m, 3H), 7.21 (d, 4H), 5.65 (s, 4H), 4.64 (s, 2H), 2.98 (t, 4H), 2.73-2.70 (m, 4H), 2.17-2.02 (m, 4H); ^{13}C-NMR (63 MHz, *CD_3CN*) δ ppm 164.0, 152.0, 150.8, 149.3, 148.9, 145.3, 143.6, 134.3, 128.2, 124.2, 63.1, 62.6, 34.7, 34.0, 30.5, 29.6; Anal. Calcd for $C_{35}H_{38}N_4P_2F_{12}O$: C, 51.23; H, 4.66; N, 6.82. Found C, 51.60; H, 4.77; N, 7.04.

$W_3.4PF_6$:

$W_2.2PF_6$ (0.2 g, 243 μmol) and 4-*t*-BuBnBr (0.13 mL, 731 μmol) were dissolved in 20mL CH_3CN, refluxed for 1 d. The solution was cooled, solvent was removed under reduced pressure and the residue was washed with EtOAc to remove excess 4-*t*-BuBnBr. The residue

was then dissolved in MeOH/H_2O, precipitated with 3M NH_4PF_6, filtered, washed with H_2O and dried to yield **W_3.4PF_6** as a brown solid, 0.23 g (68%); ^{1}H-NMR (250 MHz, *CD_3CN*) δ

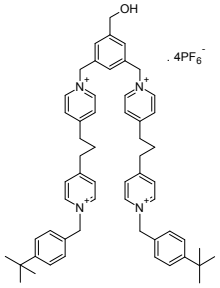

ppm 8.63 (s, 8H), 7.89 (s, 8H), 7.56 (d, 4H), 7.47 (s, 2H), 7.40 (d, 5H), 5.66 (s, 8H), 4.61 (s, 2H), 3.00 (t, 8H), 2.11 (m, 4H), 1.34 (s, 18H); ^{13}C-NMR (63 MHz, *CD_3CN*) δ ppm 163.1, 162.8, 153.1, 143.9, 143.7, 134.2, 130.2, 128.8, 128.3, 128.1, 126.4, 63.5, 63.2, 62.6, 34.4, 30.4, 28.7; Anal. Calcd for $C_{57}H_{68}N_4P_4F_{24}O.H_2O$: C, 48.11; H, 4.96; N, 3.94. Found C, 47.85; H, 4.84; N, 4.23.

W_3'.4PF_6:

W_2.2PF_6 (0.2 g, 243 μmol) and CH_3I (0.15 mL, 2.43mmol) were dissolved in 20mL CH_3CN, stirred at 50°C for 1 d. The solution was cooled, solvent was removed under reduced pressure, the residue was dissolved in MeOH/H_2O, precipitated with 3M NH_4PF_6, filtered, washed with H_2O and dried to yield **W_3'.4PF_6** as a brown solid, 0.17 g (61%); ^{1}H-NMR (250 MHz, *CD_3CN*) δ ppm 8.57 (s, 8H), 7.89 (s, 8H), 7.49 (s, 2H), 7.41 (s, 1H), 5.68 (s, 4H), 4.62 (s, 2H), 4.27 (s, 6H), 3.00 (s, 8H), 2.12 (m, 4H); ^{13}C-NMR (63 MHz, *CD_3CN*) δ ppm 163.1, 161.9, 145.1, 144.6, 143.9, 134.2, 128.4, 128.1, 127.8, 63.2, 62.6, 47.6, 34.3, 34.2, 28.8.

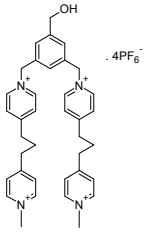

4.3.3 Estimation of association constant of the first AQDS complexation with an empty G_2- dendrimer

DOSY experiment: c(**G_2**)$_{initial}$ = c(**AQDS**) $_{initial}$ = 0.97 mM = 1 * 10^{-3} M

at 8 equiv. addition of AQDS there is no free AQDS observed leading to the assumption, that more than 90 % of AQDS is complexed at the first addition.

first association equilibrium:

$$G_2 + AQDS \rightleftharpoons G_2\text{-}AQDS \qquad K$$

$$K = c(\mathbf{G_2\text{-}AQDS})_{eq} / (c(\mathbf{AQDS})_{eq} * c(\mathbf{G_2})$$

$$= 1*10^{-3} / (1*10^{-4} * 1*10^{-4}) = 10^5\ M^{-1}$$

Thus the real K is expected > $10^5\ M^{-1}$

4.3.4 NOESY

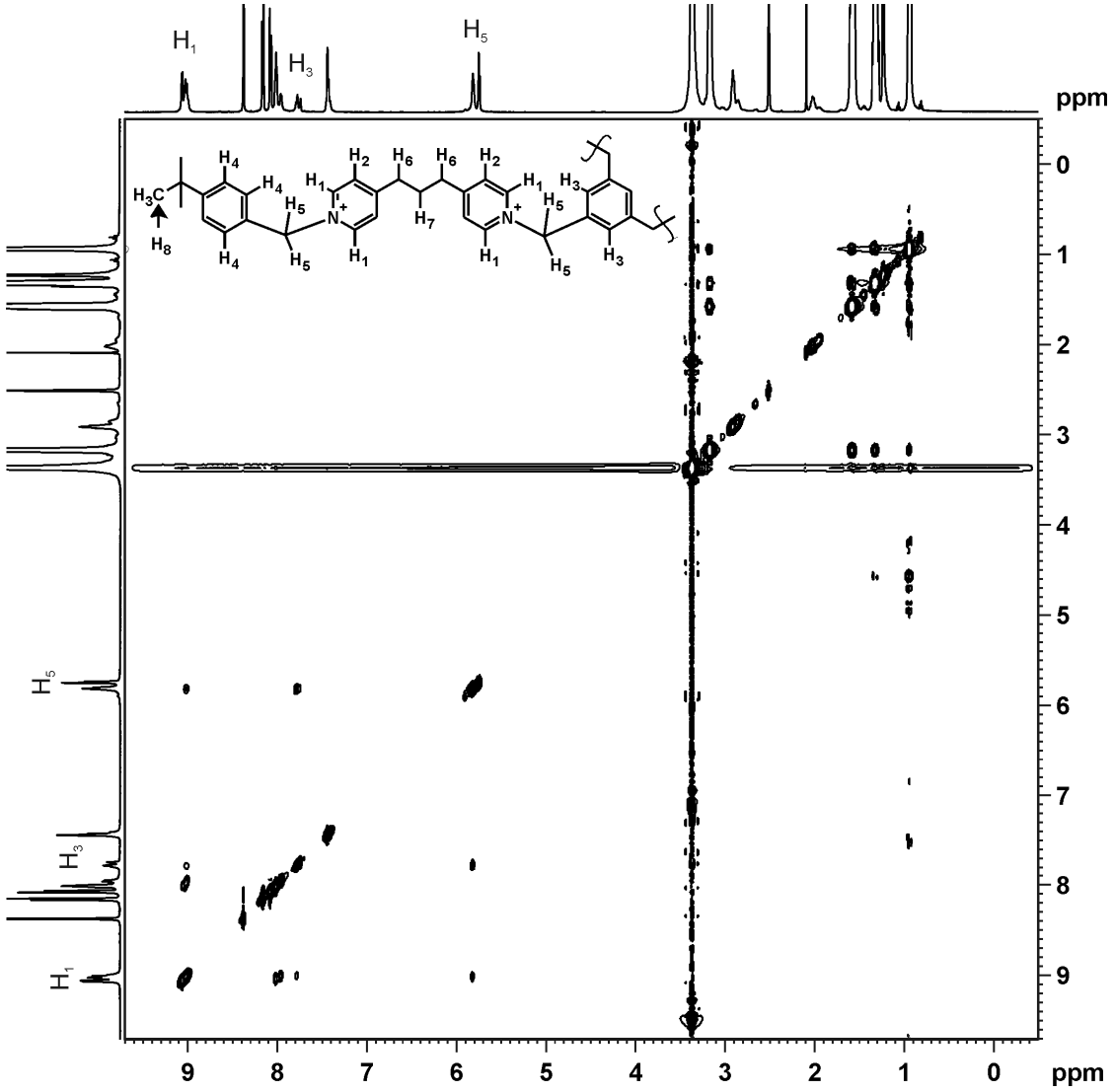

Figure 4-10*:* NOESY spectrum of G_1 dendrimer + 8equiv AQDS

NOESY spectra were done on mixtures of **G_1** and AQDS. Interestingly we do not observe any cross-peaks between the protons of the dendrimer and AQDS. However, there are well defined cross peaks corresponding to intramolecular interaction of protons H_1, H_3 and H_5 on the dendrimer (Figure 5-10).

4.3.5 MM+ simulation

The MM+ force field implemented in HyperChem 8.0.8[79] was used for the geometry optimization of G_0, G_1 and G_2. The charge was +1 on all pyridinium N and -0.33 on all oxygens of the sulfonate groups. All other atoms were at 0 charges. *Atomic charges* and *cut-off: none* was selected in the options. In most sets of optimizations the guest molecule(s) was/were *name selected*: *fixed atom* in order to let the dendrimer wrap them and to omit distortions on the AQDS.

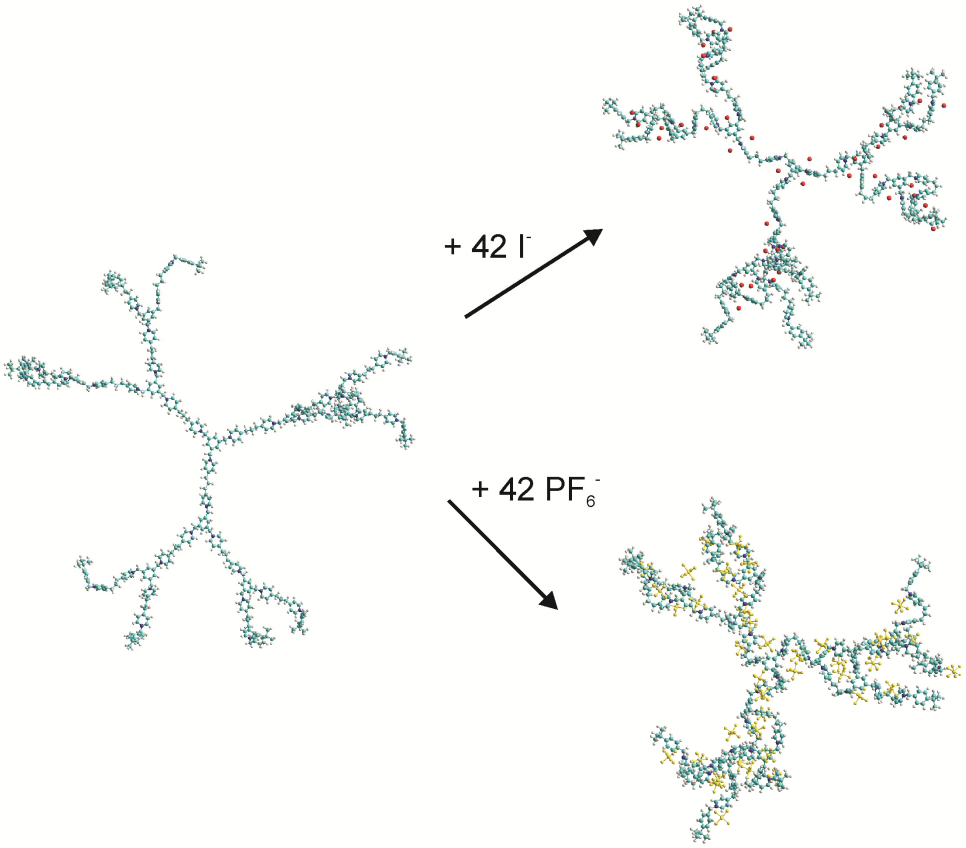

Figure 4-11: Contraction of G_2 without counter ions upon addition of 42 Iodide ions (red spheres) or 42 PF_6^- ions (yellow octahedras)

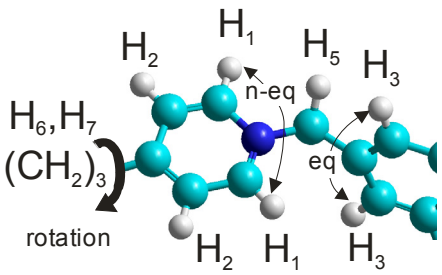

Figure 4-12: Substructure from MM+ simulation showing magnetic non-equivalency of H_1 and equivalency of H_3 in the non complexed (AQDS free) relaxed state

4.3.6 Scheme of Squares

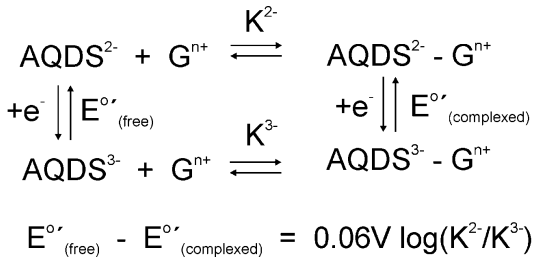

Figure 4-13: Scheme of Squares

Upon complexation of a redox active guest its standard reduction potential $E^{0'}_{(free)}$ may shift to $E^{0'}_{(complexed)}$ if one of the oxidation states has a higher affinity towards the dendrimer (larger K value) than the other oxidation state. As $AQDS^{2-}$ becomes $AQDS^{3-}$ after reduction, one might expect $K^{3-} > K^{2-}$ and thus, $E^{0'}_{(complexed)}$ to be more positive than $E^{0'}_{(complexed)}$. This is experimentally observed but (i) it is hidden by the adsorption behavior and (ii) the potential shift is rather small.[85]

5 Step-wise Radial Complexation in Pyridinium Dendrimers

Manuscript in preparation

Dendrimers can act as hosts for smaller molecular guests, a fact that has been used for fundamental studies[50f,90] as well as for drug delivery applications.[91] Depending on the functionalities present on the dendrimer (ionic,[10c,11a,38,43,76] hydrophobic,[50f,91c] H-bonding[17,50f] etc.) charged,[92] neutral,[93] or H-bonding[17] guest molecules can be complexed and transported.[23b] The usual divergent synthetic procedures allow producing such functionalities exclusively at the core, along the branches or at the periphery, opening the design of localized complexation sites within a dendrimer.[22,71g,72a] Complexation can occur either in a random or in a step-wise fashion.[12,83] Another approach can be based mainly on a steric phenomenon, i.e., the voids in the innermost molecular shell of highly branched dendrimers appearing close to their limiting generation. Such dendritic boxes are able to reversibly complex certain molecular guests.[3] On the other hand there exist dendrimers with complexation sites (e.g. positive charges) distributed all through the dendrimer (center, branches and periphery) equally. The PPI, PAMAM are examples of such structures, however exhibiting a complex pH dependent dissociation degree (nothing being known about the radial distribution of cationic sites). Most importantly, nothing has been reported about the preference of molecular guests to bind at the periphery, along the branches or in the center for a dendrimer with identical ionic complexation sites all through its structure.

Except Yamamoto et al's report on the sequential guest complexation, there are no other reports available on other dendrimer/guest combinations showing the same stepwise charging mode, and the question is still not solved, if the phenomenon observed by Yamamoto is unique or of general importance. A decade before we reported on the divergent synthesis of viologen dendrimers;[10] convergent synthesis and guest complexation of these

molecules were reported by Balzani et al[38] but the way the guest molecules fills-in the voids of the dendrimers were not reported. Though it was reported that such stepwise radial complexation cannot be observed with organic molecules due to their radial distribution, we were able to observe the stepwise complexation of anthraquinonedisulfonate in molecular shells of trimethylenedipyridinium dendrimers. Our observations were based on the NMR and

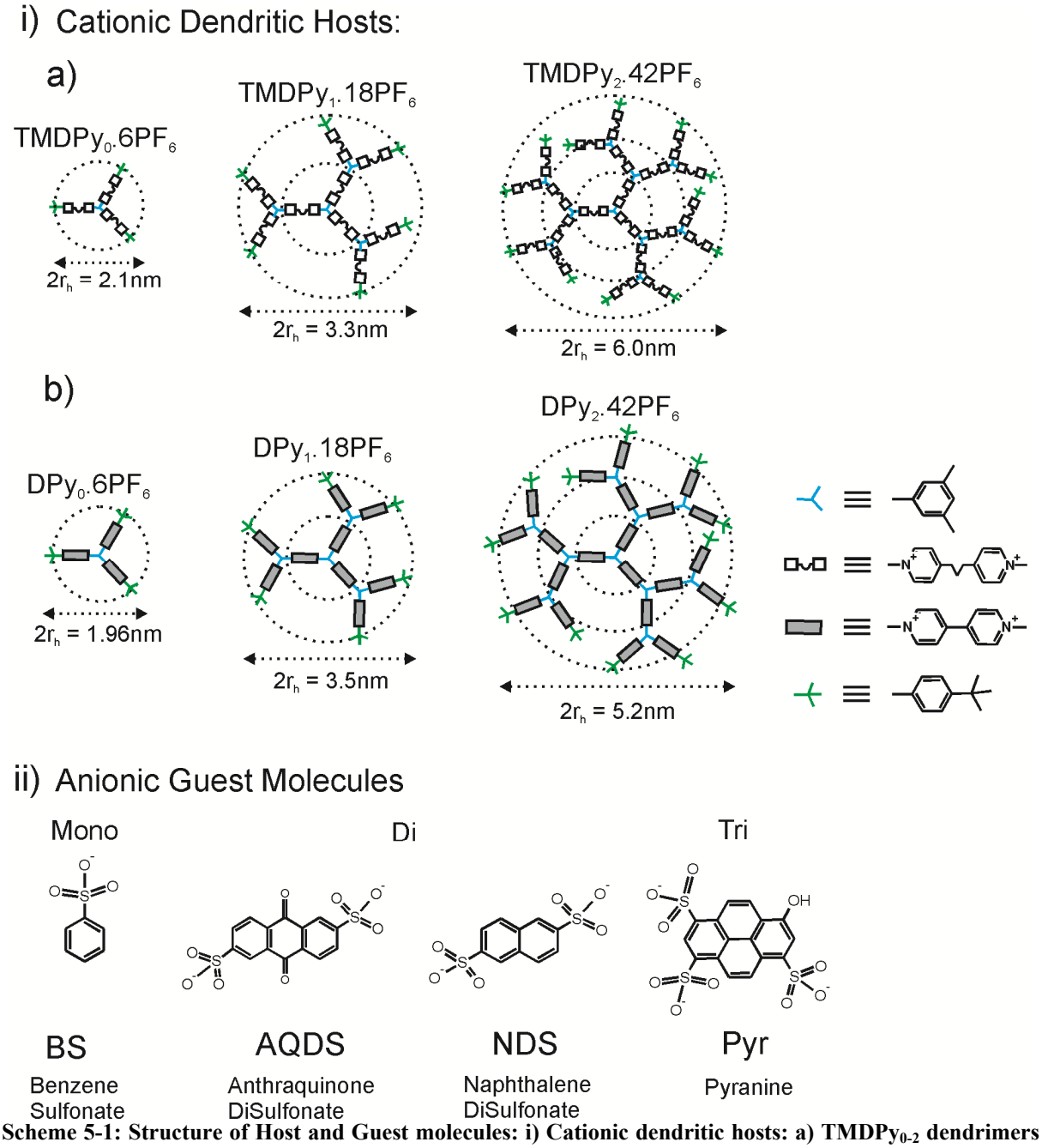

Scheme 5-1: Structure of Host and Guest molecules: i) Cationic dendritic hosts: a) $TMDPy_{0\text{-}2}$ dendrimers (non-electroactive); b) $DPy_{0\text{-}2}$ dendrimers (electroactive); ii) Anionic guest molecules (mono-, di- and trivalent); $2r_h$-hydrodynamic radii obtained from DOSY

CV titrations. This new polycationic dendrimers with their equally distributed complexation sites, arranged in molecular shells of 6, 12 and 24 pyridinium units, allowed us to deliver clear evidence for a shell-by-shell complexation of the anionic guests starting with the innermost dendritic shell and ending with the outermost.

In this study, we extended our experiments with different host and guest molecules. The benzylic trimethylenedipyridinium dendrimers (**TMDPy**) and the benzylic viologen dendrimers (**DPy**) were prepared by divergent methods as we reported before (Scheme 5-1). The purity of the compounds was checked by ^{1}H NMR, ^{13}C NMR and DEPT measurements. Further they were characterized by elemental analysis (See Experimental Section). As known earlier 4-*t*-BuBn group imparts better solubility to the dendrimers, hence we were able to perform experiments without much precipitation which we observed in the Et terminated viologen dendrimers even at low addition of the guest molecules.

Figure 5-1 shows the ^{1}H-NMR of **TMDPy$_1$** and **DPy$_1$** including the complete assignment of the proton resonances; the interacting protons were shown by dotted pink circles and in the table we summarized the protons which are responding to the different guests. Other protons respond upon guest addition, due to the overlap of these signals with the guest molecules, we were not able to monitor these shifts. The corresponding spectra of **TMDPy$_0$, DPy$_0$**, **TMDPy$_2$ and DPy$_2$** are similar except the ratio of internal to peripheral protons. The H_1 resonances on the pyridinium shows large splitting, whereas H_3 on the phenyl branching unit show only minor splitting. This points to a preferential conformation of the methylene bearing H_5 rendering the two H_1 magnetically non-equivalent, but the three H_3 magnetically almost equivalent in the absence of the guest molecule. Since the region from δ 0.9 to 4 (trimethylene (in the case of TMDPy) and *t*-Bu end groups) is dominated by solvent peaks and tetrabutyl ammonium (counter ion of the anionic guests), we focused mainly on the

changes in the region δ 5.7-9.5. The resonances due to meta-H_2 (TMDPy and DPy) at pyridinium, as well as the protons at the trimethylene bridge [TMDPy (H_6 and H_7)] show

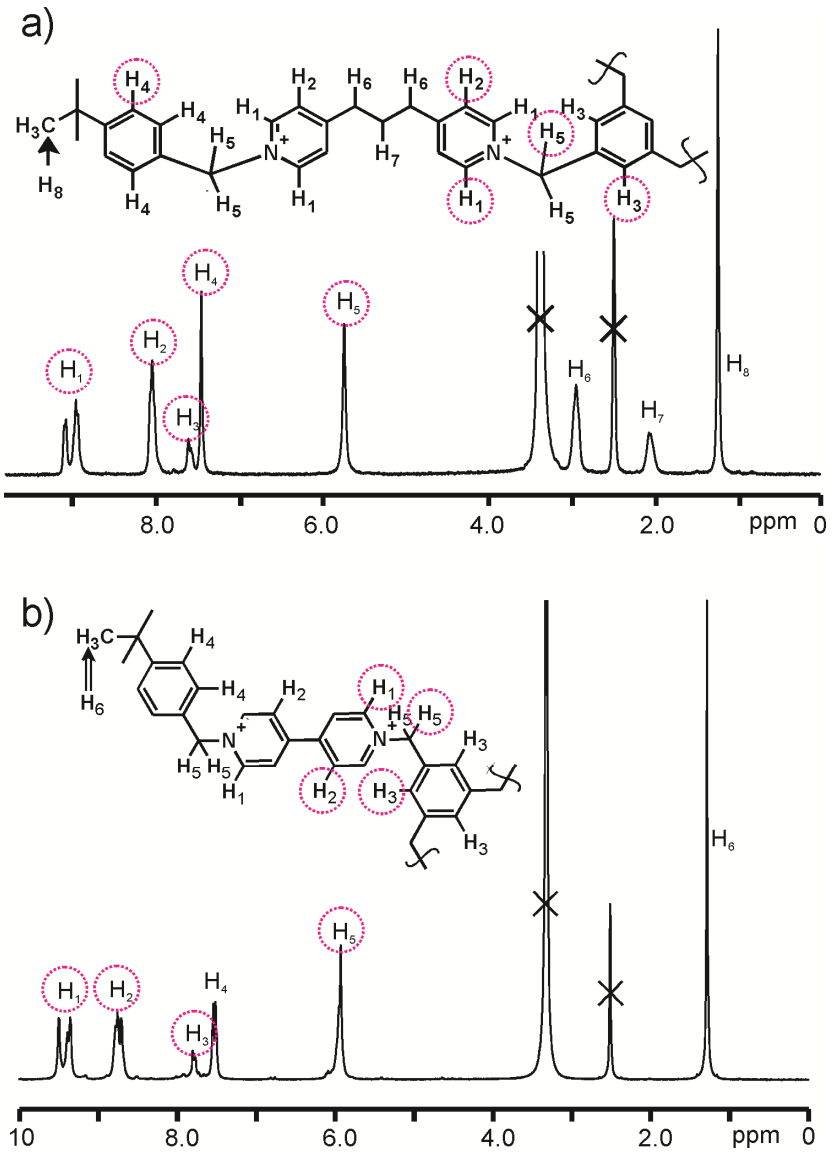

Anionic Guests	Monitored Host Protons	
	TMDPy	**DPy**
BS	H_1, H_2, H_4 & H_5	H_1, H_2, H_3 & H_5
AQDS	H_1, H_3 & H_5	H_1, H_2 & H_5
NDS	H_1 & H_5	H_1 & H_5
Pyr	H_5	H_5

Figure 5-1: ^{1}H NMR spectrum of a) $TMDPy_1$ dendrimers and b) DPy_1 dendrimers with chemical shift assignments; dotted pink circles indicates monitored host protons; Table shows the monitored host protons

almost no splitting indicating reasonable rotational freedom of the bridge methylene groups (at least before complexation).

Upon addition of the dianionic guest (AQDS and NDS), important shifts and changes in splitting of the host resonances H_1, H_2/H_3 and H_5 are observed as exemplified for the 18 fold positively charged **TMDPy$_1$** and **DPy$_1$** upon stepwise addition of 2,4,8, and 16 equiv AQDS/NDS (1 equiv = 2 stoichiometric negative charges). The changes in chemical shift reached a constant value after complete charge compensation, i.e., 9 equiv AQDS/NDS for **TMDPy$_1$** and **DPy$_1$**.

A detailed study of the NMR shifts[G] of the host protons H_1, H_2/H_3 and H_5 for all dendrimers **TMDPy$_{0-2}$** and **DPy$_{0-2}$** as a function of added AQDS and NDS equivalents is shown in Figure 2. No precipitation is observed (except Et terminated case) during the titration except at the point of charge compensation for **TMDPy$_2$** and **DPy$_2$**, we observed haziness. Generally changes become small above full charge compensation, but this is rather due to overcharging the dendrimer than to a low association constant. Remarkably, prominent changes occur at the same number of added equivalents AQDS/NDS independent of the dendrimer generation, e.g. 3 equiv AQDS added leads to splitting of H_5 in **TMDPy$_{0-2}$**, and **DPy$_{0-2}$**, or after 9 equiv added collapse of the splitting of H_1 in **TMDPy$_{1-2}$** and **DPy$_{0-2}$** is observed. The interaction with NDS showed the splitting of H_5 in **TMDPy$_{0-2}$** and **DPy$_{0-2}$** which remained constant after the end point and H_1 showed varied interactions, i.e., peak collapse and peak splitting (remained constant after the end point). We interpret this behavior as follows (Figure 2, bottom): The dendrimer **TMDPy$_0$** and **DPy$_0$** can be considered as a trimethyl benzene core with 3 doubly charged propyl bispyridinium/dipyridinium side chains

[G] NMR techniques have been widely used to study host-guest interaction mechanisms, Meijer et al investigated H-bonding interactions between urea-adamantyl modified dendrimers and carboxylic or phosphonic acid containing guests by ^{13}C NMR and ^{31}P NMR, see *Journal of the American Chemical Society* **2005**, *127*, 10334, Astruc et al analyzed ion pairing of water soluble dendrimers and different guests by ^{1}H NMR, see *Chemistry A European Journal* **2008**, *14*, 5577, as it can distinguish different protons within a molecule/complex according to their chemical environments

in a first shell, in **TMDPy$_1$** and **DPy$_1$** further 2*3 = 6 doubly charged propyl bispyridinium/dipyridinium side chains are added in a second shell, and in **TMDPy$_2$** and **DPy$_2$** another set of 4*3 = 12 doubly charged side chains are added in a third shell, yielding total amounts of 3, 3+6 = 9, and 3+6+12 = 21 doubly charged side chains organized in shells

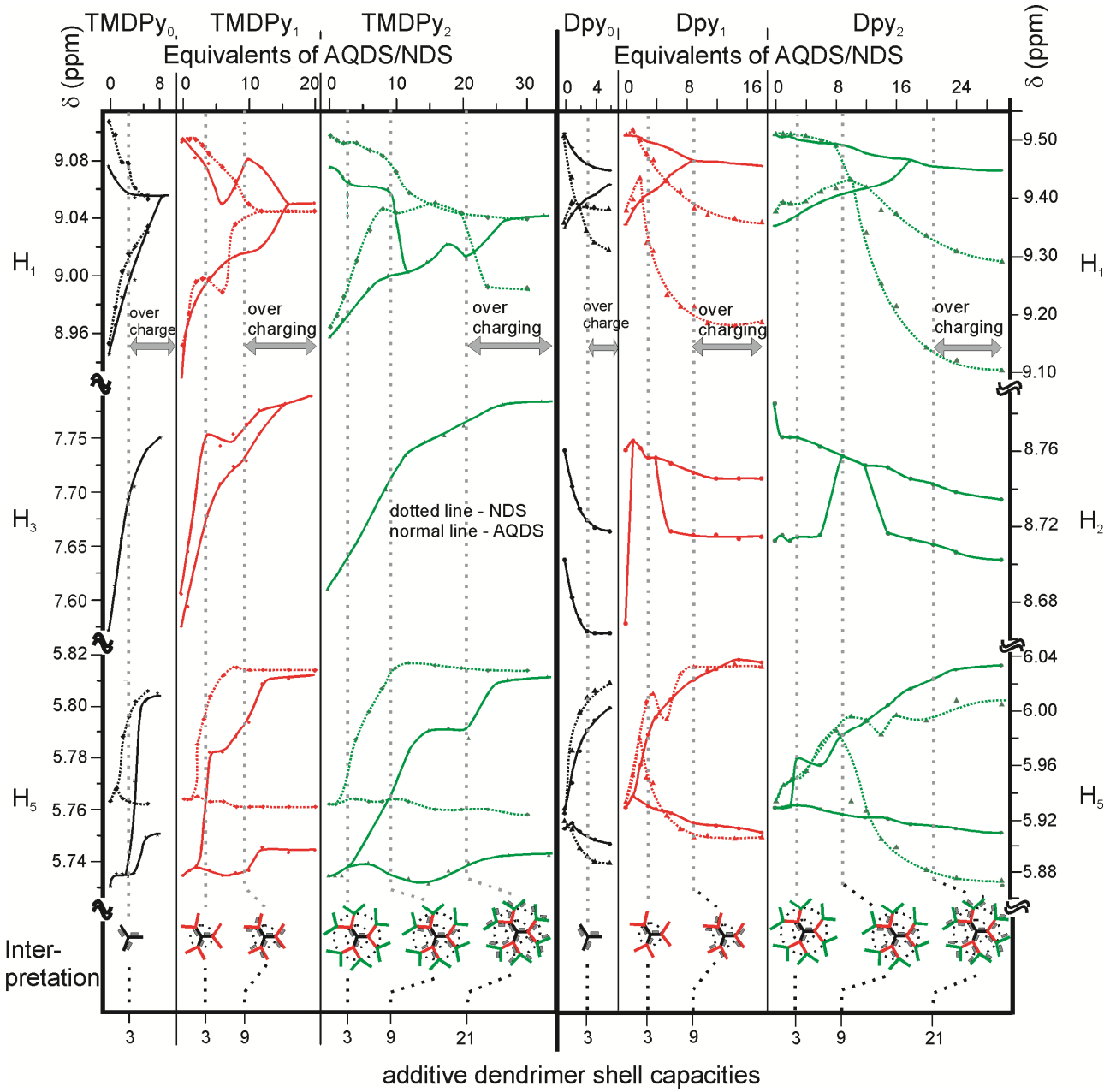

Figure 5-2: ^{1}H NMR titration: plots of the H_1, H_3 and H_5 dendrimer peaks of TMDPy$_{0\text{-}2}$ vs. AQDS (continuous line) and NDS (dotted line) equivalent additions; [TMDPy$_0$]= 3.2 mM; [TMDPy$_1$]= 1.1 mM; [TMDPy$_2$]= 0.48 mM; DPy$_{0\text{-}2}$ vs. AQDS (continuous line) and NDS (dotted line) equivalent additions; [DPy$_0$]= 3.3 mM; [DPy$_1$]= 1.2 mM; [DPy$_2$]= 0.5 mM; dotted lines: dendrimer shell capacity

for **$TMDPy_0$/DPy_0**,**$TMDPy_1$/DPy_1** and **$TMDPy_2$/DPy_2**, respectively (Figure 2 (bottom), Scheme 1). The dotted lines connecting prominent changes in the splitting at 3, 9 and 21 equiv AQDS/NDS are therefore evidence for a sequential filling of the innermost shell (3 open place), followed by the central shell (6 open places), followed by the outer most shell (12 open places).

This shell-by-shell filling ability was further verified by employing Benzene Sulfonate (monoanionic) and Pyranine[H] (trianionic) with all generations (Supporting Information). The monoanionic guest showed very weak interactions with the dendrimers, i.e., the end points were observed before the theoretical end points, as well as we do not observe larger peak splitting or peak collapse as we observed in the case of dianionic/trianionic guest molecules. This is attributed to a low association constant of BS as well as the competition of the monoanionic guest with the PF_6^- counter ions of the dendrimer. The trianionic guest (Pyr) showed very strong interaction[I] and we were able to observe shell-by-shell filling behavior in the case of **$TMDPy_0$**, **DPy_0**, **$TMDPy_1$** and **DPy_1** but we were unable to titrate **$TMDPy_2$** and **DPy_2** dendrimers due to precipitation till their theoretical end points. Thus NMR titration shows clear evidence for the shell-by-shell filling behavior. The anions with matching symmetry showed the best interaction. Trimethylenedipyridinium dendrimer with its propyl bridge was able to adopt its conformation to both the dianionic guests, showing very good interaction with AQDS as well as NDS whereas Viologen showed best interaction with NDS due to its matching symmetry as evident from NMR titrations. Each endpoint/filling is shown by peak splitting or peak collapse. Also, higher the charge of the anion, stronger the interaction and it follows the order: Pyr >> NDS ≈ AQDS >> BS.

[H] Pyranine- leads to precipitation of the higher generation dendrimers at/before the theoritical end points. This is attributed to the higher molecular weight of the complex

[I]This is observed from the Cyclic voltammetry, we complexed NDS with Viologen dendrimers and monitored the complexation by conventional CV, upon addition of Pyr to this complex, we observed a larger shift in potential to the negative direction due to the excessive stabilisation of the positive charges by the trianionic guest

In this work, we have shown the step-wise radial complexation of cationic dendrimers with different anionic guests. The dendrimers **TMDPy$_0$/DPy$_0$**, **TMDPy$_1$/DPy$_1$** and **TMDPy$_2$/DPy$_2$** consists of 1, 2 and 3 concentric shells. The first shell can accommodate 6 counter ions (3 equiv AQDS/NDS), the second can accommodate 12 counter ions (6 equiv AQDS/NDS) and the third can host 24 counter ions (12 equiv AQDS/NDS). If charging occurs shell by shell we expect - in analogy to the Bohr atomic model - prominent changes in experimental observables for **TMDPy$_2$/DPy$_2$** at 3, 9 and 21 equiv AQDS/NDS added, if – and only if – the dendrimer is loaded "shell-wise" starting with the innermost shell. All these observations are possible only if the cationic dendrimer possesses persistent positive charge from the core to the periphery.

Table 5-1: Physical Chemical data

	M [g/mol]	q^+	*Shell capacity for* q^{2-}	$D_{exp}x10^{-10}[m^2/s]$[a]	$r_h(nm)$[b]
TMDPy$_0$	2023.45	6	3	1.12	1.07
TMDPy$_1$	5745.81	18	3+6	0.74	1.63
TMDPy$_2$	13190.53	42	3+6+9	0.4	3.03
DPy$_0$	1897.21	6	3	1.258	0.98
DPy$_1$	5367.09	18	3+6	0.708	1.75
DPy$_2$	12306.85	42	3+6+9	0.478	2.59

[a]Reproducibility and analysis error is ± 5%[J] [b] r_h is the hydrodynamic radius calculated for a hard sphere model with Stokes-Einstein equation. q^+ is the no. of positive charges; q^{2-} is the dianionic guest.

The appearance of such "magic numbers" was first and so far exclusively reported by Yamamoto et al for dendrimer-guest complexation based on Lewis base-Lewis acid interactions. Experiments with other molecular guests, e.g. Pyranine, BS also showed strong complex formation but slightly less structured NMR shift vs. anion equivalent results, still giving access the same magic numbers. We found – to the best of our knowledge for the first

[J] The diffusion coefficients reported are median values of the distribution. The error estimations reported in this work were the difference between maximum and minimum diffusion values.

time for cationic dendrimers– clear evidence for a stepwise shell charging of the dendrimer from inside towards the periphery.

5.1 Experimental Section

5.1.1 Synthesis

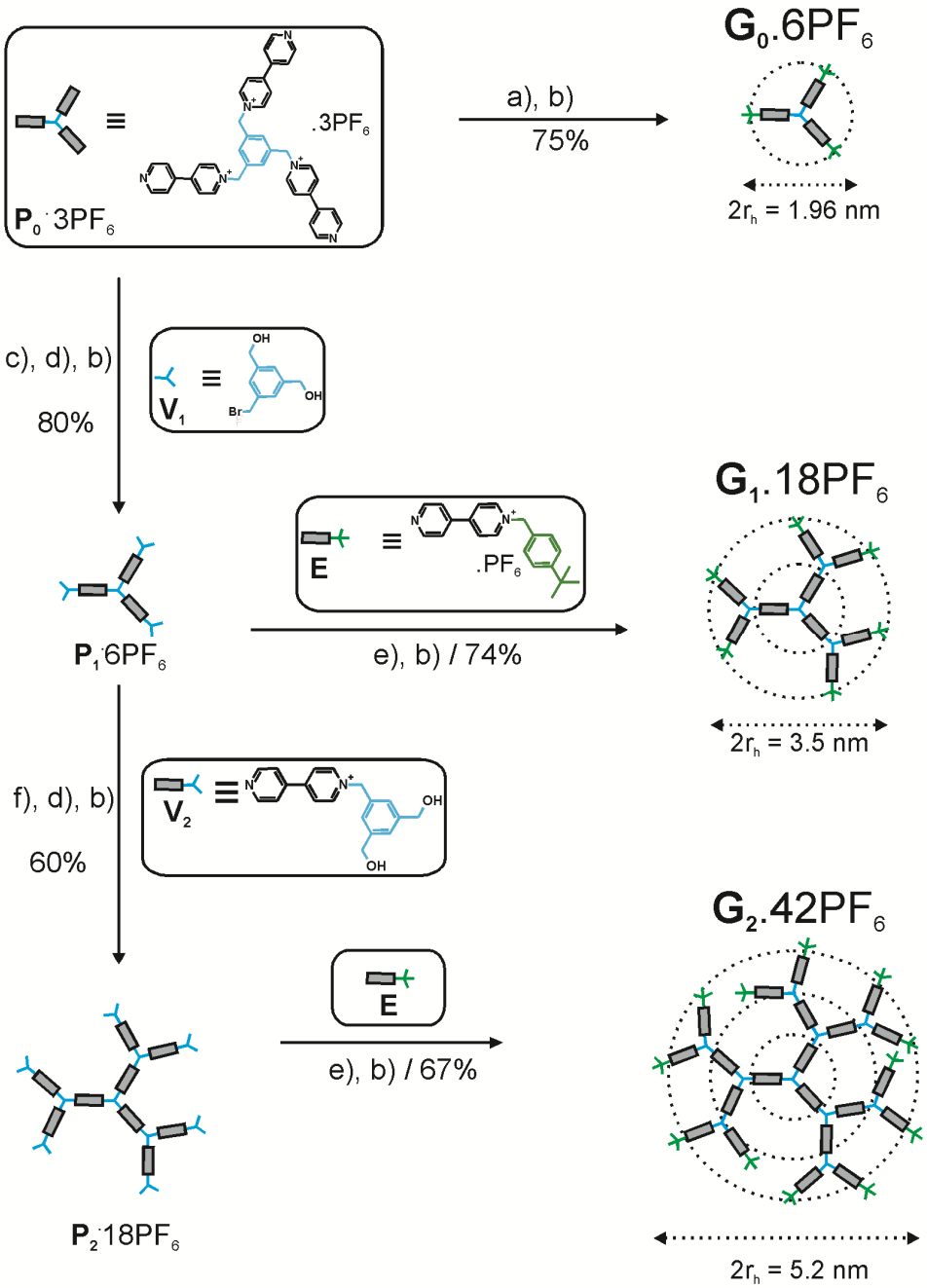

Scheme 5-2: Divergent synthesis of viologen dendrimers with 4-*tert*-butylbenzyl end group; a) 4-*t*-Bu-BnBr/CH_3CN/80°C; b) NH_4PF_6/H_2O; c) V_1/CH_3CN/80°C; d) HBr/HOAc/RT; e) E/CH_3CN/80°C, f) V_2/CH_3CN/80°C; yields reported are the isolated yields of the title compounds; dotted circles represent generation shells, r_h is the experimental hydrodynamic radius from DOSY

The dendrimers of generations zero to two were synthesized following the "divergent method with preformed branching units"[10b] (Scheme 4-1). The three peripheral nitrogens in **P$_0$**.3PF$_6$ react quantitatively with excess of 4-*t*-Bu-BnBr. Its reaction with **P$_0$**.3PF$_6$ followed by ion exchange yielded **G$_0$**.6PF$_6$ in 75%. The dendrimers **G$_1$**.18PF$_6$ and **G$_2$**.42PF$_6$ were available from the reaction of the corresponding precursors **P$_1$**.6PF$_6$ and **P$_2$**.18PF$_6$ with the end group **E.PF$_6$,** yielding 74 and 67%, respectively after ion exchange.

5.1.2 Cyclic Voltammetry

Viologen dendrimers can be characterized by measuring cyclic voltammetry. A typical viologen dendrimer shows two reduction waves corresponding to the radical cation at -0.4V approx and for the neutral species at -0.8V approx for a dialkylated viologen species. We observe the same behavior (Figure 4-1). Apart from this, generation dependent potential shifts and the diffusion behavior of the dendrimers was observed as reported by Heinen et al.[10]

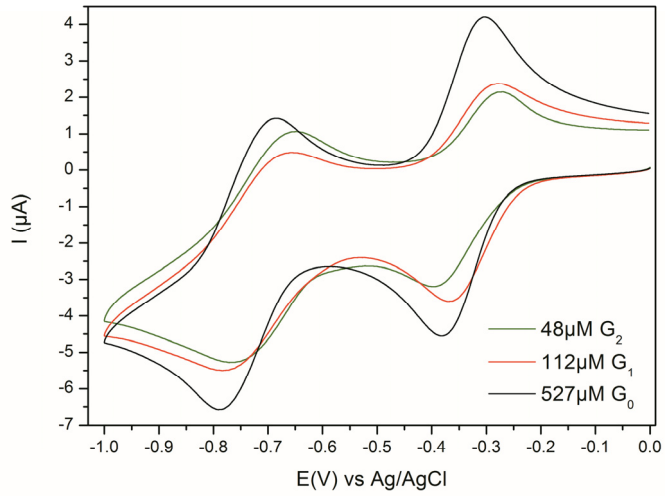

Figure 5-3: Cyclic voltammograms of G$_0$-G$_2$ benzylic viologen dendrimers in 0.1M TBA.PF$_6$/DMSO

5.1.3 DOSY

The diffusion coefficients of the dendrimers **TMDPy$_{0\text{-}2}$**, and **DPy$_{0\text{-}2}$** were measured in DMSO-d_6. Generation-dependent diffusion behavior was observed in both the dendrimers

(Table-1,). In the non-complexed state each dendrimer displays relatively a narrow band of signals centered on their average diffusion coefficient. Upon complexation with the anionic guest molecules, we observed larger fluctuation on the particle size of the complex; hence we were unable to give a reliable data.

a) Generation dependent hydrodynamic radii

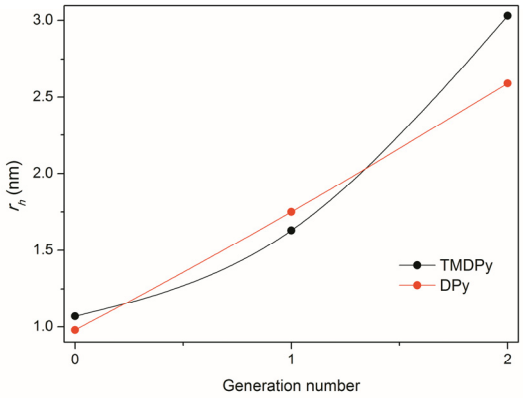

b) Generation dependent diffusion behavior

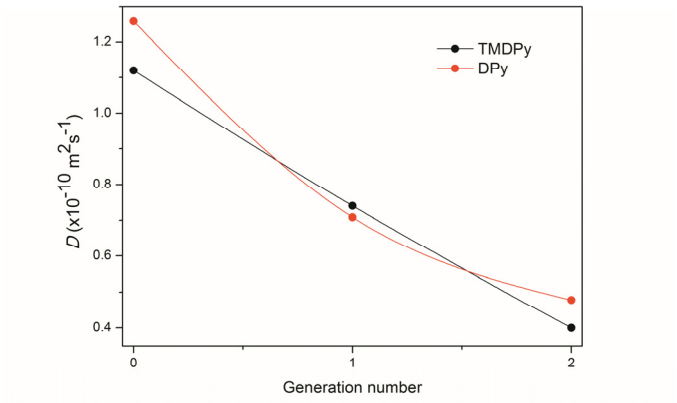

Figure 5-4: Plot of hydrodynamic radius r_h and D vs. generation number

5.1.4 Detailed Synthetic Procedures

All reactions were carried out under dry conditions. All starting materials and solvents were purchased from Sigma-Aldrich and used without further purification. Detailed syntheses of $P_0.3PF_6$, $P_1.6PF_6$, $P_2.18PF_6$, V_2, and V_1 (intermediates for the viologen dendrimers) were

discussed in chapters 2 and 3. Detailed synthetic procedure for the trimethylenedipyridinium dendrimers were discussed in chapter 4.

E.PF_6^-:

4,4′-Bipyridine (1.72g, 11mmol) and 4-*tert*-butylbenzyl bromide (1g, 4.4 mmol) were dissolved in 50 mL DCM, stirred for 2h at 60°C. The reaction mixture was then cooled, filtered, washed with DCM and dried. It was then dissolved in a minimum quantity of water, precipitated with 3M NH_4PF_6, filtered, washed and dried to yield **E**.PF_6 as a white powder

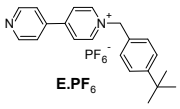

(1.45g, 73%). ^{1}H-NMR (250 MHz, *CD_3CN*) δ ppm 8.87 (s, 4H), 8.33 (s, 2H), 7.79 (s, 2H), 7.50 (dd, 4H), 5.74 (s, 2H), 1.34 (s, 9H); ^{13}C-NMR (63 MHz, *CD_3CN*) δ ppm 154.5, 153.3, 151.1, 144.8, 141.2, 130.1, 128.9, 126.5, 126.3, 121.9, 63.9, 34.4, 30.4; Anal. Calcd for $C_{21}H_{23}F_6N_2P$: C, 56.25; H, 5.17; N, 6.25. Found C, 55.89; H, 5.16; N, 6.21.

G_0.6PF_6^-:

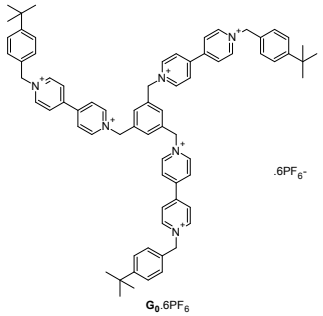

P_0.3PF_6 (0.2g, 195μmol) and 4-*tert*-butylbenzyl bromide (0.27g, 1.2 mmol) were dissolved in 20 mL CH_3CN, stirred at 80°C for 2d. The solution was cooled, filtered, washed with CH_3CN and dried. It was then dissolved in MeOH:H_2O (1:1) mixture, precipitated with 3M NH_4PF_6, filtered, washed and dried to yield **G_0**.6PF_6 as a pale yellow powder (0.28g, 75%). ^{1}H-NMR (500 MHz, *DMSO-d_6*) δ ppm 9.50 (d, ^3J(H,H) = 6.5 Hz, 6H), 9.35 (d, ^3J(H,H) = 6 Hz, 6H), 8.75 (d, ^3J(H,H) = 7 Hz, 6H), 8.71 (d, ^3J(H,H) = 6.5 Hz, 6H), 7.78 (s, 3H), 7.53 (dd, 12H), 5.92 (s, 12H), 1.28 (s, 27H); ^{13}C-NMR (125 MHz, *DMSO-d_6*) δ ppm 152.8, 150.1, 149.3,

149.3, 146.4, 146.2, 135.9, 131.6, 131.2, 129.2, 127.6, 127.5, 126.6, 63.9, 63.2, 34.9, 31.4; Anal. Calcd for $C_{72}H_{78}F_{36}N_6P_6.3H_2O$: C, 44.32; H, 4.34; N, 4.31. Found C, 44.35; H, 4.36; N, 4.39.

$G_1.18PF_6^-$:

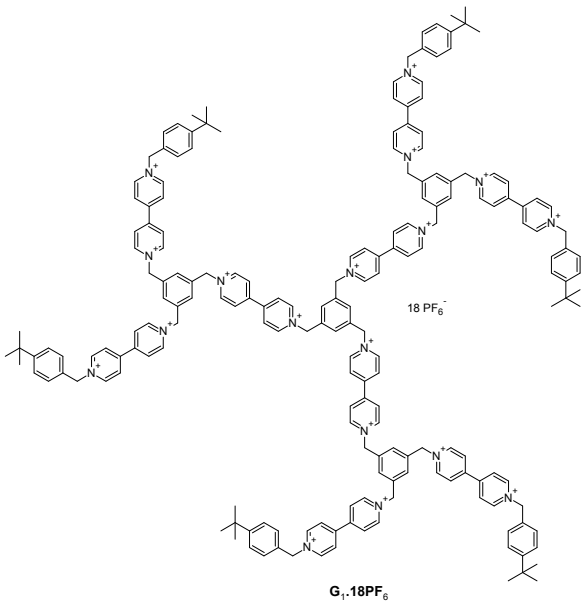

P_1.$6PF_6$ (0.15g, 65μmol) and **E**.PF_6 (0.22g, 492 μmol) were dissolved in 50 mL CH_3CN, stirred at 80°C for 4d. The solution was cooled, filtered, washed with CH_3CN and dried. It was then dissolved in MeOH:H_2O (1:1) mixture, precipitated with 3M NH_4PF_6, filtered, washed and dried to yield **G_1**.$18PF_6$ as a pale yellow powder (0.26g, 74%). ^{1}H-NMR (500 MHz, *DMSO-d_6*) δ ppm 9.45 (m, 36H), 8.73 (m, 36H), 7.79 (m, 12H), 7.53 (dd, 24H), 5.93 (s, 36H), 1.28 (s, 54H); ^{13}C-NMR (125 MHz, *DMSO-d_6*) δ ppm 152.8, 150.1, 149.4, 146.4, 146.2, 135.8, 131.6, 131.2, 129.2, 127.6, 127.5, 126.6, 63.9, 63.2, 34.9, 31.4; Anal. Calcd for $C_{192}H_{198}F_{108}N_{18}P_{18}.9H_2O$: C, 41.71; H, 3.93; N, 4.56. Found C, 41.64; H, 3.80; N, 4.49.

$G_2.42PF_6^-$:

P_2.$18PF_6$ (0.2g, 32μmol) and **E**.PF_6 (0.20g, 455 μmol) were dissolved in 50 mL CH_3CN, stirred at 80°C for 4d. The solution was cooled, filtered, washed with CH_3CN and

dried. It was then dissolved in MeOH:H_2O (1:1) mixture, precipitated with 3M NH_4PF_6, filtered, washed and dried to yield **G_2**.42PF_6 as a pale yellow powder (0.27g, 67%).

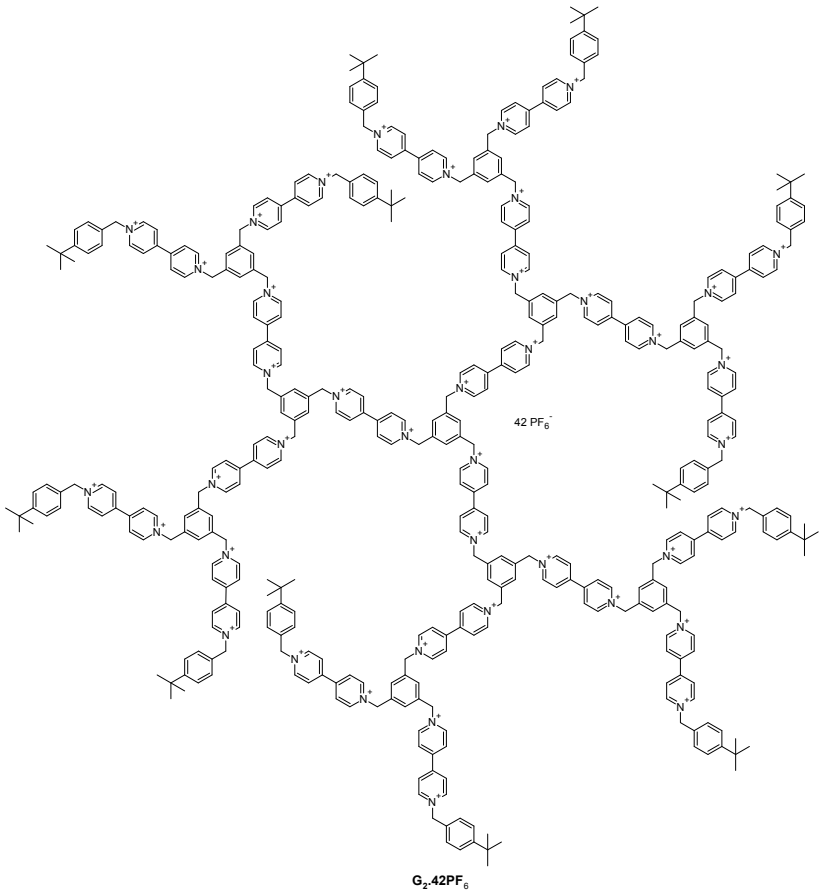

G_2·42PF_6

^{1}H-NMR (500 MHz, *DMSO-d_6*) δ ppm 9.44 (m, 84H), 8.74 (m, 84H), 7.80 (m, 30H), 7.53 (dd, 48H), 5.93 (s, 84H), 1.28 (s, 108H); ^{13}C-NMR (125 MHz, *DMSO-d_6*) δ ppm 152.8, 150.1, 149.7, 149.4, 146.6, 146.4, 146.2, 135.8, 131.6, 131.2, 129.2, 127.6, 127.5, 126.6, 63.9, 63.3, 34.9, 31.4; Anal. Calcd for $C_{432}H_{438}F_{252}N_{42}P_{42}$.21$H_2O$: C, 40.90; H, 3.81; N, 4.64. Found C, 40.77; H, 3.91; N, 4.53.

5.2 NMR titrations with BS and Pyranine

5.2.1 a) NMR titration: Plots of H_1, H_2, H_3/H_4 and H_5 dendrimer peaks (TMDPy_{0-2} and DPy_{0-2}) vs. BenzeneSulfonate (BS)

The titration curves of TMDPy and DPy dendrimers with monoanionic benzene sulfonate (BS) are shown in Figure 5-4. The expected stoichiometric sphere occupancies are 6, 18 and

42. These values are indicated by vertical broken lines. The protons H_1, H_2, H_4 and H_5 of the TMDPy dendrimers and H_1, H_2, H_3 and H_5 of the DPy dendrimers are monitored. Mostly monotonic increasing or decreasing dependences are observed. However, the following discontinuities are remarkable:

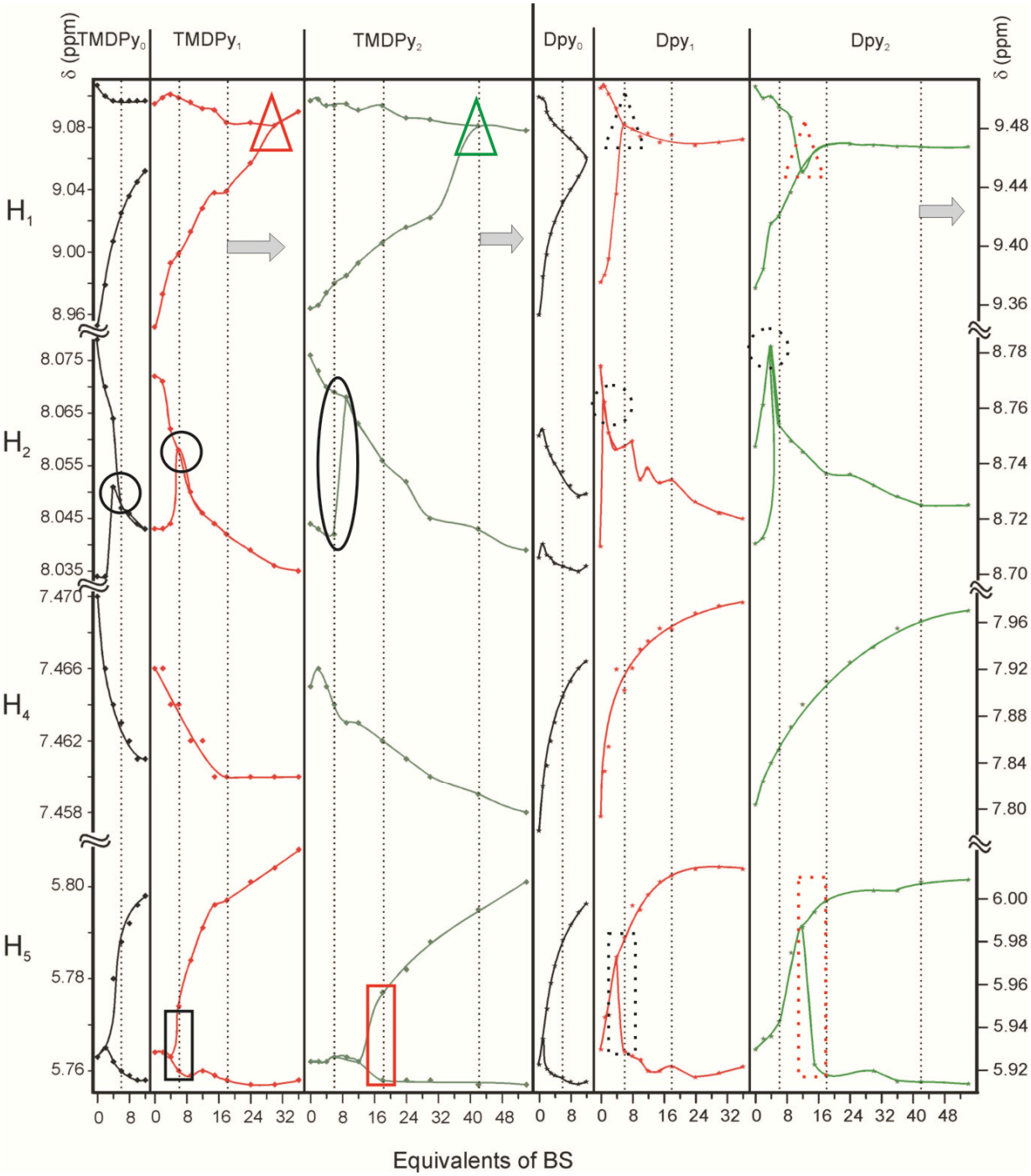

Figure 5-5: NMR titration plots of H_1, H_2, H_3/H_4 and H_5 dendrimer peaks ($TMDPy_{0\text{-}2}$ and $DPy_{0\text{-}2}$) vs. BenzeneSulfonate (BS)

1. Black full circles: the TMDPy series shows discontinuities for H_2 at ca. 6 equiv in all generations, indicating complete filling of the innermost void at low guest concentration predominantly.
2. Black broken circles: In the DPy series similar discontinuities are observed, but occurring at 2-4 equiv.
3. Black and red full rectangles: The TMDPy series shows discontinuities for H_5 at 6 and 18 equiv for generation 1 and 2, i.e. for the full 1st and 2nd sub-shells, respectively.
4. Black and red broken rectangles: The DPy series shows discontinuities at 6 and 13 equiv, for H_5 i.e. slightly below the theoretical endpoint of sub-shell capacities.
5. Red and green full triangles: These discontinuities are observed at the stoichiometric end point. They do not display sub-shell filling.

Red and green broken triangles: These discontinuities display sub-shell filling.

5.2.2 b) NMR titration: Plot of H_5 dendrimer peaks ($TMDPy_{0-2}$ and DPy_{0-2}) vs. Pyranine (Pyr)

The titration curves of TMDPy and DPy dendrimers with Pyranine were shown in Figure 5-5. We were able to monitor the response of the host resonances only at H_5 as the other protons merged with the guest signals with increase in concentration of the guest molecules. Dendrimers showed well-structured response upon guest addition. $TMDPy_0$ and DPy_0 have only one void and the addition of the guest molecule resulted in larger peak shifts (coupling) till the theoretical end point, after which it remained constant. $TMDPy_1$ and DPy_1 dendrimers showed the innermost filling by peak splitting and upon complete neutralization we observed no changes in the host signals, i.e., we observed coupling constant after first filling which reached a maximum value and after the second filling it almost remained constant. The same trend, i.e., innermost filling accompanied by peak splitting, was seen in the case of $TMDPy_2$

and DPy_2 but we were unable to titrate till the theoretical end points due to the precipitation of the complex.

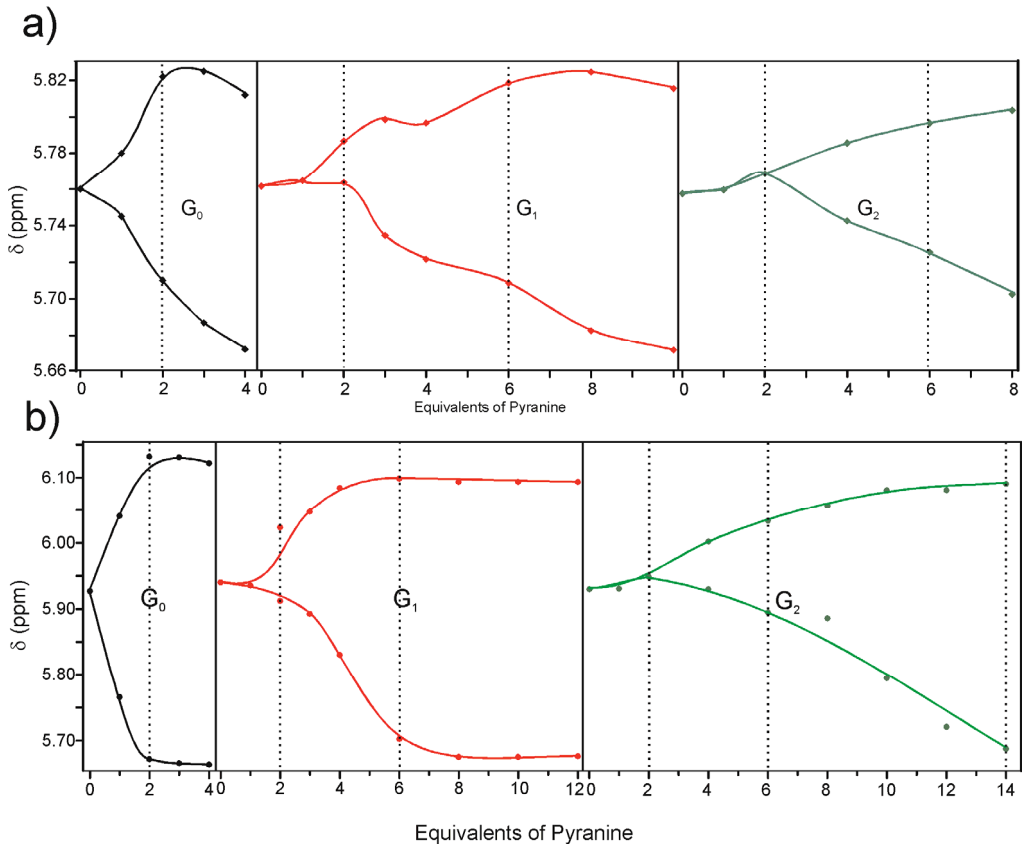

Figure 5-6: NMR titration plot of H_5 dendrimer peaks ($TMDPy_{0\text{-}2}$ and $DPy_{0\text{-}2}$) vs. Pyranine (Pyr)

6 Synthesis of *n*-Pyridinium- and *n*-Sulfonoalkylphosphonic acids for the surface modification of metal oxides

Part of the SI from *Langmuir*, **2009**, *25*, 5371 and *Phys. Chem. Chem. Phys.* **2010**, *12*, 1473.

Organophosphonates are a class of organic phosphorous compounds containing the P-C bond. They attracted considerable synthetic and pharmacological interest due to their diverse biological activity. The Michaelis-Arbuzov rearrangement,[94] also known as the Arbuzov reaction, is very versatile way to form P-C bond from the reaction of an aryl / alkyl halide and trialkyl phosphite. This reaction is one of the most extensively investigated and is widely used to prepare phosphonates, phosphinates and phosphine oxides. In my work I synthesized ω-alkylpyridinium, ω-alkyltrimethylenedipyridinium, ω-alkylbipyridinium or ω-sulfonoalkylphosphonates for the surface modification of pore walls of mesoporous TiO_2. Host-guest interaction studies were carried out between sulfonoalkylphosphonic acid modified TiO_2 electrodes and viologen guests.[95] In this thesis, I have discussed the synthesis of different alkyl phosphonic acids and the synthesis of viologen guest molecules.

6.1 Synthesis of alkylphosphonic acids

The synthesis involves two steps starting from the respective dibromides. The first step was an Arbuzov reaction where we extended the reported procedure for 1,10-dibromotetradecane[96] to 1,6-dibromohexane[97] and to 1,14-dibromotetradecane with minor modifications (Scheme 6-1). 1,6-dibromohexane and 1,10-dibromodecane were commercially available whereas 1,14-dibromotetradecane was synthesized from the commercially available 1,14-tetradecanedioic acid using 1M Borane-THF complex in high yields (reported literature procedure[98] was extended). 1,14-tetradecanediol thus obtained was brominated using 5.7M HBr in acetic acid which gave higher yield than the reported procedure.[99] The intermediate obtained in the first step was common for N-alkylation as well as for sulfonation where we

extended the same approach with minor modifications of the reported literatures[45b,100] respectively.

These bifunctional linkers were used as surface modifiers to build a biomimetic membrane on the pore walls of mesoporous TiO_2 electrodes via phosphorous coordination. Host-guest interaction studies were carried out between synthesized viologen derivatives and sulfonoalkylphosphonic acids.[95] A detailed synthetic procedure along with their characterization is presented in this thesis.

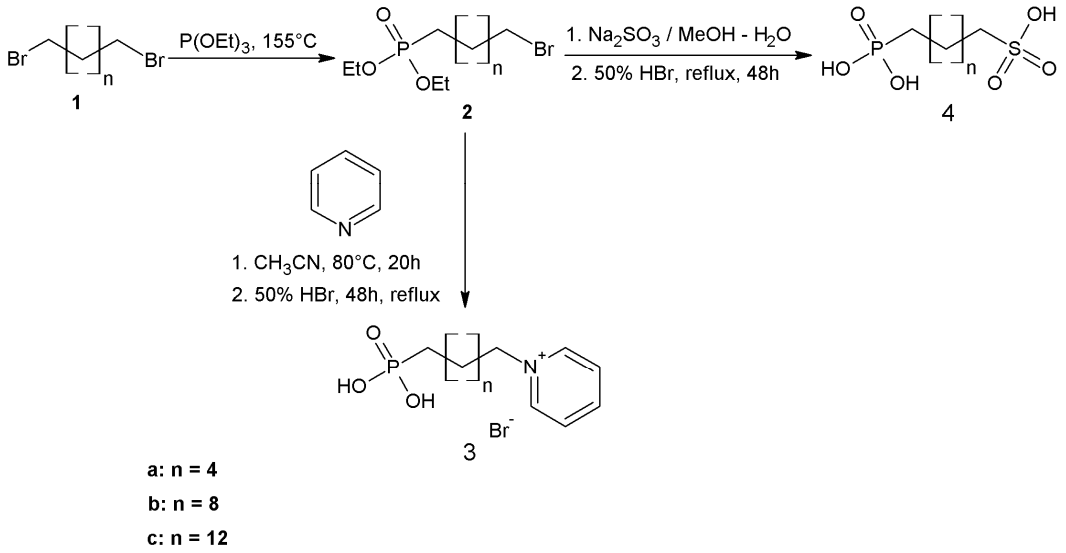

Scheme 6-1: Synthesis of pyridinium and sulfonoalkylphosphonic acids

Bifunctional molecular linkers, i.e., ω-derivatised alkyl (6, 10 and 14 methylene groups) phosphonic acids were synthesized; the reaction conditions and yields were optimized. It is shown that by proper tailoring, we were able to introduce pyridinium, trimethylenedipyridinium, and bipyridinium or sulfonate groups on the ω end of these linkers creating a bifunctionalized system. These bifunctional linkers were used as surface modifiers to build a biomimetic membrane on the pore walls of mesoporous TiO_2, Host-guest interaction studies with on purpose synthesized viologen compounds have been performed in collaboration.

6.2 Detailed Synthetic Procedures

6.2.1 Synthesis of *n*-pyridinium- and *n*-sulfonoalkylphosphonates

General:1,6-dibromohexane, 1,10-dibromodecane, 1-bromohexane, 1-bromodecane, 1-bromotetradecane, 4,4´-bipyridine, pyridine, sodium sulfite, triethylphosphite and HBr were purchased from Sigma-Aldrich co. Methyl iodide was purchased from Merck. 1,14-tetradecanedioic acid was purchased from ABCR chemicals. CH_3CN used for the reactions was of spectroscopic grade. THF, pyridine and DCM were distilled using standard procedures before use. Aqueous solutions were prepared with deionized water. ^{1}H NMR was recorded on Bruker 250 MHz Spectrometer at 25°C using solvent as the internal standard.

Synthesis of 2a:1,6-dibromohexane (10 g, 32 mmol) was heated to 150°C under Argon. To this liquid, triethylphosphite (1.4 mL, 8 mmol) was added dropwise over 1 h. The mixture was stirred for 1h and the excess dibromohexane was removed at 40°C under reduced pressure (3.2 x 10^{-3} mbar). The residue was purified by silica gel column chromatography with EtOAc/Hexane (1:1) as eluent, solvent evaporation of the second fraction gave a colorless oil, 1.63 g (66%); ^{1}H-NMR (250 MHz, $CDCl_3$): 4.11 (m, 4H), 3.42 (t, *J*(H,H) = 6.7Hz, 2H), 1.78 (m, 8H), 1.46-1.26 (unresolved coupling, combined integral, 8H).

Synthesis of 2b: Reported literature[96] procedure was followed.

Synthesis of 2c: Tetradecanedioic acid (8.87 g, 34 mmol) dissolved in 150 mL THF was cooled to 0°C under argon. To this solution, 118 mL 1M BH_3-THF complex (103 mmol) was added slowly over 1 h. The mixture was stirred at RT for 6 h and cooled to 0°C. To this mixture 1:1 THF-H_2O (100 mL) was added carefully, THF was removed under reduced pressure and the organic layer was extracted with DCM, dried over anhydrous MgSO4, evaporated and dried to yield a colorless solid, 7.8 g (99%), (m.pt: 85°C); ^{1}H-NMR (250 MHz, $CDCl_3$)[99]: 3.67 (t, 4H), 1.57 (m, 4H), 1.29 (unresolved coupling, combined integral 20H).

1,14-dihydroxytetradecane (7.5 g, 32 mmol) and 300 mL of 33% HBr in acetic acid was stirred at RT for 48 h under dry condition. The excess acid was removed under reduced pressure; the residue was dissolved in DCM. The organic layer was washed with water until neutral pH, was dried over anhydrous $MgSO_4$, filtered and evaporated to yield a colorless solid which was then recrystallized from hot methanol yielding 9.6 g (83%), (m.pt: 46-48°C); ^{1}H-NMR (250 MHz, $CDCl_3$)[99]: 3.43(t, 4H), 1.89 (m, 4H), 1.47-1.21 (unresolved coupling, combined integral 20H).

1,14-dibromotetradecane (8 g, 21 mmol) was heated to 150°C under inert condition. To this liquid, triethylphosphite (0.8 mL, 4 mmol) was added dropwise over 1 h. Then the mixture was stirred for 24 h and the solution was cooled to 5°C to remove the excess dibromodecane by filtration. The residue was purified by silica gel column chromatography with EtOAc/Hexane (1:1) as eluent, solvent evaporation of the second fraction gave a colorless oil, (turns into solid at RT after several days) yielding 1.24 g (67%); ^{1}H-NMR (250 MHz, $CDCl_3$): 4.12 (m, 4H), 3.43 (t, 2H), 1.84 (m, 2H), 1.75-1.25(unresolved coupling, combined integral 30H).

Synthesis of 3a: Freshly distilled pyridine (0.85 mL, 10 mmol), diethyl(6-bromohexyl)phosphonate (0.500 g, 1.6 mmol) and CH_3CN (7.5mL) were heated to 80°C and stirred for 20 h. The solvent was removed under reduced pressure, the residue was dissolved in H_2O and excess pyridine was removed by washing with DCM. The aqueous layer was concentrated under reduced pressure; the residue thus obtained was dissolved in 50% HBr (25 mL) and refluxed for 48 h. The acid was removed under reduced pressure to yield a brown viscous liquid, 0.5 g (93%); ^{1}H-NMR (250 MHz, D_2O): 8.72 (d, *J*=5.4Hz, 2H), 8.43 (t, *J*=7.8Hz, 1H), 7.95 (t, *J*=6.8Hz, 2H), 4.50 (t, *J*=7.3Hz, 2H), 1.89 (t, 2H), 1.62 (m, 2H), 1.46-1.25 (unresolved coupling, combined integral, 6H).

3b: 88%; ^{1}H-NMR (250 MHz, D_2O): 8.72 (d, *J*=5.5Hz, 2H), 8.42 (t, *J*=7.9Hz, 1H), 7.94 (t, *J*=6.6Hz, 2H), 4.49 (t, *J*=7.2Hz, 2H), 1.90 (t, 2H), 1.66 (m, 2H), 1.45-1.16 (unresolved coupling, combined integral, 14H).

3c: 85%; ^{1}H-NMR (250 MHz, CD_3OD): 9.02 (d, 2H, J=5.6Hz), 8.63 (t, 1H, J=7.8Hz), 8.14 (t, 2H, J=6.8Hz), 4.66 (t, 2H), 2.05 (t, 2H), 1.74-1.31 (unresolved coupling, combined integral 24H).

Synthesis of 4a: Diethyl(6-bromohexyl)phosphonate (0.5 g, 1.6 mmol) in 5 mL MeOH and saturated solution of Na_2SO_3 (0.523 g, 4.1 mmol) in water were first refluxed for 1 h and heated to 120°C until complete evaporation of the solvents. The residue was then slurred with MeOH under refluxing condition, the hot solution was filtered. The filtrate containing the sodium salt was then evaporated and the residue obtained was kept for hydrolysis with 25 mL 50% HBr under reflux for 48 h. The acid was removed under reduced pressure which gave a pale-black powder yielding 0.32 g (80%); ^{1}H-NMR (250 MHz, D_2O): 2.79 (t, 2H), 1.64 (m, 4H), 1.47-1.33 (unresolved coupling, combined integral, 6H).

4b: 81%; ^{1}H-NMR (250 MHz, D_2O): 2.81 (t, 2H), 1.63 (m, 4H), 1.45 (d, 2H), 1.21 (unresolved coupling, combined integral, 12H).

4c: 72%; ^{1}H-NMR (250 MHz, CD_3OD): 2.80 (t, 2H), 1.79 (m, 4H), 1.70 (m, 2H), 1.32 (unresolved coupling, combined integral, 20H).

6.2.2 Synthesis of Guest molecules (Viologen derivatives)

1-methyl-4-(pyridin-4-yl)pyridinium iodide and 1,1´-dimethyl-4,4´-bipyridinium diiodide were synthesized according to the reported procedures[101]. The other derivatives were synthesized using the same procedure as reported for dimethylbipyridinium diiodide.

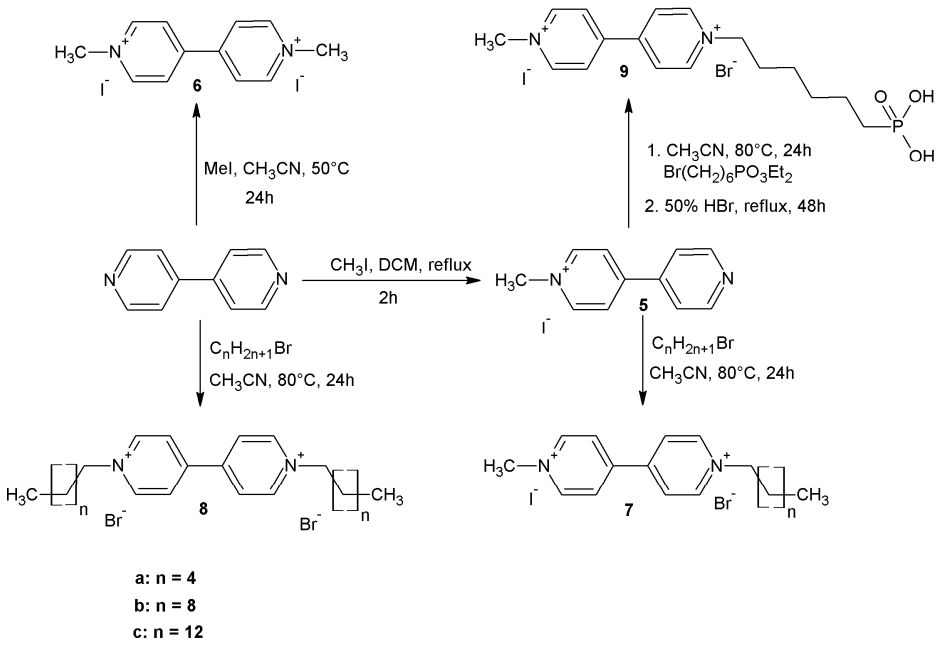

Scheme 6-2: Synthesis of guest viologen molecules

Synthesis of 7a:

1-methyl-4-(pyridin-4-yl)pyridinium iodide (0.5 g, 1.6 mmol), 1-bromohexane (0.8 mL, 5 mmol) in 25 mL CH_3CN was stirred at 75°C for 24 h. The reaction mixture was cooled, filtered, the solid thus obtained was washed with CH_3CN and dried to yield a red-orange powder weighing 0.69 g (90%); ^{1}H-NMR (250MHz, D_2O): 9.00 (dd, *J*(H,H) = 5Hz, 4H), 8.45 (t, 4H), 4.61 (t, 2H), 4.42 (s, 3H), 2.00 (bs, 2H), 1.26 (s, 6H), 0.78 (t, 3H).

7b: orange solid, 79%; ^{1}H-NMR (250MHz, DMSO-d_6): 9.42 (d, *J*(H,H) = 5Hz, 2H), 9.31 (d, *J*(H,H) = 5Hz, 2H), 8.80 (t, 4H), 4.70 (t, 2H), 4.45 (s, 3H), 1.97 (bs, 2H), 1.28 (unresolved coupling, combined integral, 14H), 0.85 (t, 3H).

7c: yellow-orange solid, 73%; ^{1}H-NMR (250MHz, DMSO-d_6): 9.41 (d, *J*(H,H) = 7.5Hz, 2H), 9.31 (d, *J*(H,H) = 7.5Hz, 2H), 8.79 (t, 4H), 4.69 (t, 2H), 4.45 (s, 3H), 1.97 (bs, 2H), 1.28 (unresolved coupling, combined integral, 22H), 0.85 (t, 3H).

8a: yellow solid, 68%; ^{1}H-NMR (250MHz, D_2O): 9.03 (d, *J*(H,H) = 5Hz, 4H), 8.45 (d, *J*(H,H) = 5Hz, 4H), 4.64 (t, 4H), 2.00 (bs, 4H), 1.26 (unresolved coupling, combined integral 12H), 0.79 (t, 6H).

8b: pale-yellow solid, 87%; ^{1}H-NMR (250MHz, DMSO-d_6): 9.43 (d, *J*(H,H) = 7.5Hz, 4H), 8.82 (d, *J*(H,H) = 5Hz, 4H), 4.70 (t, 4H), 1.98 (bs, 4H), 1.28 (unresolved coupling, combined integral 28H), 0.84 (t, 6H).

8c: pale-brown solid, 67%; ^{1}H-NMR (250MHz, DMSO-d_6): 9.39 (d, *J*(H,H) = 5Hz, 4H), 8.78 (d, *J*(H,H) = 7.5Hz, 4H), 4.68 (t, 4H), 1.97 (bs, 4H), 1.24 (unresolved coupling, combined integral 44H), 0.85 (t, 6H).

9: Alkylation procedure was the same as mentioned above, the alkylated product was kept for hydrolysis with 50% HBr for 48 h, the acid was evaporated under reduced pressure, the residue obtained was dissolved in MeOH, precipitated with diethyl ether, filtered, washed with ether and dried to yield an yellow solid 20%. ^{1}H-NMR (250MHz, D_2O): 9.02 (d, *J*(H,H) = 5Hz, 2H), 8.96 (d, *J*(H,H) = 5Hz, 2H), 8.44 (t, 4H), 4.67 (t, 2H), 4.40 (s, 3H), 2.00 (bs, 2H), 1.62 (m, 2H), 1.35 (s, 6H).

6.3 Synthesis of dicationic alkyl phosphonates[95a]

Synthesis of 1-methyl-4-(3-[1-(10-phosphonodecyl)pyridinium-4-yl]propyl)pyridinium bromide iodide

The selective monoalkylation of 4,4´-trimethylenedipyridine is been a challenging task unlike other dipyridine or bipyridine systems because of the presence of trimethylene bridge which influences the overall solubility of the alkylated products as well as the free trimethylenedipyridine unit to a greater extent. Dialkylation of 4,4´-trimethylenedipyridine has been known since longtime.[102] It is been known that monoalkylation of 4,4´-bipyridine can be stopped without further alkylation by using solvents such as dichloromethane[101a,103], chloroform[79c], diethyl ether[104], benzene[105] or using the excess alkylating agent as a solvent. We tried this same strategy for our trimethylenedipyridine system, but we observed dialkylation in all those solvents mentioned above including ethylacetate and in hexane. We used methyliodide as a solvent and carried out the alkylation, we obtained dialkylated

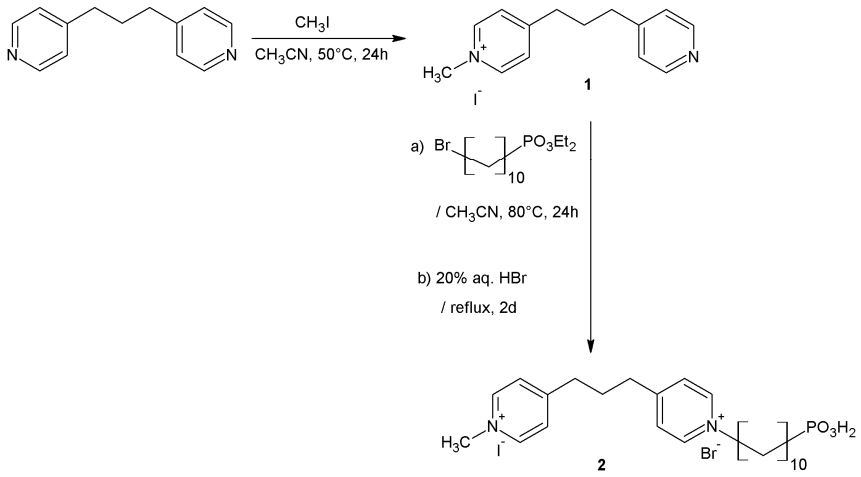

Scheme 6-3: Synthesis of dicationic alkyl phosphonate

product. Finally using the excess equivalents of 4,4′-trimethylenedipyridine and one equivalent of methyl iodide in acetonitrile gave us the desired product in good yield and the procedure is reported as below:

Synthesis of 1-methyl-4-[3-(pyridin-4-yl)propyl]pyridinium iodide (1)

2 g (10.08 mmol) of 4,4′-trimethylenedipyridine was dissolved in 20 mL acetonitrile and the solution was heated to 50°C. To this solution, 0.13 mL (2.017 mmol) methyl iodide dissolved in 20 mL acetonitrile was added dropwise over 4 h and the solution was stirred for another 20 h. The progress of the reaction was monitored using TLC (0.2 mm Silicagel coated on aluminium sheets) using 10:4:1 (MeOH:HOAc:H_2O) as the eluent. After 24 h, the reaction mixture was cooled to room temperature; excess acetonitrile was distilled under reduced pressure. The slurry thus obtained was dissolved in water, washed with dichloromethane to remove the excess 4,4′-trimethylenedipyridine. Removal of the water under reduced pressure gave dark blackish brown solid which was then dried under high vacuum to afford 0.6 g of 1-methyl-4-[3-(pyridin-4-yl)propyl]pyridinium iodide, (87%) ^{1}H NMR (250 MHz, *D_2O*): 8.46 (d, *J* = 6.52 Hz, 2H), 8.33 (d, *J* = 6.16 Hz, 2H), 7.72 (d, *J* = 6.42 Hz, 2H), 7.37 (d, *J* = 6.09 Hz, 2H), 4.18 (s, 3H), 2.84 (t, 2H), 2.71 (t, 2H), 2.09-1.93 (m, 2H).

Synthesis of 1-methyl-4-(3-[1-(10-phosphonodecyl)pyridinium-4-yl]propyl) pyridinium bromide iodide (2)

0.4 g (1.17 mmol) of 1-methyl-4-[3-(pyridin-4-yl)propyl]pyridinium iodide and 0.84 g (2.35 mmol) diethyl-(10-bromodecyl)phosphonate were dissolved in 20 mL acetonitrile and the solution was heated to 80°C for 24 h. The progress of the reaction was monitored using TLC (0.2 mm Silicagel coated on aluminium sheets) using 10:4:1 (MeOH:HOAc:H_2O) as the eluent. After 24 h, the reaction mixture was cooled to room temperature; excess acetonitrile was distilled under reduced pressure. The slurry thus obtained was dissolved in water, washed with ethylacetate to remove the excess diethyl-(10-bromodecyl)phosphonate. Removal of the water under reduced pressure gave dark reddish brown solid which was then hydrolyzed using 20 mL of 20% aqueous HBr at 100°C for 2 d. The solution was then cooled to room temperature; the solvent was evaporated under reduced pressure to yield a black oily residue. It was then dissolved in 20 mL MeOH. To this solution, 0.5 g of activated charcoal was added, heated and the mixture was filtered through Celite. The filtrate thus obtained was evaporated under reduced pressure leaving pale brown semisolid of 0.55 g (73%). ^{1}H NMR (250 MHz, D_2O): 8.56 (dd, J = 6.34 Hz, 4H), 7.81 (t, J = 5.65 Hz, 4H), 4.44 (t, 2H), 4.22 (s, 3H), 2.92 (t, 4H), 2.08 (t, 2H), 1.96-1.81 (m, 2H), 1.75-1.56 (m, 2H), 1.53-1.33 (m, 2H), 1.17 (d, 12H).

6.4 Synthesis of tricationic alkyl phosphonate

Synthesis of tricationic alkyl phosphonate is shown in scheme 6-4. 1,3-dibromopropane is selectively reacted with pyridine to yield 1-(3-bromopropyl)pyridinium bromide which was further reacted with 4,4´-trimethylenedipyridine to yield 4-(3-(pyridin-4-yl)propyl)-1-(3-(pyridinium-1-yl)propyl)pyridinium bromide. Reaction of this compound with diethyl-phosphonoethyl bromide gave the ester derivative which was hydrolyzed to yield the title compound.

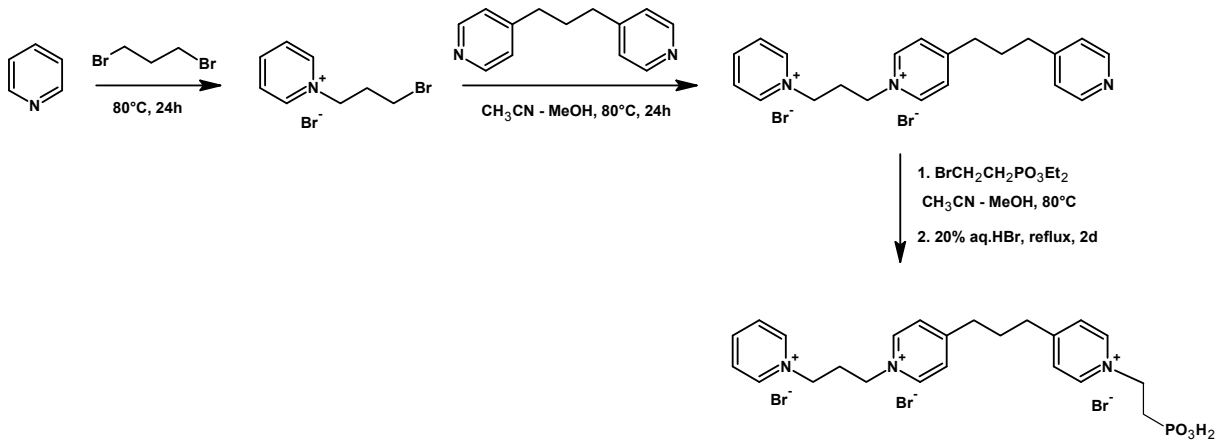

Scheme 6-4: Synthesis of tricationic alkyl phosphonate

Synthesis of 1-(3-bromopropyl)pyridinium bromide

1,3-dibromopropane (12.5 g, 62 mmol) was dissolved in 30 mL CH_3CN, heated to 80°C. To this solution, pyridine (0.98 g, 12 mmol) dissolved in 20 mL CH_3CN was added dropwise over 6 h and the mixture was stirred for 18 h. The reaction mixture was cooled, the solvent was evaporated under reduced pressure, and the residue thus obtained was partitioned between EtOAc and water. The aqueous layer was washed with EtOAc to remove unreacted 1,3-dibromopropane, and finally concentrated to yield 1-(3-bromopropyl)pyridinium bromide as pale yellow powder (2.5 g, 72%); ^{1}H NMR (250 MHz, D_2O) δ ppm 8.79 (d, 2H), 8.46 (t, 1H), 7.98 (t, 2H), 4.67 (t, 2H), 3.38 (t, 2H), 2.47 (m, 2H); ^{13}C NMR (63 MHz, D_2O) δ ppm 144.9, 144.6, 128.3, 59.9, 32.65, 28.7.

Synthesis of 4-(3-(pyridin-4-yl)propyl)-1-(3-(pyridinium-1-yl)propyl)pyridinium bromide

4,4′-Trimethylenedipyridine (2.6 g, 13 mmol) was dissolved in 30 mL CH_3CN, heated to 80°C. To this solution, 1-(3-bromopropyl)pyridinium bromide (0.75 g, 2.7 mmol) dissolved in 20 mL MeOH was added drop wise over 6h and the mixture was stirred for 18 h. The reaction mixture was cooled, the solvent was evaporated under reduced pressure, and the residue thus obtained was partitioned between CH_2Cl_2 and water. The aqueous layer was washed with

CH_2Cl_2 to remove unreacted trimethylenedipyridine, and finally concentrated to yield 4-(3-(pyridin-4-yl)propyl)-1-(3-(pyridinium-1-yl)propyl)pyridinium bromide as red oil (1.08 g, 84%); ^{1}H NMR (250 MHz, D_2O) δ ppm 8.81 (d, 2H), 8.58 (d, 2H), 8.50 (t, 1H), 8.25 (d, 2H), 8.01 (t, 2H), 7.78 (d, 2H), 7.20 (d, 2H), 4.64 (m, 2H), 2.85 (t, 2H), 2.68 (m, 2H), 2.00 (m, 2H); ^{13}C NMR (63 MHz, D_2O) δ ppm 148.2, 146.3, 144.4, 143.4, 128.6, 128.4, 124.7, 58.1, 57.2, 34.5, 33.8, 31.7, 29.0.

Synthesis of tricationic alkyl phosphonate

4-(3-(pyridin-4-yl)propyl)-1-(3-(pyridinium-1-yl)propyl)pyridinium bromide (0.7 g, 1.4 mmol) and 2-diethylphosphonoethyl bromide (1.3 mL, 7 mmol) were dissolved in 15 mL 1:1 CH_3CN/MeOH mixture, heated to 80°C for 24 h. The solution was cooled to RT, the solvent was evaporated under reduced pressure and the residue was hydrolyzed with 50 mL of 20% HBr for 2 d. The acid was removed under reduced pressure and the product thus obtained was dried to yield tricationic alkyl phosphonate as brown oil (0.95 g, 97%); ^{1}H NMR (250 MHz, D_2O) δ ppm 8.79 (d, 2H), 8.63 (d, 4H), 8.47 (t, 1H), 7.99 (t, 2H), 7.82 (t, 4H), 4.63 (m, 6H), 2.68 (t, 4H), 2.70 (m, 2H), 2.24 (m, 2H); 2.07 (m, 2H); ^{13}C NMR (63 MHz, D_2O) δ ppm 146.2, 144.3, 143.6, 128.6, 128.3, 127.9, 58.1, 57.3, 56.3, 34.2, 31.6, 28.4.

7 Summary and Outlook

7.1 Summary

The aim of this work was to synthesize and study the host-guest complexation of cationic dendritic and linear pyridinium derivatives based on bipyridinium and trimethylenedipyridinium subunits. The prominent steps and results can be summarized as follows:

i) An alternate way to synthesize benzylic bromide precursors which represent important intermediates for the synthesis of viologen and trimethylenedipyridinium dendrimers is described. The usual procedure involving the non-regioselective Appel reaction was replaced by a new method that allows the production of this intermediate in large quantities without tedious column purification. Apart from this I optimized the procedure for the synthesis of viologen dendron. The analysis of crystal structure of the viologen dendron opens new insight into the possible conformation of the corresponding benzylic viologen dendrimers.

ii) Viologen dendrimers were successfully spin-labeled at their periphery via a divergent method using 1-(2,4-dinitrophenyl)-4-(pyridin-4-yl)pyridinium hexafluorophosphate (**A**.PF_6) as the peripheral group. Such activated dendrimers were spin-labeled with 4-amino TEMPO. Cyclic voltammetry and ESR measurements showed the existence of the additional N-O$^{\cdot}$ electroactive subunit and good spin-label efficiency. The distance measurements are in progress. We intend to study chemical trigger induced conformational changes.

iii) A new class of polycationic dendrimers based on 1,3,5-tris-methylbenzene branching units interconnected by trimethylenedipyridinium was reported. The synthetic strategy follows here a divergent approach but the intermediates necessary for a convergent route are also reported. The syntheses described are conceptually similar to the synthesis of the corresponding viologen dendrimers. In contrast to the viologen (4,4´-bipyridinium)

dendrimers, the new trimethylendipyridinium dendrimers show no reversible electrochemistry (disruption of conjugation), they show higher flexibility (additional trimethylene), and they are expected to have a higher limiting generation (0.3 nm larger distance between the trimethylbenzene branching units). This makes them in their water soluble state (halide counter ion) ideal candidates for gene transfection and antiviral applications (lower toxicity and higher flexibility). The model anti-cancer drug anthraquinone-2,6-disulfonic acid (AQDS) is a tailored guest for the new dendrimers. The two sets of negatively charged sulfonate oxygens (distance 1.1 nm) correspond well to the distance between the pyridinium nitrogens (distance 1.1 nm) in the trimethylenedipyridinium unit. Upon addition of substoichiometric amounts of the AQDS guest, the dendrimers contract and reach their smallest diameter (ca 2/3 of their original hydrodynamic radius) in the range of total charge compensation. Overcharging with the AQDS guest is possible as evidenced by NMR (NMR titration) and cyclic voltammetry and leads to re-opening of the dendrimer structure. Charging occurs shell by shell in analogy to the Bohr atomic model. It is evidenced by the NMR titration which definitely exhibits prominent shift changes mainly at the magic numbers 3, 9 and 21.

iv) Step-wise radial complexation of cationic dendrimers with different anionic guests was studied to establish a generality of this phenomenon. For this purpose, viologen dendrimers bearing 4-*t*-BuBn at their periphery was synthesized and the experiments were carried out between different anionic guests with TMDPy and DPy dendrimers. As in the case of the trimethylene bridged pyridinium dendrimers, the dendrimers **TMDPy$_0$/DPy$_0$**, **TMDPy$_1$/DPy$_1$** and **TMDPy$_2$/DPy$_2$** consists of 1, 2 and 3 concentric shells which have 3, 6 and 12 double charges. If charging occurs shell by shell we expect - in analogy to the Bohr atomic model - prominent changes in experimental observables for **TMDPy$_2$/DPy$_2$** at 3, 9 and 21 equiv AQDS/NDS added, if – and only if – the dendrimer is loaded "shell-wise" starting with the innermost shell. The appearance of such "magic numbers" was first and so far

exclusively reported by Yamamoto et al for dendrimer-guest complexation based on Lewis base-Lewis acid interactions. Experiments with other molecular guests, e.g. Pyranine, BS also showed strong complex formation but slightly less structured NMR shift vs. anion equivalent results, still allowing access to the corresponding magic numbers. We found – to the best of our knowledge for the first time for cationic dendrimers– clear evidence for a stepwise shell charging of the dendrimer from inside towards the periphery.

v) α,ω-bromoalkanes were successfully tailored to bifunctional derivatives. The first step involves Arbuzov reaction where an α,ω-dibromoalkane is monofunctionalized to ω-dialkylphosphono-α-alkylbromide. In the second step, nucleophilic substitution was carried out with nucleophiles such as pyridine or sodium sulfite to yield the corresponding ω-functionalized pyridinium or sulfonate derivative. Thus by proper tailoring, we were able to introduce pyridinium, trimethylenedipyridinium, bipyridinium or a sulfonate at their ω end. These compounds were used as surface modifiers to build a biomimetic membrane on the pore walls of mesoporous TiO_2. Host-guest interaction studies with on purpose synthesized viologen compounds have been performed in collaboration.

7.2 Outlook

There are several interesting aspects of these molecules which are not addressed in this study. Phenomena like anion recognition and applications like gene transfection can be easily visualized from this study. Further studies in this direction can give more insight into the physico-chemical or biological aspects of these molecules in detail.

Also from synthetic point of view, cavitand synthesis would be interesting and that can be achieved by complexing the cationic subunits with the dianionic guests.

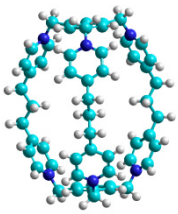

G_0 trimethylene diypridinium closed with tris bromomethyl benzene

Two G_0 trimethylene dipyridium bridged with 1,4-dibromoxylene

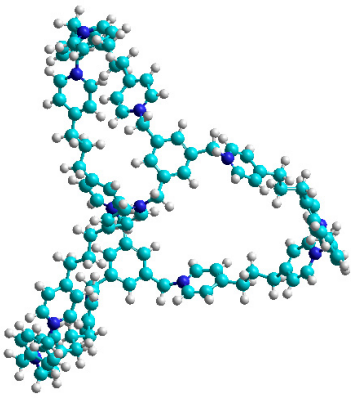

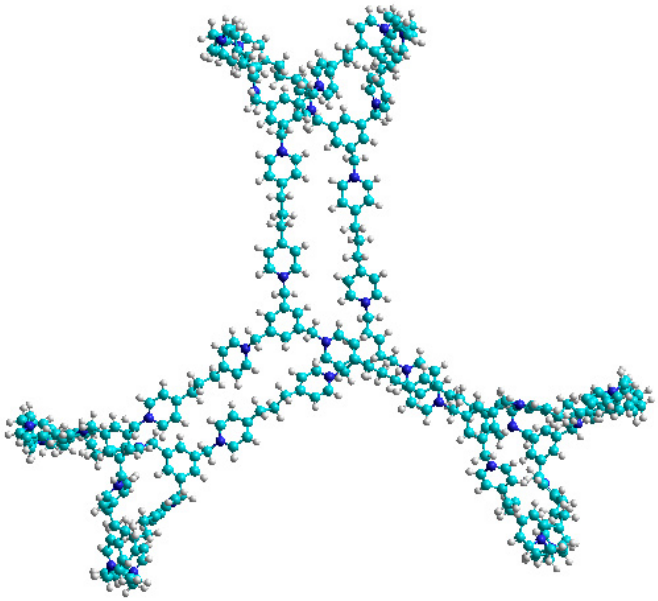

Two G_1 trimethylenedipyridinium briged with 1,4-dibromoxylene

References

(1) Voegtle, F.; Newkome, G. R.; Moorefield, C.; Editors *Dendritic Molecules: Concepts, Syntheses, Perspectives*, 1996.

(2) Fischer, M.; Vogtle, F. *Angewandte Chemie, International Edition* **1999**, *38*, 885.

(3) Aulenta, F.; Hayes, W.; Rannard, S. *European Polymer Journal* **2003**, *39*, 1741.

(4) a)Denkewalter, R. G.; Kolc, J.; Lukasavage, W. J.; (Allied Corp., USA). Application: US US, 1981, p 8 pp; b)Denkewalter, R. G.; Kolc, J. F.; Lukasavage, W. J.; (Allied Corp., USA). Application: US US, 1983, p 9 pp Cont

(5) Tomalia, D. A.; Baker, H.; Dewald, J.; Hall, M.; Kallos, G.; Martin, S.; Roeck, J.; Ryder, J.; Smith, P. *Polymer Journal* **1985**, *17*, 117.

(6) Newkome, G. R.; Yao, Z.; Baker, G. R.; Gupta, V. K. *Journal of Organic Chemistry* **1985**, *50*, 2003.

(7) a)Hawker, C.; Frechet, M. J. *Journal of the Chemical Society, Chemical Communications* **1990**, 1010; b)Hawker, C. J.; Frechet, J. M. J. *Journal of the American Chemical Society* **1990**, *112*, 7638; c)Hawker, C. J.; Frechet, J. M. J. *Macromolecules* **1990**, *23*, 4726.

(8) a)Xu, Z.; Kahr, M.; Walker, K. L.; Wilkins, C. L.; Moore, J. S. *Journal of the American Chemical Society* **1994**, *116*, 4537; b)Xu, Z.; Moore, J. S. *Angewandte Chemie* **1993**, *105*, 1394; c)Xu, Z.; Shi, Z. Y.; Tan, W.; Kopelman, R.; Moore, J. S. *Polymer Preprints* **1993**, *34*, 130.

(9) a)Balzani, V.; Ceroni, P.; Maestri, M.; Vicinelli, V. *Current Opinion in Chemical Biology* **2003**, *7*, 657; b)Patel, T. D.; Parikh, B. N.; Gothi, G. D.; Dave, J. B.; Patel, C. N. *Journal of Global Pharma Technology* **2010**, *2*, 5; c)Zeng, Y.; Li, Y.-Y.; Chen, J.; Yang, G.; Li, Y. *Chemistry An Asian Journal* **2010**, *5*, 992; d)Takada, K.; Goldsmith, J. I.; Bernhard, S.; Abruna, H. D. *Encyclopedia of Electrochemistry* **2007**, *11*, 729; e)Kim, C.; Hong, J. H. *Molecules* **2009**, *14*, 3719; f)Li, J.; Liu, D. *Journal of Materials Chemistry* **2009**, *19*, 7584.

(10) a)Heinen, S. *Dissertation; University of Osnabrueck* **1999**; b)Heinen, S.; Walder, L. *Angewandte Chemie, International Edition* **2000**, *39*, 806; c)Heinen, S.; Meyer, W.; Walder, L. *Journal of Electroanalytical Chemistry* **2001**, *498*, 34.

(11) a)Boisselier, E.; Ornelas, C.; Pianet, I.; Aranzaes, J. R.; Astruc, D. *Chemistry A European Journal* **2008**, *14*, 5577; b)Ornelas, C.; Boisselier, E.; Martinez, V.; Pianet, I.; Ruiz Aranzaes, J.; Astruc, D. *Chemical communications* **2007**, 5093.

(12) Yamamoto, K.; Higuchi, M.; Shiki, S.; Tsuruta, M.; Chiba, H. *Nature* **2002**, *415*, 509.

(13) Kaifer, A. E. *European Journal of Inorganic Chemistry* **2007**, 5015.

(14) Newkome, G. R.; Yao, Z.; Baker, G. R.; Gupta, V. K.; Russo, P. S.; Saunders, M. J. *Journal of the American Chemical Society* **1986**, *108*, 849.

(15) Newkome, G. R.; Baker, G. R.; Saunders, M. J.; Russo, P. S.; Gupta, V. K.; Yao, Z. Q.; Miller, J. E.; Bouillion, K. *Journal of the Chemical Society, Chemical Communications* **1986**, 752.

(16) a)Vladimirov, N. *Encyclopedia of Chromatography (3rd Edition)* **2010**, *1*, 559; b)Voronina, N. V.; Tatarinova, E. A.; Bystrova, A. V.; Ignat'eva, G. M.; Myakushev, V. D.; Muzafarov, A. M. *Polymer Preprints* **2009**, *50*, 487.

(17) Astruc, D.; Boisselier, E.; Ornelas, C. *Chemical Reviews* **2010**, *110*, 1857.

(18) Therien-Aubin, H.; Zhu, X. X. *Polymer Preprints* **2008**, *49*, 712.

(19) a)Giordanengo, R.; Mazarin, M.; Wu, J.; Peng, L.; Charles, L. *International Journal of Mass Spectrometry* **2007**, *266*, 62; b)Schalley, C. A.; Baytekin, B.; Baytekin, H. T.; Engeser, M.; Felder, T.; Rang, A. *Journal of Physical Organic Chemistry* **2006**, *19*, 479.

(20) Frechet, J.; Tomalia, D. *Dendrimers and Other Dendritic Polymers*, 2001.

(21) Marchioni, F.; Venturi, M.; Credi, A.; Balzani, V.; Belohradsky, M.; Elizarov, A. M.; Tseng, H.-R.; Stoddart, J. F. *Journal of the American Chemical Society* **2004**, *126*, 568.

(22) Boas, U.; Christensen, J. B.; Heegaard, P. M. H. *Journal of Materials Chemistry* **2006**, *16*, 3785.

(23) a)Calderon, M.; Quadir, M. A.; Sharma, S. K.; Haag, R. *Advanced Materials* **2010**, *22*, 190; b)Menjoge, A. R.; Kannan, R. M.; Tomalia, D. A. *Drug Discovery Today* **2010**, *15*, 171.

(24) Wiener, E.; Narayanan, V. V. *Advances in Dendritic Macromolecules* **2002**, *5*, 129.

(25) Teertstra, S. J.; Gauthier, M. *Progress in Polymer Science* **2004**, *29*, 277.

(26) King, A. S. H.; Twyman, L. J. *Journal of the Chemical Society, Perkin Transactions 1* **2002**, 2209.

(27) Bourrier, O.; Kakkar, A. K. *Macromolecular Symposia* **2004**, *209*, 97.

(28) Balzani, V.; Bandmann, H.; Ceroni, P.; Giansante, C.; Hahn, U.; Klaerner, F.-G.; Mueller, U.; Mueller, W. M.; Verhaelen, C.; Vicinelli, V.; Voegtle, F. *Journal of the American Chemical Society* **2006**, *128*, 637.

(29) Astruc, D.; Ornelas, C.; Ruiz, J. *Accounts of Chemical Research* **2008**, *41*, 841.

(30) Chase, P. A.; Gebbink, R. J. M. K.; van Koten, G. *Journal of Organometallic Chemistry* **2004**, *689*, 4016.

(31) Smith, D. K.; Diederich, F. *Topics in Current Chemistry* **2000**, *210*, 183.

(32) Nishide, H.; Oyaizu, K. *Science* **2008**, *319*, 737.

(33) Ceroni, P.; Credi, A.; Venturi, M.; Editors *Electrochemistry of Functional Supramolecular Systems*, 2010.

(34) a)Oyaizu, K.; Ando, Y.; Konishi, H.; Nishide, H. *Journal of the American Chemical Society* **2008**, *130*, 14459; b)Cho, S. I.; Lee, S. B. *Accounts of Chemical Research* **2008**, *41*, 699.

(35) a)Ling, X. Y.; Reinhoudt, D. N.; Huskens, J. *Langmuir* **2006**, *22*, 8777; b)Budny, A.; Novak, F.; Plumere, N.; Schetter, B.; Speiser, B.; Straub, D.; Mayer, H. A.; Reginek, M. *Langmuir* **2006**, *22*, 10605.

(36) a)Bongard, D.; Bohr, W.; (Germany). Application: DE DE, 2008, p 10pp; b)Bongard, D.; (Germany). Application: DE DE, 2010, p 9pp; c)Bongard, D. *Dissertation; University of Osnabrueck* **2008**.

(37) Asaftei, S.; De Clercq, E. *Journal of Medicinal Chemistry* **2010**, *53*, 3480.

(38) a)Marchioni, F.; Venturi, M.; Ceroni, P.; Balzani, V.; Belohradsky, M.; Elizarov, A. M.; Tseng, H. R.; Stoddart, L. F. *Chemistry A European Journal* **2004**, *10*, 6361; b)Ronconi, C. M.; Stoddart, J. F.; Balzani, V.; Baroncini, M.; Ceroni, P.; Giansante, C.; Venturi, M. *Chemistry A European Journal* **2008**, *14*, 8365.

(39) a)Fujii, A.; Ochi, Y.; Nakajima, R.; Yamamoto, K. *Chemistry Letters* **2009**, *38*, 418; b)Higuchi, M.; Tsuruta, M.; Chiba, H.; Shiki, S.; Yamamoto, K. *Journal*

of the American Chemical Society **2003**, *125*, 9988; c)Ochi, Y.; Fujii, A.; Nakajima, R.; Yamamoto, K. *Macromolecules* **2010**, *43*, 6570.

(40) Azagarsamy, M. A.; Krishnamoorthy, K.; Sivanandan, K.; Thayumanavan, S. *Journal of Organic Chemistry* **2009**, *74*, 9475.

(41) a)Diez-Barra, E.; Garcia-Martinez, J. C.; Merino, S.; del Rey, R.; Rodriguez-Lopez, J.; Sanchez-Verdu, P.; Tejeda, J. *Journal of Organic Chemistry* **2001**, *66*, 5664; b)Menzer, S.; White, A. J. P.; Williams, D. J.; Belohradsky, M.; Hamers, C.; Raymo, F. M.; Shipway, A. N.; Stoddart, J. F. *Macromolecules* **1998**, *31*, 295.

(42) a)Sivakumar, C.; Nasar, A. S. *Journal of Polymer Science, Part A: Polymer Chemistry* **2009**, *47*, 3337; b)Shimizu, S.; Suzuki, T.; Shirakawa, S.; Sasaki, Y.; Hirai, C. *Advanced Synthesis & Catalysis* **2002**, *344*, 370.

(43) Felderhoff, M.; Heinen, S.; Mulisho, N.; Webersinn, S.; Walder, L. *Helvetica Chimica Acta* **2000**, *83*, 181.

(44) Arendt, M.; Sun, W.; Thomann, J.; Xie, X.; Schrader, T. *Chemistry An Asian Journal* **2006**, *1*, 544.

(45) a)Esser, B.; Bandyopadhyay, A.; Rominger, F.; Gleiter, R. *Chemistry A European Journal* **2009**, *15*, 3368; b)Allard, E.; Delaunay, J.; Cousseau, J. *Organic Letters* **2003**, *5*, 2239.

(46) Leon, J. W.; Kawa, M.; Frechet, J. M. J. *Journal of the American Chemical Society* **1996**, *118*, 8847.

(47) a)Komissarov, V. V.; Panova, N. G.; Kritzyn, A. M. *Russian Journal of Bioorganic Chemistry* **2008**, *34*, 67; b)Drescher, S.; Meister, A.; Blume, A.; Karlsson, G.; Almgren, M.; Dobner, B. *Chemistry A European Journal* **2007**, *13*, 5300; c)Snider, B. B.; Lu, Q. *Journal of Organic Chemistry* **1996**, *61*, 2839.

(48) Cooke, G.; Woisel, P.; Bria, M.; Delattre, F.; Garety, J. F.; Hewage, S. G.; Rabani, G.; Rosair, G. M. *Organic Letters* **2006**, *8*, 1423.

(49) Schon, P.; Degefa, T. H.; Asaftei, S.; Meyer, W.; Walder, L. *Journal of the American Chemical Society* **2005**, *127*, 11486.

(50) a)Dickson, S. J.; Wallace, E. V. B.; Swinburne, A. N.; Paterson, M. J.; Lloyd, G. O.; Beeby, A.; Belcher, W. J.; Steed, J. W. *New Journal of Chemistry* **2008**, *32*, 786; b)Porter, W. W.; Vaid, T. P. *Journal of Organic Chemistry* **2005**, *70*,

5028; c)Scheytza, H.; Rademacher, O.; Reissig, H. U. *European Journal of Organic Chemistry* **1999**, 2373; d)Soleimannejad, J.; Aghabozorg, H.; Hooshmand, S. *Acta Crystallographica Section E-Structure Reports Online* **2008**, *64*, M564; e)Spruell, J. M.; Paxton, W. F.; Olsen, J. C.; Benitez, D.; Tkatchouk, E.; Stern, C. L.; Trabolsi, A.; Friedman, D. C.; Goddard, W. A.; Stoddart, J. F. *Journal of the American Chemical Society* **2009**, *131*, 11571; f)Hu, J.; Cheng, Y.; Wu, Q.; Zhao, L.; Xu, T. *J. Phys. Chem. B* **2009**, *113*, 10650.

(51) Inoue, M. B.; Inoue, M.; Machi, L.; Brown, F.; Fernando, Q. *Inorganica Chimica Acta* **1995**, *230*, 145.

(52) García, M. D.; Blanco, V. c.; Platas-Iglesias, C.; Peinador, C.; Quintela, J. M. *Crystal Growth & Design* **2009**.

(53) Stewart, J. J. P. *Journal of Computational Chemistry* **1989**, *10*, 209.

(54) Dimick, S. M.; Powell, S. C.; McMahon, S. A.; Moothoo, D. N.; Naismith, J. H.; Toone, E. J. *Journal of the American Chemical Society* **1999**, *121*, 10286.

(55) Nielsen, A. T.; Christian, S. L.; Moore, D. W.; Gilardi, R. D.; George, C. F. *Journal of Organic Chemistry* **1987**, *52*, 1656.

(56) Reschke, T. *Bachelor Thesis, University of Osnabrück.* **2009**.

(57) Flanagan, J. B.; Margel, S.; Bard, A. J.; Anson, F. C. *Journal of the American Chemical Society* **1978**, *100*, 4248.

(58) a)Thompson, M. A.; Glendening, E. D.; Feller, D. *Journal of Physical Chemistry* **1994**, *98*, 10465; b)Thompson, M. A.; Schenter, G. K. *Journal of Physical Chemistry* **1995**, *99*, 6374; c)Thompson, M. A. *Journal of Physical Chemistry* **1996**, *100*, 14492; d)Thompson, M. A.; Zerner, M. C. *Journal of the American Chemical Society* **1991**, *113*, 8210.

(59) Dandliker, P. J.; Diederich, F.; Zingg, A.; Gisselbrecht, J. P.; Gross, M.; Louati, A.; Sanford, E. *Helvetica Chimica Acta* **1997**, *80*, 1773.

(60) Selby, T. D.; Blackstock, S. C. *Journal of the American Chemical Society* **1998**, *120*, 12155.

(61) Miller, L. L.; Duan, R. G.; Tully, D. C.; Tomalia, D. A. *Journal of the American Chemical Society* **1997**, *119*, 1005.

(62) Moulines, F.; Djakovitch, L.; Boese, R.; Gloaguen, B.; Thiel, W.; Fillaut, J. L.; Delville, M. H.; Astruc, D. *Angewandte Chemie* **1993**, *105*, 1132.

(63) Valerio, C.; Fillaut, J.-L.; Ruiz, J.; Guittard, J.; Blais, J.-C.; Astruc, D. *Journal of the American Chemical Society* **1997**, *119*, 2588.

(64) Ottaviani, M. F.; Furini, F.; Casini, A.; Turro, N. J.; Jockusch, S.; Tomalia, D. A.; Messori, L. *Macromolecules* **2000**, *33*, 7842.

(65) Ottaviani, M. F.; Matteini, P.; Brustolon, M.; Turro, N. J.; Jockusch, S.; Tomalia, D. A. *Journal of Physical Chemistry B* **1998**, *102*, 6029.

(66) a)Ottaviani, M. F.; Cossu, E.; Turro, N. J.; Tomalia, D. A. *Journal of the American Chemical Society* **1995**, *117*, 4387; b)Ottaviani, M. F.; Turro, N. J.; Jockusch, S.; Tomalia, D. A. *Journal of Physical Chemistry* **1996**, *100*, 13675.

(67) Ottaviani, M. F.; Sacchi, B.; Turro, N. J.; Chen, W.; Jockusch, S.; Tomalia, D. A. *Macromolecules* **1999**, *32*, 2275.

(68) Bosman, A. W.; Janssen, R. A. J.; Miejer, E. W. *Macromolecules* **1997**, *30*, 3606.

(69) a)Yordanov, A. T.; Lodder, A. L.; Woller, E. K.; Cloninger, M. J.; Patronas, N.; Milenic, D.; Brechbiel, M. W. *Nano Letters* **2002**, *2*, 595; b)Yordanov, A. T.; Yamada, K.; Krishna, M. C.; Mitchell, J. B.; Woller, E.; Cloninger, M.; Brechbiel, M. W. *Angewandte Chemie, International Edition* **2001**, *40*, 2690.

(70) Yamaguchi, I.; Higashi, H.; Shigesue, S.; Shingai, S.; Sato, M. *Tetrahedron Letters* **2007**, *48*, 7778.

(71) a)Carlmark, A.; Hawker, C.; Hult, A.; Malkoch, M. *Chem Soc Rev* **2009**, *38*, 352; b)Grayson, S. M.; Frechet, J. M. J. *Chemical Reviews* **2001**, *101*, 3819; c)Merkel, O. M.; Mintzer, M. A.; Sitterberg, J.; Bakowsky, U.; Simanek, E. E.; Kissel, T. *Bioconjugate Chemistry* **2009**, *20*, 1799; d)Laufersweiler, M. J.; Rohde, J. M.; Chaumette, J.-L.; Sarazin, D.; Parquette, J. R. *Journal of Organic Chemistry* **2001**, *66*, 6440; e)Goh Sarah, L.; Francis Matthew, B.; Frechet Jean, M. J. *Chemical communications* **2002**, 2954; f)Goodwin Andrew, P.; Lam Stephanie, S.; Frechet Jean, M. J. *Journal of the American Chemical Society* **2007**, *129*, 6994; g)Hourani, R.; Kakkar, A. *Macromolecular Rapid Communications* **2010**, *31*, 947.

(72) a)Hecht, S. *Journal of Polymer Science, Part A: Polymer Chemistry* **2003**, *41*, 1047; b)Nierengarten, J.-F. *Angewandte Chemie, International Edition* **2005**, *44*, 2830; c)Gitsov, I.; Lin, C. *Current Organic Chemistry* **2005**, *9*, 1025.

(73) a)Smith, D. K. *Advanced Materials* **2006**, *18*, 2773; b)Lee, C. C.; MacKay, J. A.; Frechet, J. M. J.; Szoka, F. C. *Nature Biotechnology* **2005**, *23*, 1517; c)Welsh, D. J.; Jones, S. P.; Smith, D. K. *Angewandte Chemie, International Edition* **2009**, *48*, 4047; d)Medina, S. H.; El-Sayed, M. E. H. *Chemical Reviews* **2009**, *109*, 3141; e)Schultz, L. G.; Zimmerman, S. C. *Pharmaceutical News* **1999**, *6*, 25; f)Mintzer, M.; Merkel, O. M.; Kissel, T.; Simanek, E. E. *PMSE Preprints* **2008**, *99*, 132; g)Smith, D. K. *Current Topics in Medicinal Chemistry* **2008**, *8*, 1187.

(74) a)Pittelkow, M.; Christensen, J. B.; Meijer, E. W. *Journal of Polymer Science, Part A: Polymer Chemistry* **2004**, *42*, 3792; b)Pittelkow, M.; Nielsen, C. B.; Broeren, M. A. C.; van Dongen, J. L. J.; van Genderen, M. H. P.; Meijer, E. W.; Christensen, J. B. *Chemistry A European Journal* **2005**, *11*, 5126.

(75) Hofacker, A. L.; Parquette, J. R. *Angewandte Chemie, International Edition* **2005**, *44*, 1053.

(76) Therien-Aubin, H.; Zhu, X. X.; Moorefield, C. N.; Kotta, K.; Newkome, G. R. *Macromolecules* **2007**, *40*, 3644.

(77) A. J. Bard, L. R. Faulkner, Electrochemical Methods: Fundamentals and Applications, 2nd ed., Wiley, New York, 2001.

(78) a)Sobransingh, D.; Kaifer, A. E. *Langmuir* **2006**, *22*, 10540; b)Kaifer, A. E. *Accounts of Chemical Research* **1999**, *32*, 62.

(79) a)Pluth, M. D.; Raymond, K. N. *Chemical Society Reviews* **2007**, *36*, 161; b)Kleppinger, R.; Mortensen, K.; Meijer, E. W. *PMSE Preprints* **2002**, *86*, 139; c)Aloshyna, M.; Medina, B. M.; Poulsen, L.; Moreau, J.; Beljonne, D.; Cornil, J.; Di Silvestro, G.; Cerminara, M.; Meinardi, F.; Tubino, R.; Detert, H.; Schrader, S.; Egelhaaf, H.-J.; Botta, C.; Gierschner, J. *Advanced Functional Materials* **2008**, *18*, 915; d)Gitsov, I.; Lambrych, K. R.; Remnant, V. A.; Pracitto, R. *Journal of Polymer Science, Part A: Polymer Chemistry* **2000**, *38*, 2711.

(80) a)Bus, J. S.; Aust, S. D.; Gibson, J. E. *Environmental health perspectives* **1976**, *16*, 139; b)O'Fallon, J. V.; Wright, R. W., Jr. *Analytical biochemistry* **1991**, *198*, 179; c)Ross, J. H.; Krieger, R. I. *Drug and chemical toxicology* **1979**, *2*, 207.

(81) McNerny, D. Q.; Leroueil, P. R.; Baker, J. R. *Wiley Interdisciplinary Reviews: Nanomedicine and Nanobiotechnology* **2010**, *2*, 249.

(82) Wolfdieterich, M. *Dissertation; University of Osnabrueck* **2005**.

(83) Satoh, N.; Cho, J.-S.; Higuchi, M.; Yamamoto, K. *Journal of the American Chemical Society* **2003**, *125*, 8104.

(84) a)Wong, E. L. S.; Gooding, J. J. *Analytical Chemistry* **2003**, *75*, 3845; b)Zagotto, G.; Mitaritonna, G.; Sissi, C.; Palumbo, M. *Nucleosides & Nucleotides* **1998**, *17*, 2135; c)Batchelor-McAuley, C.; Li, Q.; Dapin, S. M.; Compton, R. G. *Journal of Physical Chemistry B* **2010**, *114*, 4094.

(85) Komura, T.; Mori, Y.; Yamaguti, T.; Takahasi, K. *Electrochimica Acta* **1997**, *42*, 985.

(86) a)Morris, K. F.; Johnson, C. S., Jr. *Journal of the American Chemical Society* **1992**, *114*, 3139; b)Johnson, C. S., Jr. *Progress in Nuclear Magnetic Resonance Spectroscopy* **1999**, *34*, 203; c)Cohen, Y.; Avram, L.; Frish, L. *Angewandte Chemie, International Edition* **2005**, *44*, 520; d)Stejskal, E. O.; Tanner, J. E. *Journal of Chemical Physics* **1965**, *42*, 288.

(87) a)Pregosin, P. S.; Kumar, P. G. A.; Fernandez, I. *Chemical Reviews* **2005**, *105*, 2977; b)Brand, T.; Cabrita, E. J.; Berger, S. *Progress in Nuclear Magnetic Resonance Spectroscopy* **2005**, *46*, 159.

(88) Kang, H.; Facchetti, A.; Jiang, H.; Cariati, E.; Righetto, S.; Ugo, R.; Zuccaccia, C.; Macchioni, A.; Stern, C. L.; Liu, Z.; Ho, S.-T.; Brown, E. C.; Ratner, M. A.; Marks, T. J. *Journal of the American Chemical Society* **2007**, *129*, 3267.

(89) Hoefer, M.; Bandaru, P. R. *Applied Physics Letters* **2009**, *95*, 183108/1.

(90) Cheng, Y.; Wu, Q.; Li, Y.; Xu, T. *Journal of Physical Chemistry B* **2008**, *112*, 8884.

(91) a)Boas, U.; Heegaard, P. M. H. *Chemical Society Reviews* **2004**, *33*, 43; b)Gillies, E. R.; Frechet, J. M. J. *Drug Discovery Today* **2005**, *10*, 35; c)Morgan, M. T.; Carnahan, M. A.; Immoos, C. E.; Ribeiro, A. A.; Finkelstein, S.; Lee, S. J.; Grinstaff, M. W. *Journal of the American Chemical Society* **2003**, *125*, 15485.

(92) Braun, M.; Atalick, S.; Guldi, D. M.; Lanig, H.; Brettreich, M.; Burghardt, S.; Hatzimarinaki, M.; Ravanelli, E.; Prato, M.; van Eldik, R.; Hirsch, A. *Chemistry A European Journal* **2003**, *9*, 3867.

(93) Morara, A. D.; McCarley, R. L. *Organic Letters* **2006**, *8*, 1999.

(94) Michaelis, A.; Kaehne, R. *Berichte der Deutschen Chemischen Gesellschaft* **1898**, *31*, 1048.

(95) a)Taffa, D. *Dissertation; University of Osnabrueck* **2010**; b)Taffa, D.; Kathiresan, M.; Walder, L. *Langmuir* **2009**, *25*, 5371.

(96) Li, S. J.; Liu, M.; Zheng, B.; Zhu, K. L.; Wang, F.; Li, N.; Zhao, X. L.; Huang, F. H. *Organic Letters* **2009**, *11*, 3350.

(97) Nakamura, C. E.; Chu, S. H.; Stoeckler, J. D.; Parks, R. E., Jr. *Biochemical Pharmacology* **1986**, *35*, 133.

(98) Yoon, N. M.; Pak, C. S.; Brown Herbert, C.; Krishnamurthy, S.; Stocky, T. P. *Journal of Organic Chemistry* **1973**, *38*, 2786.

(99) Akkerman Hylke, B.; Blom Paul, W. M.; de Leeuw Dago, M.; de Boer, B. *Nature* **2006**, *441*, 69.

(100) Montoneri, E.; Ricca, G. *Phosphorus, Sulfur Silicon and Related Elements* **1991**, *55*, 111.

(101) a)Feng, D.-J.; Li, X.-Q.; Wang, X.-Z.; Jiang, X.-K.; Li, Z.-T. *Tetrahedron* **2004**, *60*, 6137; b)Bhowmik, P. K.; Han, H.; Ndedeltchev, I. K.; Cebe, J. J.; Kang, S.-W.; Kumar, S. *Liquid Crystals* **2006**, *33*, 891.

(102) a)Katritzky, A. R.; Fan, W. Q.; Li, Q. L. *Journal of Heterocyclic Chemistry* **1988**, *25*, 1311; b)Jiao, X.; Niu, Y.; Zhang, H.; Zhu, L.; Zhao, F. *Journal of Chemical Crystallography* **2006**, *36*, 685.

(103) Veling, N.; Thomassen, P. J.; Thordarson, P.; Elemans, J. A. A. W.; Nolte, R. J. M.; Rowan, A. E. *Tetrahedron* **2008**, *64*, 8535.

(104) Weber, J. M.; Rawls, M. T.; MacKenzie, V. J.; Limoges, B. R.; Elliott, C. M. *Journal of the American Chemical Society* **2007**, *129*, 313.

(105) Stehle, P.; Fuerst, P.; Ratz, R.; Rau, H. *Journal of Chromatography* **1988**, *449*, 299.

Appendix

Table 1. Atomic coordinates (x 10^4) and equivalent isotropic displacement parameters (A^2 x 10^3) for **A**.PF_6. U(eq) is defined as one third of the trace of the orthogonalized U_{ij} tensor.

	x	y	z	U(eq)
P(1)	3562(1)	1092(1)	2925(1)	17(1)
F(1)	5344(1)	1801(1)	2540(1)	35(1)
F(2)	2311(1)	743(1)	1499(1)	25(1)
F(3)	3693(1)	-354(1)	2795(1)	36(1)
F(4)	1739(1)	377(1)	3294(1)	20(1)
F(5)	4760(1)	1439(1)	4341(1)	38(1)
F(6)	3375(1)	2527(1)	3043(1)	27(1)
N(1)	-1458(2)	-4779(1)	3177(1)	22(1)
N(2)	2307(1)	677(1)	8128(1)	13(1)
N(3)	6012(2)	2397(1)	9846(1)	16(1)
N(4)	3354(2)	4909(1)	11760(1)	17(1)
O(1)	5808(1)	1235(1)	9499(1)	26(1)
O(2)	7480(1)	3398(1)	10191(1)	24(1)
O(3)	2000(2)	4820(1)	12023(1)	27(1)
O(4)	4884(1)	5822(1)	12242(1)	22(1)
C(1)	64(2)	-3690(1)	3267(1)	19(1)
C(2)	969(2)	-2606(1)	4251(1)	16(1)
C(3)	258(2)	-2648(1)	5216(1)	15(1)
C(4)	-1316(2)	-3788(1)	5146(1)	19(1)
C(5)	-2114(2)	-4812(2)	4119(1)	22(1)
C(6)	1095(2)	-1497(1)	6264(1)	14(1)
C(7)	1947(2)	-152(1)	6090(1)	16(1)
C(8)	2527(2)	922(1)	7026(1)	16(1)
C(9)	1589(2)	-614(1)	8352(1)	15(1)
C(10)	990(2)	-1714(1)	7438(1)	15(1)
C(11)	2660(2)	1804(1)	9052(1)	13(1)
C(12)	4392(2)	2622(1)	9867(1)	13(1)
C(13)	4661(2)	3668(1)	10750(1)	14(1)
C(14)	3129(2)	3850(1)	10793(1)	15(1)
C(15)	1396(2)	3084(1)	9987(1)	17(1)
C(16)	1172(2)	2053(1)	9096(1)	16(1)

Abbreviations

$(CD_3)_2CO$	deuterated acetone
µ	micro
^{13}C NMR	Carbon13 NMR
^{1}H NMR	Proton NMR
4-*t*-BuBnBr	4-*tert*-butylbenzyl bromide
Ag/AgCl	Silver/Silver Chloride
AQDS	Anthraquinone-2,6-disulfonicacid disodium salt
Ar	Argon
BH_3	Borane
BS	BenzeneSulfonic acid sodiumsalt
bs	broadsinglet
Bz_2O_2	Benzoylperoxide
CD_3CN	deuterated acetonitrile
$CDCl_3$	deuterated Chloroform
CH_3CN	Acetonitrile
$CHCl_3$	Chloroform
CT	Charge Transfer
CV	cyclic voltammetry
d	days (in reaction scheme); doublet (in NMR data)
D	Diffusion Coefficient
D_2O	deuterated water
DCM (CH_2Cl_2)	Dichloromethane
DEPT	**D**istortionless **E**nhancement by **P**olarization **T**ransfer
DIBAL	Diisobutylaluminium hydride
DMF	Dimethylformamide
DMSO	Dimethylsulfoxide
DMSO-d_6	deuterated Dimethylsulfoxide
DNA	Deoxyribo Nucleic Acid
DOSY	Diffusion Ordered Spectroscopy
E	Electrochemical Potential
E^0	Formal potential

equiv	Equivalents
ESR	Electron Spin Resonance
EtOAc	Ethylacetate
EtOH	Ethanol
Fig	Figure
g	grams
Gn	Generation number of the dendrimers
h	hours
H_2O	water
H_2SO_4	Sulfuric acid
HBr	Hydrobromic acid
HPLC	High Performance Liquid Chromatography
Hz	Hertz
I	Current
J	Coupling Constant
K	association constant
KOH	Potassium hydroxide
LAH ($LiAlH_4$)	Lithium Aluminium Hydride
M	molar
m	multiplet
m.pt	melting point
mbar	millibar
MeOH	Methanol
$MgSO_4$	Magnesium sulfate
MHz	megahertz
mL	milliliter
mmol	millimoles
MRI	Magnetic Resonance Imaging
Na_2SO_3	Sodiumsulfite
Na_2SO_4	Sodiumsulfate
$NaHCO_3$	Sodium bicarbonate
NBS	N-Bromosuccinimide
NDS	Naphthalene-2,6-disulfonicacid disodium salt

NH_4PF_6	Ammonium hexafluorophosphate
NMR	Nuclear Magnetic Resonance
NOESY	Nuclear Overhauser Effect Spectroscopy
PAMAM	Polyamidoamine
PPh_3	Triphenylphosphine
ppm	parts per million
Pyr	Pyranine
r_h	hydrodynamic radius
RT	room temperature
s	singlet
Sat.	Saturated
t	triplet
TBA	Tetrabutylammonium
$TBA.PF_6$	Tetrabutylammonium hexafluorophosphate
TEMPO	-2,2,6,6-TetramethylPiperidine 1-Oxyl free radical
THF	Tetrahydrofuran
TiO_2	Titanium dioxide
TLC	Thin Layer Chromatography
Uv-Vis	UltraViolet-Visible
δ	chemical shift
ν	scan rate

CURRICULUM VITAE

Personal details

Name	Kathiresan Murugavel
Date of Birth	11-06-1984
Place of Birth	Cuddalore, TamilNadu, India
Citizenship	Indian
2001-2004	Bachelor of Science in Chemistry, St. Joseph's College of Arts & Science, Affiliated to the University of Madras, Cuddalore.
2004-2006	Master of Science in Organic Chemistry, Department of Organic Chemistry, University of Madras, Chennai.
2006-2007	Junior Scientist, Shasun Research Centre, a unit of Shasun Chemicals and Drugs Limited, Chennai.
2007-2010	Research Student, AG Walder, Institut für Chemie, Universität Osnabrück, Germany.

Publications

1. DerejeHailu Taffa, Murugavel Kathiresan and Lorenz Walder; *Tuning the Hydrophilic, Hydrophobic, and Ion Exchange Properties of Mesoporous TiO_2,* Langmuir, **2009**, 25 (9), 5371.

2. Dereje Hailu Taffa, Murugavel Kathiresan, Lorenz Walder, Britta Seelandt and Michael Wark; *Pore size and surface charge control in mesoporous TiO_2 using post-grafted SAMs*, Physical Chemistry Chemical Physics, **2010**, 12, 1473.

3. Murugavel Kathiresan, Lorenz Walder, Fei Ye and Hans Reuter; *Viologen-based benzylic dendrimers: selective synthesis of 3,5-bis(hydroxymethyl)benzyl bromide and conformational analysis of the corresponding viologen dendrimer subunit*, Tetrahedron Letters, **2010**, 51(16), 2188.

4. Dereje Hailu Taffa, Murugavel Kathiresan, Tamara Arnold, Lorenz Walder, Martin Erbacher, Daniela Bauer, Franz-Peter Montforts, Jörg Nordmann and Markus Haase; *Dye sensitized membranes within mesoporous TiO_2: Photocurrents in aqueous solution,* Journal of Photochemistry and Photobiology A: Chemistry, **2010**, 216(1), 35-43.

5. Murugavel Kathiresan, Lorenz Walder, *Trimethylenedipyridinium Dendrimers: Synthesis and Sequential Guest Complexation in Molecular Shells,* Macromolecules, **2010**, *ASAP.*

6. Murugavel Kathiresan, Lorenz Walder, *Stepwise Radial Complexation in Pyridinium Dendrimers*, Manuscript in preparation.

Earlier Publication

Ekambaram Ramesh, Murugavel Kathiresan and Raghavachary Raghunathan; *Solvent-free microwave-assisted conversion of Baylis–Hillman adducts of ninhydrin into functionalized spiropyrrolidines/pyrrolizidines through 1,3-dipolar cycloaddition,* Tetrahedron Letters, **2007,** 48(10), 1835.

Conference Talks

1. Pore wall modification of Mesoporous TiO_2 with Organic phosphonic acid; Dereje Hailu Taffa, Murugavel Kathiresan, Lorenz Walder, Second German-Danish Meeting on Interface phenomena, July 14-16, **2008**, Sonderborg, Denmark.

2. Electrostatic and Hydrophobic Interactions on Mesoporous TiO_2 Electrodes, Dereje H. Taffa, M. Kathiresan, L. Walder, B. Seelandt, and M. Wark, Electrochemistry in Interfacial Nanoscience, 6th ECHEMS meeting, June 20-23, **2010** Sandbjerg, Denmark.

Posters

1. A versatile surface modification Method for Mesoporous TiO_2, Dereje Hailu Taffa, Murugavel Kathiresan, Lorenz Walder, Deutschen Physikalischen Gesellschaft, March 22-27, **2009**, Dresden.

2. Synthesis and Electrochemistry of Viologen and Pyridinium dendrimer, Murugavel Kathiresan, Lorenz Walder, Electrochemistry in Interfacial Nanoscience, 6th ECHEMS meeting, June 20-23, **2010** Sandbjerg, Denmark.

Declaration

I hereby declare that this thesis is the summary of my Ph.D work and has not been submitted to any other university. All the sources and materials used in this thesis are duly acknowledged and cited.

Osnabrück, November 2010

Kathiresan Murugavel.